An investigation into treatment options to improve the performance of re-used seed crystals for gypsum precipitation in the presence of an anti-scalant

by

Izak Adolf Cronje

Thesis presented in partial fulfilment

of the requirements for the Degree

of

MASTER OF ENGINEERING
CHEMICAL ENGINEERING

in the Faculty of Engineering

at Stellenbosch University

Supervisor

Prof A.J Burger

March 2020

Plagiarism declaration

By submitting this thesis electronically, I declare that the entirety of the work contained therein is my own, original work, that I am the sole author thereof (save to the extent explicitly otherwise stated), that reproduction and publication thereof by Stellenbosch University will not infringe any third party rights and that I have not previously in its entirety or in part submitted it for obtaining any qualification.

March 2020

Abstract

Many mines in South Africa generate large volumes of acid mine drainage (AMD), containing relatively high concentrations of sulphates. Several mine water treatment plants utilise intermediate seeded slurry crystallisation between stages of reverse osmosis (RO), where gypsum ($CaSO_4 2H_2O$) is precipitated and removed to enable further desalination by RO in the presence of antiscalants.

This study aimed to determine the effect of various methods of treatment on re-used seed crystals, considering the efficiency and rate of gypsum precipitation in the presence of antiscalants. Four different treatment methods were evaluated. These were two physical and two chemical treatments: 1. vigorous mixing; 2. air scouring; 3. addition of hydrogen peroxide; 4. addition of aluminum. The experiments were performed in sets of three 2.5 hour experiments, while 2000 ppm seed crystals were re-used and introduced into a three-times supersaturated gypsum solution in the presence of 9 ppm polycarboxylic acid antiscalant.

The effectiveness of gypsum precipitation was characterised in terms of calcium removal by means of precipitation, while assuming an equivalent sulphate removal. In the presence of antiscalant, the calcium removal decreased with the re-use of seed crystals, indicating that the seeding became less effective with every re-use cycle. The average calcium removal over three runs with re-used seed crystals decreased from 42.8% in the absence of antiscalant to 15.3% in the presence of antiscalant.

Mixing of the seed crystal slurry for 10 minutes at a G-factor of 188 s^{-1} was the most effective physical treatment method, removing an average of 31.4% calcium, compared to the control in the presence of antiscalant where only 15.3% calcium was removed without treatment. Air scouring as a treatment method was found to be less effective, with a maximum calcium removal of 18.6%. The dosing of aluminum proved to be very effective. In the presence of 4.5 ppm aluminum in the form of $AlCl_3$, 41.2% of the calcium was removed, compared to maximum removal of only 25.3% in the presence of 90 ppm hydrogen peroxide.

It was found that the presence of hydrogen peroxide, the presence of aluminum and mixing as seed-crystal treatment method increased the average calcium removal significantly when seed crystals were re-used, and are viable options to improve the crystallisation process in the presence of antiscalant when seed crystals are re-used.

Opsomming

Baie myne in Suid-Afrika genereer groot volumes suurmynafloop wat hoë konsentrasies sulfate bevat. Verskeie mynwater behandelingsaanlegte gebruik intermediëre saadkristalslik kristallisasie tussen omgekeerde osmose (RO) fases, waar gips ($CaSO_4 2H_2O$) gepresipiteer en verwyder word om verdere ontsouting deur RO in die teenwoordigheid van teenskaalmiddels moontlik te maak.

Die studie het gepoog om die effek van verskillende behandelingsmetodes op hergebruikte saadkristalle vas te stel terwyl die effektiwiteit en tempo van gips presipitasie in die teenwoordigheid van teenskaalmiddels in ag geneem word. Vier verskillende behandelingsmetodes is geëvalueer. Dit het twee fisiese en twee chemiese metodes ingesluit: 1. Kragtige vermenging; 2. Lugskuring; 3. Byvoeging van waterstof peroksied; 4. Byvoeging van aluminium. Die eksperimente is uitgevoer in stelle van drie 2.5 uur eksperimente, terwyl 2000 ppm saadkristalle hergebruik is en bygevoeg is in ‘n drie keer superversadigde gips oplossing in die teenwoordigheid van 9 ppm polikarboksielsuur teenskaalmiddel.

Die effektiwiteit van gips presipitasie is gekarakteriseer in terme van kalsium verwydering deur presipitasie, terwyl die aanname gemaak is van ekwivalente sulfaatverwydering. In die teenwoordigheid van teenskaalmiddel het die kalsiumverwydering afgeneem met hergebruik van die saadkristalle, wat aandui dat die saadkristalle minder effektief geword het met elke hergebruik siklus. Die gemiddelde kalsiumverwydering oor drie eksperimentele lopies met hergebruikte saadkristalle het afgeneem van 42.8% in die afwesigheid van teenskaalmiddel tot 15.3% in die teenwoordigheid van teenskaalmiddel.

Vermenging van die saadkristal slik vir 10 minute teen ‘n G-faktor van 188 s^{-1} was die mees effektiewe fisiese behandelingsmetode, wat ‘n gemiddeld van 31.4% kalsium verwyder het, in vergelyking met die kontrole in die teenwoordigheid van teenskaalmiddel waar slegs 15.3% van die kalsium verwyder is sonder behandeling. Lugskuring as ‘n behandelingsmetode was minder effektief, met ‘n maksimum kalsiumverwydering van 18.6%. Dosering met aluminium was baie effektief. In die teenwoordigheid van 4.5 ppm aluminium in die vorm van $AlCl_3$, is 41.2% van die kalsium verwyder in vergelyking met die maksimum kalsiumverwydering van 25.3% in die teenwoordigheid van 90 ppm waterstof peroksied.

Daar is gevind dat vermenging as die saadkristal behandelingsmetode, in die teenwoordigheid van waterstof peroksied en aluminium, die gemiddelde kalsiumverwydering noemenswaardig verhoog het wanneer saadkristalle hergebruik is. Hierdie benadering is geïdentifiseer as ‘n lewensvatbare opsie om

die kristallisasieproses te verbeter in die teenwoordigheid van teenskaalmiddel wanneer saadkristalle hergebruik word.

Nomenclature

Symbol	Description	Unit
A	Pre-exponential factor	-
A_c	Surface area of crystal	m^2
B_0	Nucleation rate	Nuclei/time
C	Solute concentration in the supersaturated solution	mol/l
c	Concentration	mol/l
c^*	Equilibrium concentration	mol/l
$[Ca^{2+}]^i$	Initial calcium concentration	mol/l
$[Ca^{2+}]_{eq}$	Calcium concentration at equilibrium	mol/l
$[Ca^{2+}]_s$	Solubility calcium concentration	mol/l
D/d	Impeller Diameter	m
d	Normal particle size	m
Da	Daltons	-
E	Activation energy	J/mol
F	Air flux	m/h
F^*	Specific air flux (F* = F.t)	m
g	Gravity constant	m/s^2
G	G-factor	$1/s$
G^*	Specific G-factor (G.t.10^{-5})	-
ΔG	Gibs free energy	J
ΔG_{crit}	Max excess free energy	J
ΔG_v	Volume excess free energy	J
H	Dimensionless constant	-
σ	Interfacial tension	J/m
$\propto$	Ionic activity	-
IP	Product of free calcium sulphate ions	-
K_G	Overall growth coefficient	
k'	Growth rate constant	$l.mol.m^{-2}.\min^{-1}$

Symbol	Description	Unit
k_B	Boltzmann constant	$m^2 kg.s^{-2}\min^{-1}$
k_d	Diffusion mass transfer coefficient	$l.mol.m^{-2}\min^{-1}$
K_{sp}	Solubility product	-
L	Vessel diameter	M
m	Mass solute concentration	mg/l
M	Molar concentration	mol/l
n	Overall order of growth rate	-
n	Agitation speed	rpm
n	Count	-
N	Impeller speed	rev/s
N_P	Power number	-
ρ	Density	kg/m^3
P	Power	W
R	Gas constant	$J.mol^{-1}K^{-1}$
R_G	General growth rate	
r	Particle radius	mm
r	Stirrer bar radius	m
s	Standard deviation	Various
S	Supersaturation ratio	-
T	Temperature	K
V	Volume	L
v	Molecular volume	
t	Time	Min
x	Fraction of solids in the system	-
Δ	Uncertainty parameter	Various
γ	Activity coefficient	-
α	Significance level	-

Abbreviation	Description
ANOVA	Analysis of variance
AMD	Acid mine drainage
ICP-OES	Inductively Coupled Plasma Optical Emission Spectrometer
lpm	Liter per minute
MS	Mean of squares
ppm	Parts per million
RO	Reverse osmosis
RCF	Relative centrifugal forces
rpm	Revolution per minute
SEM	Scanning Electron Microscope
SS	Sum of squares
SS	Supersaturation
TDS	Total dissolved solids

Table of Contents

Chapter 1: Introduction

The supply of fresh water is becoming problematic worldwide (Smedley, 2017). One solution is the desalination of seawater. However, this process is costly due to the high energy requirements and low water recovery. The reduction of freshwater usage in the chemical industry would have a significant positive effect on the reserve of fresh water. To lessen their freshwater intake, plants have been using water treatment technology to recover and re-use water. Processes such as biological treatment, ion-exchange, adsorption, filtration and reverse osmosis (RO) are used to recover the water. It was found that intermediate crystallisation stages can be used to achieve higher levels of recovery in the case of brine streams and acid mine drainage (AMD).

Acid mine drainage contains high concentrations of sulphates, that need to be removed for the water to be re-used. This sulphate removal can be done by intermediate crystallisation. In the supersaturated state, some salts become insoluble and precipitate out of the solution. In a system that only contains pure water, calcium and sulphate ions, three different crystals can form: calcium sulphate dihydrate (gypsum) [Reaction 1.1], calcium sulphate hemihydrate [Reaction 1.2] and calcium sulphate anhydrite [Reaction 1.3]. The formation of these crystals is temperature dependent.

$$Ca^{2+}(aq) + SO_4^{2-} + 2H_2O \rightleftharpoons CaSO_4 \cdot 2H_2O\ (s) \qquad [1.1]$$

$$Ca^{2+}(aq) + SO_4^{2-} + \tfrac{1}{2}H_2O \rightleftharpoons CaSO_4 \cdot \tfrac{1}{2}H_2O\ (s) \qquad [1.2]$$

$$Ca^{2+}(aq) + SO_4^{2-} \rightleftharpoons CaSO_4\ (s) \qquad [1.3]$$

Gypsum is the most common precipitate of the solution and through the gypsum crystallisation the calcium and sulphate ions are removed from the water. The crystallisation process is typically achieved by the addition of seed crystals. Inhibitors can slow the crystallisation process even in the presence of seed crystals (Amjad, 1988).

It is however not economical to have a fresh feed of gypsum crystals to serve as seed crystals on big water treatment plants. Thus, the seed crystals and the crystals formed need to be re-used as seeding crystals. However, antiscalants and other inhibitors in the water cause for the reduction of active growth sites on seed crystal, thereby reducing their seeding efficiency. Therefore, if such seed material could be treated to increase their efficiency, they can be re-used more effectively to maximise gypsum precipitation. In the end, improving the efficiency of re-used seed material will reduce the cost of capital and operation on relevant plants.

1.1 Aim of the study and key questions

The study aims to determine the effect of various treatment methods and conditions on re-used seed crystals, considering the efficiency and rate of gypsum precipitation in the presence of antiscalants.

Key questions:

- What is the effect of re-used seed crystals on the efficiency and rate of gypsum crystallisation in the presence of antiscalants?
- Will re-used seed crystals that were physically treated affect the efficiency and rate of gypsum crystallisation in the presence of antiscalants?
- Will re-used seed crystals with chemical treatment affect the efficiency and rate of gypsum crystallisation in the presence of antiscalants?
- How does the efficiency and rate of gypsum crystallisation compare between physical and chemical treatments?

1.2 Objectives

To be able to achieve the aim of the study and answer the key questions, the following objectives were formulated:

1. Experimentally generate the desupersaturation curves for the crystallisation of gypsum from equimolar solutions of sodium sulphate and calcium chloride in the presence of seed crystals and antiscalants.
    - Study the effect of re-used seed crystals.
    - Study the effect of re-used seed crystals with various physical seed crystal treatment methods.
    - Study the effect of re-used seed crystals in the presence of various chemicals.
2. Interpret experimental data by evaluating the calcium removal and the kinetics of the gypsum crystallisation.
3. Determine the effect of re-used seed crystals on crystallisation.
4. Determine the effect of re-used seed crystals on crystallisation with various physical seed crystal treatment methods.
    - Mixing as seed crystal treatment method.
    - Air scouring as seed crystal treatment method.

5. Determine the effect of re-used seed crystals on crystallisation in the presence of various chemicals.
    - In the presence of hydrogen peroxide.
    - In the presence of aluminum as $AlCl_3$ and $Al_2(SO_4)_3$.
    - In the presence of hydrogen peroxide and aluminum.

Chapter 2: Literature review

2.1 Crystals

Crystals are formed by atoms in repeating or periodic order over larger atomic distances. The atoms will be in repetitive three-dimensional structures (lattices) and bonded to one another. The rigid lattice of atoms, ions, or molecules is one of the characteristics of the crystal. The internal structure of the crystal results in a characteristic shape, smoothness or face development. The faces that develop during crystal growth are parallel to the atomic planes of the lattice (Callister & Rethwisch, 2015).

2.1.1 Crystal symmetry

Some of the shapes found in crystals are recognised to have some symmetry and is used for crystal classification. Although some crystals have more than one type of symmetry, others might not have any. The three simple symmetries are:

- Symmetry about a point (center)
- Symmetry about a line (axis)
- Symmetry about a plane

2.1.2 Crystal systems

The different combinations of symmetry observed in crystals are grouped into seven systems which are known as:

1. Regular
2. Tetragonal
3. Orthorhombic
4. Monoclinic
5. Triclinic
6. Trigonal
7. Hexagonal

The first six of the seven systems can be described using three axes, namely x, y and z, as illustrated in Figure 2.1 (a), and the seventh system (hexagonal) uses four axes, namely x, y, z and u, as illustrated in Figure 2.1 (b).

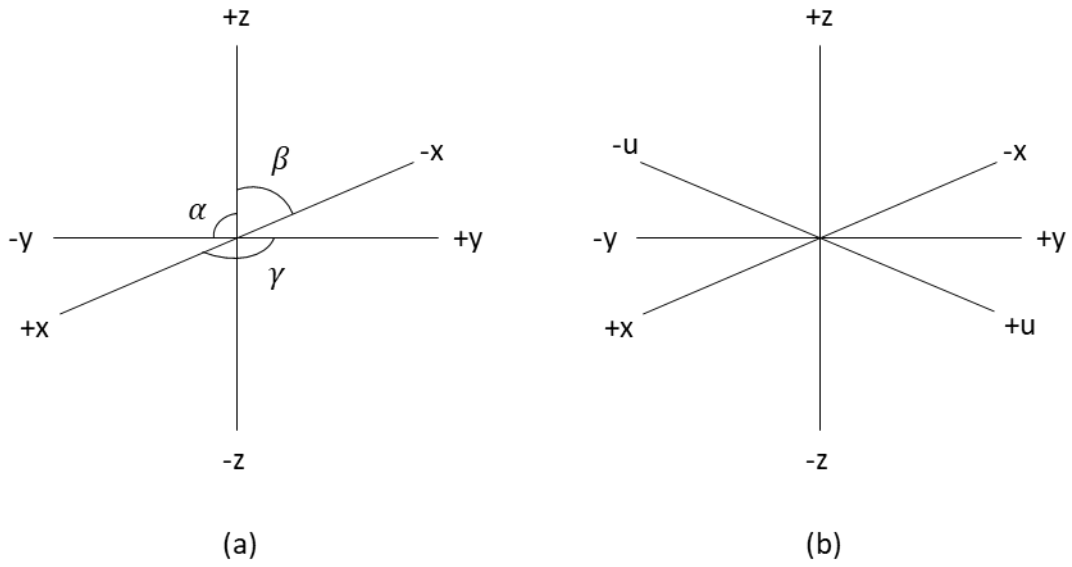

Figure 2.1: *Symmetry axis of crystals.*

For the first six systems the angle between the x and y-axis is known as γ, between the x and z-axis as β and between the y and z-axis as α. The angles between the axes and the length of the axes for the different crystal systems are summarized in Table 2.1.

Table 2.1: *Crystal systems.*

System	Other names	Angles between axes	Length of axes
Regular	Cubic Octahedral Isometric Tesseral	$\propto = \beta = \gamma = 90°$	$x = y = z$
Tetragonal	Pyramidal Quadratic	$\propto = \beta = \gamma = 90°$	$x = y \neq z$
Orthorhombic	Rhombic Prismatic Isoclinic Trimetric	$\propto = \beta = \gamma = 90°$	$x \neq y \neq z$
Monoclinic	Monosymmetric Clinorhombic	$\propto = \beta = 90° \neq \gamma$	$x \neq y \neq z$
Triclinic	Anorthic Asymmetric	$\propto \neq \beta \neq \gamma \neq 90°$	$x \neq y \neq z$

System	Other names	Angles between axes	Length of axes
Trigonal	Rhombohedral	$\propto = \beta = \gamma \neq 90°$	$x = y = z$
Hexagonal	-	z-axis is perpendicular to the x,y, and u axes, which are inclined at $60°$	$x = y = u \neq z$

2.1.3 Lattice

The lattice is based on the internal structure of the crystal and is a regular arrangement of points in three dimensions, with each point presenting a unit in the crystal, such as a molecule or atom. Since the structure is homogenous, all points in the lattice are identical to one another. It has been concluded that 14 basic types of lattice can be found. These 14 lattices can be grouped into seven groups by their symmetry, and these groups correspond with the seven different crystal systems, as specified in Section 2.1.2. The 14 different lattices are summarized in Table 2.2 with the corresponding crystal system.

Table 2.2: *Crystal lattices.*

Type of symmetry	Lattice	Crystal system
Cubic	Cube Body-centered cube Face-centered cube	Regular
Tetragonal	Square prism Body-centered square prism	Tetragonal
Orthorhombic	Rectangular prism Body-centered rectangular prism Rhombic prism Body-centered rhombic prism	Orthorhombic
Monoclinic	Monoclinic parallelepiped Clinorhombic prism	Monoclinic
Triclinic	Triclinic parallelepiped	Triclinic
Rhomboidal	Rhombohedron	Trigonal
Hexagonal	Hexagonal prism	Hexagonal

For a lattice that is not body-centered or face-centered, the points are arranged on the corners of the structure. The body-centered lattice points are arranged on the corners as well as one in the center of the structure. The face-centered lattice points are arranged on the corners of the structure as well as in the middle of each face/plane between the corners. The different lattices for the regular crystal system and cubic symmetry are illustrated in Figure 2.2.

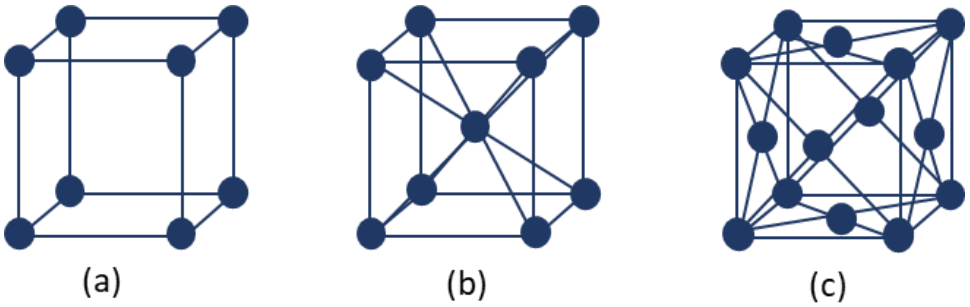

Figure 2.2: *Lattices for the regular system with cubic symmetry.*

2.2 Calcium sulphate

Calcium sulphate consists of three different crystal phases, namely anhydrite, hemihydrate and dihydrate (gypsum). Of the three crystal phases, gypsum is most likely to form at lower temperatures, and the other two crystals form at higher temperatures (Amjad, 2013). The chemical reaction takes place with the formation of gypsum:

$$Ca^{2+}(aq) + SO_4^{2-}(aq) + 2H_2O \rightleftharpoons CaSO_4 \cdot 2H_2O\ (s)$$

2.2.1 Solubility

Studies have found that the solubility of gypsum increases from 0° C to 25°C and then starts decreasing with further increase in temperature (Nancollas, et al., 1973; Power, et al., 1966; Mullin, 1972; Partridge & White, 1929; Ostroff & Metler, 1966; Bock, 1961; Power, et al., 1964). The solubility of gypsum at 25℃ is found to be approximately 0.015 mol/l. The hemihydrate was found to be unstable in the temperature range 0℃ $-$ 200℃ and the solubility of the anhydrate, similar to that of gypsum, decreased with the increase in temperature. However, the solubility of the anhydrate is more stable than that of gypsum at higher temperatures, but gypsum is more stable up until around 42℃ (Zeng & Wang, 2011).

Various studies, including Bock (1961), Power et al. (1964) and Marshall & Slusher (1966), have investigated the solubility of gypsum, in the presence of sodium chloride, and found that the solubility

increases drastically with the addition of sodium chloride up until a concentration of 3 mol/l. The solubility of gypsum increases from 0.015 mol/l up to 0.056 ml/l at 2.5 mol/l sodium chloride.

2.2.2 Thermodynamics

The driving force for gypsum formation from a supersaturation solution can be defined by using the Gibbs free energy of transfer (Amjad, 2004).

$$\Delta G = -\frac{RT}{2}\ln\left(\frac{IP}{K_{sp}}\right) \quad [2.1]$$

In equation 2.1, R is the universal gas constant of $8.314\ J/mol.K$, T the absolute temperature in K, IP the free ion activity at time t, as defined by equation 2.2 and K_{sp} the product solubility defined by equation 2.3.

$$IP = (\alpha_{Ca^{2+}})(\alpha_{SO_4^{2-}}) \quad [2.2]$$

$$K_{sp} = \gamma_{Ca^{2+}}[Ca^{2+}]_{eq} \cdot \gamma_{SO_4^{2-}}[SO_4^{2-}]_{eq} \quad [2.3]$$

In these equations α is the ionic activity of the different species (i), γ the activity coefficients of the different species (i) and $[i]$ is the equilibrium concentration of the ions in the solution after crystal growth has stopped. The equilibrium concentration ($[i]$) is a function of temperature, and thus the product solubility (K_{sp}) would also be a function of temperature.

2.2.3 Crystals

A summary of gypsum crystals, their classification, and characteristics are presented in Table 2.3. (Minerals.net, 2018; Mullin, 1972).

Table 2.3: *Gypsum crystal summary (Minerals.net, 2018; Mullin, 1972).*

	Gypsum
Colour	White
Crystal system	Monoclinic
Fracture	Uneven
Characteristics	Low hardness and flexibility

Two types of gypsum crystals are normally found, namely plate-shaped and needle (tubular crystals). These types are identified by their size, shape and surface area. The plate-shaped crystals are normally synthesized from more concentrated solutions, while the needle-shaped crystals are synthesized from less concentrated solutions. The plate-shaped crystals are shorter, more robust crystals with a size range of 25-50 µm, compared to the thinner, elongated needle crystals with a size range of 80-120 µm (Liu & Nancollas, 1970).

The presence of other chemicals can also have an effect on the shape of the gypsum crystals that can be formed. In the presence of sodium citrate, alkyl aryl and sulphonates it was found that the gypsum crystal shape changed from needle-shaped, to prism-shaped (plate-shaped) (Mullin, 1972).

2.3 Crystallisation

In order to understand crystallisation, the mechanism of crystal growth must first be understood. The crystallisation process can be classified into two phases (Mullin, 1972):

- Nucleation phase
- Crystal growth phase

The desupersaturation curve (Figure 2.3) illustrates the different phases of crystallisation.

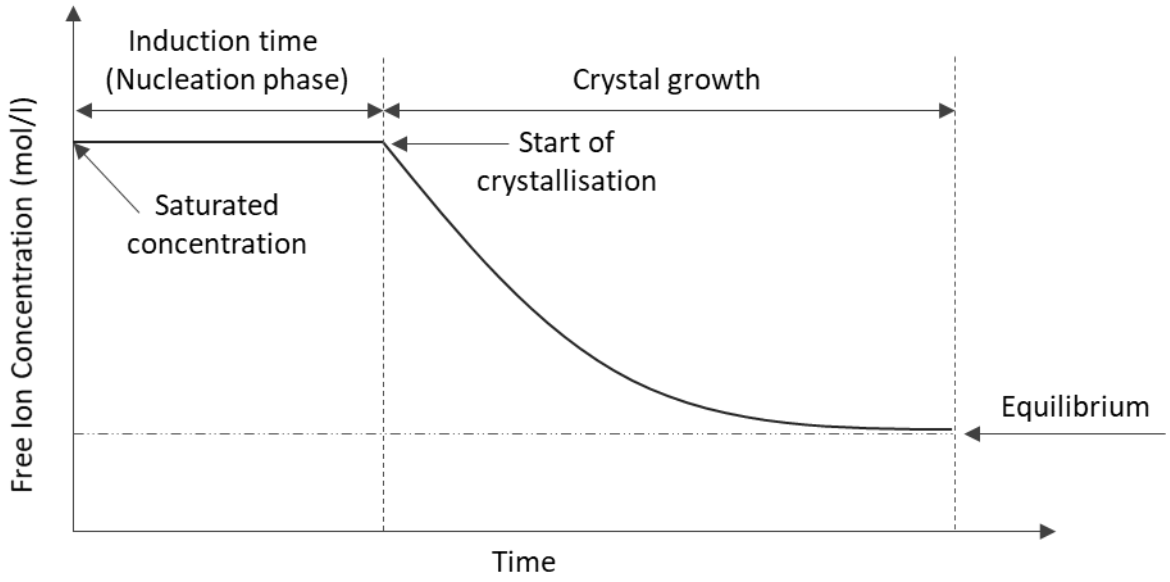

Figure 2.3: *Conceptional illustration of crystallisation desupersaturation curve (Mullin, 1972).*

The nucleation phase is expressed as the induction time, the time it takes for physical changes to appear. These changes can be in the form of an increase in turbidity (which is the presence of microscopic crystals), decrease in concentration, decrease in conductivity, or the presence of visually detectable crystals. Quantifying the induction time is difficult and is generally measured visually, but turbidity can be measured for more accuracy (Mullin, 1972). Once the concentration of the free ions of the insoluble salts starts to decrease, the nucleation phase is complete and the process has proceeded to the crystal growth phase. The growth phase will produce more prominent and visible crystals. The growth phase terminates once the system has reached equilibrium. Equilibrium is reached as soon as the free ions of the insoluble salts stabilize and remain constant.

2.3.1 Nucleation

The phenomenon of nucleation can be described as the transition from one phase (X) to another (Y). Nucleation will only take place once some Y-nucleases have formed in phase X. Once this has happened, phase Y can increase until a complete transition (Söhnel & Garside, 1992). For crystallisation to start there should be a finite amount of stable solid crystals present to start and these solids can only be present in the supersaturated state. This means that the salt ions should be above their solubility limit (Mullin, 1972).

The different mechanisms of nucleation are illustrated in Figure 2.4. Nucleation can either happen spontaneously or it can be artificially induced, classified as primary and secondary nucleation. Primary nucleation can then be further divided into homogeneous and heterogeneous nucleation. Homogeneous nucleation is the formation of nuclei over some time without any additions and the process is entirely spontaneous. This type of nucleation is very difficult to achieve. Heterogeneous nucleation, on the other hand, also forms nuclei over some time, but with the help of added foreign crystals or particles (Mullin, 1972). Secondary nucleation takes place in the presence of crystals of the same substance, known as seeding crystals. With the addition of the seed crystals, active growth sites are provided, which can reduce or eliminate the induction period since no new nuclei need to be formed to serve as growth sites (Mullin, 1972).

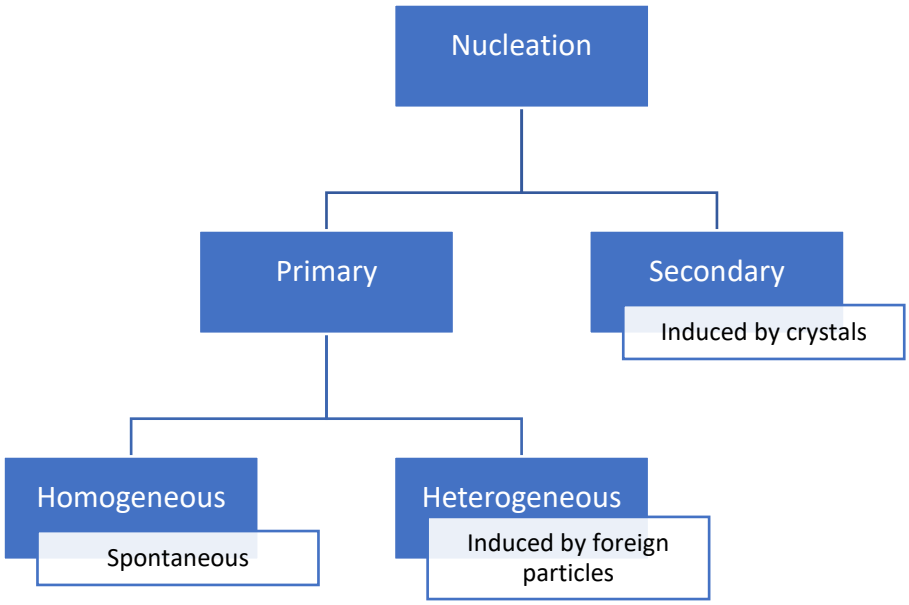

Figure 2.4: *Mechanisms of nucleation (Mullin, 1972).*

The homogeneous primary nucleation rate (B_0) can be presented using the Arrhenius reaction rate that is generally used for thermally activated processes. (Mullin, 1972; Seader, et al., 2011)

$$B_0 = A \exp\left(\frac{-\Delta G}{k_B T}\right) \quad [2.4]$$

In equation 2.4, A is the frequency factor, ΔG the total excess free energy, k_B the Boltzmann constant and T is the temperature in Kelvin. The volume excess free energy (ΔG_v) is given as equation 2.5 and the maximum value (ΔG_{crit}) required for a new crystalline structure to form is given as equation 2.6.

$$-\Delta G_v = \frac{2\sigma}{r} = \frac{ln(S)Tk_B}{v} \quad [2.5]$$

$$-\Delta G_{crit} = \frac{16\pi\sigma^3}{3(\Delta G_v)^2} \quad [2.6]$$

In these equations, σ is the interfacial tension, r the particle radius, v the molecular volume and S is the saturation ratio expressed using the Gibbs-Thomson relationship for solid-liquid systems as equation 2.7. The saturation ratio is discussed in detail in section 3.2.

$$\ln\left(\frac{c}{c^*}\right) = \ln(S) = \frac{2\sigma v}{k_B T r} \quad [2.7]$$

To describe the nucleation rate of crystallisation, equation 2.6 is substituted into equation 2.5 and then equation 2.5 is substituted into equation 2.4 and simplified to equation 2.8.

$$B_o = A \exp\left(\frac{16\pi\sigma^3 v^2}{3k_B^3 T^3 (ln(S))^2}\right) \quad [2.8]$$

From equation 2.8 it is clear that the nucleation rate is controlled by the level of saturation, temperature, interfacial tension, and the molecular volume.

2.3.2 Growth

Once the nucleation phase is complete, the crystals grow until equilibrium is reached. The crystal growth is based on equilibrium at the crystal-solution interface and is defined in the form of equation 2.9.

$$\frac{dm}{dt} = k_c A_c (c - c_s) \quad [2.9]$$

In equation 2.9, $\frac{dm}{dt}$ is the rate at which mass is deposited on the surface of the crystal, k_c the mass transfer coefficient, A_c the surface area of the crystal, c the solute concentration in the supersaturated solution and c_s the solute concentration at saturation (Seader, et al., 2011). The measurement of interfacial concentration is not always possible and is very difficult (Mullin, 1972). To avoid this, the more measurable solution concentration is used to formulate an expression for crystal growth rate

(Mullin, 1972). In equation 2.10, cis the solute concentration in the bulk solution and c^* the equilibrium solute concentration.

$$\frac{dm}{dt} = k_c A_c (c - c^*) \quad [2.10]$$

The crystal growth can be divided into two steps. Thus, the crystal growth rate as defined by equation 2.9 can be broken up into two steps as well (Schram, et al., 2016).

$$\frac{dm}{dt} = k_d A_c (c_b - c_I) \quad \text{(Mass transfer)} \quad [2.11]$$

$$\frac{dm}{dt} = k_r A_c (c_I - c^*)^r \quad \text{(Integration)} \quad [2.12]$$

In these equations k_d is the mass transfer rate coefficient, c_I the concentration at the solid-liquid interface, k_r the integration rate coefficient and r the integration rate order. When $k_d < k_r$ the mass transfer is slower than the integration and the process is mass transfer controlled. When $k_r < k_d$ the integration process is slower; thus, the process is integration controlled. When the process is integration controlled $c_I \approx c_b$ and equation 2.12 can be adjusted (Schram, et al., 2016).

$$\frac{dm}{dt} = k_r A_c (c_b - c^*)^r \quad [2.13]$$

These equations are not generally applied because of the difficulty of the measurements. A general equation based on the overall driving force can be written and used (Mullin, 1972).

$$R_G = \frac{1}{A_c} . \frac{dm}{dt} = K_G (c_b - c^*)^n \quad [2.14]$$

$$K_G = \frac{k_d k_r}{k_d + k_r} \quad [2.15]$$

In equation 2.14, R_G is the general growth rate, K_G the overall growth coefficient defined by equation 2.15 and n the order of the growth process. Most inorganic salts that crystallise from aqueous solutions have a growth rate order between 1.5 to 2 (Mullin, 1972). Previous studies, including Lui & Nancollas (1970), Smith & Sweett (1971) and Klima & Nancollas (1987), have shown that crystallisation reactions follow a second-order rate equation and, more specifically, the crystal growth rate based on calcium concentration was determined to be second-order as well.

2.4 Factors influencing crystallization

Multiple factors influence the crystallisation process. The factors that have some of the largest influences are listed below (Nyvlt, 1971; Mullin, 1972; Bock, 2017):

- Level of supersaturation

- Seed crystals
- pH
- Agitation
- Temperature
- Ionic strength
- Impurities

2.4.1 Level of supersaturation

From equation 2.8 it can be seen that the nucleation rate of crystallisation is a function of the saturation ratio of the solution. Thus, the higher the level of supersaturation, the faster the crystallisation will take place. The level of supersaturation is defined by the supersaturation ratio. The supersaturation ratio (S) is mostly defined by the relation between the solution concentration (c) and the equilibrium concentration (c^*) at specific ionic strength and temperature (Mullin, 1972).

$$S = \frac{c}{c^*} \qquad [2.16]$$

For soluble electrolytes in aqueous media, the supersaturation ratio can be defined by the following relation (Mullin, 1972):

$$S = \left(\frac{IP}{K_a}\right)^{\frac{l}{v}} \qquad [2.17]$$

Where IP is the free ion activity at time t (discussed in more detail in section 2.4.2), K_a the activity solubility product of the salt and v is the amount of moles of ion per one mole of salt.

Various studies, including Sohnel & Garside (1981), Lancia et al. (1999) and Abdel-Aal et al. (2004), have shown that a higher level of supersaturation increased the level of crystallisation. When no seed crystals were added, it was found that higher levels of supersaturation reduced the induction time with spontaneous crystallisation. The level of supersaturation is one of the main factors that influence spontaneous crystallisation.

2.4.2 Seed crystals

It is known that the addition of seed crystals to the system can completely override the need for a nucleation period, since an activated surface for crystallisation is made available. Elimination of the nucleation period by addition of seed crystals would then have a significant impact on the crystallisation rate of the system.

Experimental work done in previous studies, including those of Amjad & Hooley (1986) and Amjad (1988), found that for the crystallisation of gypsum, with seeding ranging from 1820 mg/l to 3730 mg/l, the nucleation period is completely eliminated. It was also found that the growth rate constant, thus, the growth rate, increased as the amount of seed crystals increased (Table 2.4). Experiments containing seed crystals were also found to be more repeatable than experiments based on spontaneous crystallisation since the growth sites were already provided.

Table 2.4: *The effect of seeding on the induction time and growth rate constant in gypsum crystallisation.*

Temperature (°C)	Seed (mg/l)	Induction time (min)	Growth rate constant ($l.mol^{-1}.min^{-1}$)	Reference
25	1970	0	5.89	(Amjad, 1988)
25	2000	0	6.35	
25	3200	0	9.55	
35	1820	0	5.8	(Amjad & Hooley, 1986)
35	1990	0	6.4	
35	3730	0	12	

However, the study by Amjad (1988) determined that by adding seed crystals the nucleation was not always completely eliminated. It was found that in the presence of additives, such as polymers, the addition of seed crystals only shortened the nucleation period (Table 2.5). As the seed crystals increased, the induction period decreased, showing that when more seed crystals are used, faster crystallisation will occur.

Table 2.5: *The effect of seeding on the induction time in gypsum crystallisation in the presence of polymers (Amjad, 1988).*

Polymer	Dosage (ppm)	Temp. (°C)	Seed (mg/l)	Induction time (min)
Poly(acrylic acid)	0.25	35	1970	43
Poly(acrylic acid)	0.25	35	1980	21
Poly(acrylic acid)	0.25	35	2000	5

The crystal growth is, however, size and shape-dependent and therefore the size and shape of the seed crystals added will also influence the rate of crystallisation. The size of the seed crystals might be insignificant for macro-crystals, but the size of the crystals does matter when working with crystals of microscopic or sub-microscopic size. The effect of particle size is more prominent when crystals smaller than a few microns are used. Smaller crystals and crystals that are near-nucleic size grow at a prolonged rate (Mullin, 1972).

Studies done by Liu & Nancollas (1970), Lui & Nancollas (1973) and Lewis & Nathoo (2006) found that plate-shaped crystals cause higher growth rates when added to supersaturated solutions than when needle (tubular) shaped crystals were added. It was proposed that the increase in the growth rates is a result of the increase in surface area with the plate-shaped crystals, compared to that of the needle (tubular) shaped crystals (Table 2.6).

Table 2.6: *Effect of morphology on gypsum crystallisation.*

Morphology	Seed dosage (mg/l)	$[Ca^{2+}]$ (mol/l)	k' ($l.mol^{-1}.min^{-1}$)	Reference
Plates	880	0.0458	1.37	(Liu & Nancollas, 1973)
Plates	880	0.0464	1.37	(Liu & Nancillas, 1970)
Plates	980	0.0468	1.52	(Liu & Nancillas, 1970)
Plates	1890	0.0442	2.97	(Liu & Nancollas, 1973)
Plates	1890	0.0442	2.97	(Liu & Nancillas, 1970)
Needles	2520	0.0390	1.43	(Liu & Nancillas, 1970)
Needles	2780	0.0438	1.55	(Liu & Nancillas, 1970)
Needles	2780	0.0438	1.66	(Liu & Nancillas, 1970)
Needles	3030	0.0460	1.80	(Liu & Nancollas, 1973)
Needles	2870	0.0330	1.97	(Liu & Nancillas, 1970)

2.4.3 pH

It has been observed that pH affects the crystallisation of certain salts in the presence of polyelectrolytes containing carboxylic and phenolic functional groups (Amjad, 1988). By changing the pH of a system, the neutrality of the substances is affected. A positively charged particle can become negatively charged, and the same the other way around (Amjad, 1988).

A study by Amjad (1988) found that pH had no significant impact on the crystal growth rate of gypsum in the absence of additives or inhibitors (Table 2.7). The induction period does not change with the change in pH and the change in the growth rate constant is so minimal that it can be ignored.

Table 2.7: *The effect of pH on the induction time and growth rate constant in gypsum crystallisation in the absence of additives and inhibitors (Amjad, 1988).*

Temperature (°C)	Seed (mg/l)	pH	Induction time (min)	Growth rate constant x 10 ($l.mol^{-1}min^{-1}$)
25	2000	2.5	0	5.55
25	1990	3.5	0	5.83
25	2010	4.5	0	5.95
25	2000	5.5	0	5.65
25	2000	6.5	0	6.35
25	2020	7	0	5.75

Temperature (°C)	Seed (mg/l)	pH	Induction time (min)	Growth rate constant x 10 (l.mol^{-1}min^{-1})
25	2000	8	0	6.32
25	1980	9	0	5.85

However, Amjad (1988) found that in the presence of an inhibitor, such as a polymer, a change in pH has an impact on the induction time of crystallisation. As the pH increased the induction time increased as well (Table 2.8). This shows that the induction period increased as the pH increased, leading to faster spontaneous crystallisation at lower pH conditions.

Table 2.8: *The effect of pH on the induction time in gypsum crystallisation in the presence of additives (Amjad, 1988).*

Polymer	Dosage(ppm)	Temperature (°C)	Seed (mg/l)	pH	Induction period (min)
Poly(acrylic acid)	0.25	25	2000	2.5	0
Poly(acrylic acid)	0.25	25	2000	7	125
Poly(acrylic acid)	0.25	25	1990	8	245
Poly(acrylic acid)	0.25	25	1970	9	290

2.4.4 Agitation

Agitation is used to keep the crystals in suspension and also to promote interphase mass transfer between particles by means of turbulence. This turbulence can either increase or decrease the rate of crystallisation. The energy introduced to the system by mixing is absorbed by the collision of particles, which leads to crystallisation. Slow mixing is preferred for the generation of crystals since collisions increase the crystallisation rate. However, if vigorous mixing occurs, the collisions are too strong and break the desired crystals down.

Determination of the mixing rate for optimum crystallisation is very difficult. The widely used relationship by Zwietering (1985) below determines the minimum impeller speed (N) for optimal particle suspension (Mullin, 1972).

$$N = H\left[v^{0.1}d^{0.2}x^{0.13}D^{-0.85}\left(\frac{g\Delta\rho}{\rho_s}\right)^{0.45}\right] \qquad [2.18]$$

In equation 2.18, N is the impeller speed in rev/s ,v the kinematic viscosity of the liquid in m^2/s, d the normal particle size in m, x the fraction of solids in the system, D the impeller diameter in m, g the gravitational acceleration constant in m/s^2, ρ the liquid density and ρ_s the solid density. H is defined by equation 2.19.

$$H = \left(\frac{L}{D}\right)^a \qquad [2.19]$$

In equation 2.19, $a = 0.82$ for propeller agitators and $a = 1.3$ for radial flow impellers and L is the vessel diameter in meter (Mullin, 1972).

From the above relations it is clear that the speed and size of the stirrer, as well as the shape and dimensions of the vessel, need to be considered for crystallisation systems.

The mixing rate (rev/s) can further be quantified by either Relative Centrifugal Force (RCF) or G-factors. The RCF is calculated based on the speed and size of the magnetic stirrer bar (Equation 2.20) and is measured in times g (9.81 m/s^2) (BCF, 2015).

$$RCF = RPM^2 \times 1.118 \times 10^{-5} \times r \quad [2.20]$$

Where the radius (r) of the magnetic stirrer bar that was used for the treatment was measured in meters.

Further the G-factor (s^{-1}) is determined based on the power per unit volume, as well as the viscosity of the liquid (Equation 2.21) (Oldshue, 1983; Nagata, 1975).

$$G = \sqrt{\frac{P}{V\mu}} \quad [2.21]$$

Where G is the G-factor measured in s^{-1}, V is the volume of the liquid that is mixed and μ the viscosity of the liquid. The impeller power (P) was calculated based on the power number, the liquid density, the magnetic stirrer dimensions as well as the speed (Equation 2.22) (CerCell, 2019).

$$P = N_P \times \rho \times n^3 \times d^5 \quad [2.22]$$

Where N_P is the power number of the stirrer used, ρ the density of the slurry in kg/m^3, n the agitation speed in revolutions/second and d the impeller diameter in meters.

According to Degremont (2007), a G-factor in the range 0 – 100 s^{-1} is refered to as slow mixing, a G-factor in the range 100 – 400 s^{-1} is refered to as medium and a G-factor above 500 s^{-1} as rapid mixing.

2.4.5 Temperature

Temperature does not only affect solubility but also affects crystallisation. The effect of temperature on crystallisation, more specifically the crystal growth rate constant (k), is described by the Arrhenius equation (Mullin, 1972).

$$k = A \exp\left(\frac{-E}{RT}\right) \quad [2.23]$$

In equation 2.23, A is the frequency factor, E the activation energy of the reaction, R the universal gas constant and T the temperature in K. By taking the log of equation 2.23, equation 2.24 is obtained. This equation describes the growth rate constant as a function of temperature (Mullin, 1972).

$$\ln(k) = \ln(A) - \frac{E}{RT} \qquad [2.24]$$

The effect of temperature has been investigated (Table 2.9) by several studies, including those by Liu & Nancollas (1975), Amjad & Hooley (1986) and Amjad (1987), and these studies found that the growth rate increases significantly with an increase in temperature. A temperature difference of 10°C was shown to have a drastic impact on the crystal growth rate.

Table 2.9: *The effect of temperature on the induction time and growth rate constant in gypsum crystallisation.*

Temperature (°C)	Seeding (mg/l)	Induction period (min)	Growth rate constant (l/mol.min)	Reference
25	1930	0	0.255	(Liu & Nancollas, 1975)
35	1930	0	0.552	
45	1930	0	1.17	
55	1930	0	2.34	
25	2000	0	0.575	(Amjad, 1988)
35	1990	0	1.25	
50	1970	0	1.61	
25	1980	0	0.295	(Amjad & Hooley, 1986)
35	1990	0	0.61	
45	1990	0	1.23	

Mullin (1972) found that the crystal growth rate becomes diffusion controlled at higher temperatures compared to integration controlled at lower temperatures. However, both these processes can have an effect on the crystallisation over a wide temperature range. The Arrhenius plot of crystal growth data is a non-linear curve, which indicates that for the overall growth the activation energy is dependent on temperature.

2.4.6 Ionic strength

It was found that the solubility of the crystallite has a significant impact on crystal growth (Ahmed, et al., 2014). With an increase in the solubility of the crystallite, which is based on ionic strength, the driving force $(c - c^*)$ will decrease and thus the nucleation rate will decrease.

Hamdona et al. (1993) as well as Hamdona & Al Hadad (2007) found that the presence of low concentrations of metal ions in the solution can have a negative influence on gypsum crystallisation by reducing the rate of gypsum crystallisation up to 70%. The effect of the cations increases as their

concentration increases (Table 2.10). The decrease in the rate of gypsum crystallisation is due to the cations that adsorb onto the crystal surface, reducing the number of active growth sites. In controversy with these findings, Rashad et al. (2004) showed that at some concentrations of aluminum (Al^{3+}) an increase in gypsum precipitation kinetics can be observed (Table 2.10).

Table 2.10: *Effect of cations on gypsum crystallisation.*

Additive	Concentration	Effect on growth rate	% growth inhibition	Reference
Mg^{2+}	0-3%	(-)	n/a	(Rashad, et al., 2004)
	1-12x10^{-6} M	(-)	3-38% inhibition	(Hamdona & Al Hadad, 2007)
	5-50x10^{-5} M	(-)	17-65% inhibition	(Hamdona, et al., 1993)
Al^{3+}	0-2%	(+)	n/a	(Rashad, et al., 2004)
	3%	(-)	n/a	(Rashad, et al., 2004)
Cr^{3+}	1-12x10^{-6} M	(-)	16-51% inhibition	(Hamdona & Al Hadad, 2007)
Fe^{3+}	1-12x10^{-6} M	(-)	27-64% inhibition	(Hamdona & Al Hadad, 2007)
	20-50x10^{-5} M	(-)	8-18% inhibition	(Hamdona, et al., 1993
Cu^{2+}	1-12x10^{-6} M	(-)	34-70% inhibition	(Hamdona & Al Hadad, 2007)
Cd^{2+}	1-12x10^{-6} M	(-)	34-70% inhibition	(Hamdona & Al Hadad, 2007)
	5-50x10^{-5} M	(-)	12-55% inhibition	(Hamdona, et al., 1993

In other studies by Witkamp et al. (1990) and Brandse & van Rosmalen (1977), an increase in crystal growth was found with the addition of background ions, such as Na^+, Cl^- and NO_3^-. This was due to the change in solubility with the increase in ionic strength. It was suggested that the background ions influenced the surface charge of the crystals and, by doing so, prompted the transfer of ions onto the surface. Thus, crystallisation can be influenced by a change in ionic strength, but it varies from system to system.

2.4.7 Impurities

Impurities and additives in the system can have an extreme effect on crystal growth. Several studies, including Amjad & Hooley (1986), Amjad (1988) and Amjad (2004), have shown that it has a significant impact on the crystallisation of certain salts.

The most common additive considered was polyelectrolytes. It was shown to be a very effective inhibitor of crystal growth due to its nature, molecular weight and ionic charge. It contains functional groups like carboxylic acid, sulfonic acid, esters and phenolic groups.

A study by Amjad (2004) showed that an increase in polyelectrolyte concentration resulted in a decrease in the amount (in mass) of gypsum deposited, which indicates a decrease in crystallisation (Table 2.11). The most inhibiting polyelectrolyte was found to be polyacrylic acid (P-AA), inhibiting

almost all gypsum precipitation at a calcium and sulphate concentration of 0.0345M and a P-AA concentration of 1 ppm.

Table 2.11: *The effect of polyelectrolyte on gypsum crystallisation at 35°C with equimolar calcium and sulphate of 3.45 x 10^{-2} mol/l (Amjad, 2004).*

Polyelectrolyte	Polyelectrolyte concentration (ppm)	Mass of gypsum deposited (g)
None	0	1.57
	0	1.62
Tannic Acid	1.0	1.31
	2.5	0.94
	5.0	0.77
	15.0	0.44
Fulvic Acid	1.0	1.20
	2.5	0.85
	5.0	0.67
Poly-A	0.075	1.02
P-AA	0.10	0.86
	0.25	0.48
	0.50	0.20
	1.0	0.05
P-AA:SA	0.20	0.79
P-AA:SA:SS	0.20	0.88

This shows that impurities and additives affect crystal growth.

2.5 Antiscalant

When it comes to gypsum precipitation inhibition, there are a lot of different compounds, including natural products, that cause some level of gypsum inhibition. Some compounds can even cause total inhibition. These compounds include proteins, organic acids, polyelectrolytes, phosphates, metal ions and synthetically produced antiscalants.

Antiscalant is a synthetic organic polymer that was developed to slow down the kinetics of precipitation. It was initially intended for use in the pretreatment process in RO systems but was found to be useful in other processes as well. The function of antiscalants is to prolong the kinetics of precipitation to the extent that no unwanted precipitations form during the duration of the process. However, the precipitation will ultimately still occur if the solution stays supersaturated. The required amount of antiscalant is typically determined by the level of supersaturation. Antiscalant can be classified as either phosphonate based or acrylic acid-based. The acrylic acid-based antiscalant can also be blended with phosphonates (Lawler, et al., 2010).

Antiscalant interferes with the precipitation reaction in three main ways (Kucera, 2015):

- Threshold inhibition
- Crystal modification
- Dispersion

Threshold inhibition is when the antiscalant affects both the formation and the growth of the nucleation sites in the nucleation phase, thus reducing precipitation at the start. However, by preventing the crystals from growing during the nucleation phase, the antiscalant force more nucleation sites to be formed than would have been formed if no antiscalant was present. By forming more of these nucleation sites, the concentration of ions in the solution decreases, resulting in a decrease in supersaturation. This then leads to a lower concentration gradient in the solution. The lower gradient slows the rate of diffusion, which leads to slower crystallisation according to Fick's law (Lawler, et al., 2010). Therefore, threshold inhibition allows supersaturated solutions to be kept in supersaturation without precipitating soluble salts (Kucera, 2015).

The antiscalant can also modify the crystals. The antiscalant has the ability to distort the crystal shapes and this results in a soft non-adherent scale. During the nucleation phase the negative groups in the antiscalant molecule target the positive charges of the nuclei that were formed during the nucleation phase. This attack interrupts the electronic balance that is needed to allow crystal growth. When this occurs the soft scale that is formed is distorted and less compact than the crystals that would form in the absence of antiscalants (Kucera, 2015).

Some antiscalants can adsorb on the crystal. This leaves the active growth site that was available on the crystal occupied. The antiscalant that did adsorb on the crystal imparts a high anionic charge that also keeps the crystals separate, reducing crystal growth. This behaviour is classified as dispersion (Kucera, 2015).

2.6 Degrading of antiscalant

The presence of antiscalant during water treatment has many advantages, like preventing membrane scaling. However, when the wastewater leaves the system, the slow precipitation kinetics go from being an advantage to a problem since it slows the salt recovery process. Thus, the antiscalant needs to be degraded in order to allow precipitation to take place, which makes salt recovery possible. A study by Rahardianto, et al. (2007) showed a 95-98% recovery through alkaline pH adjustment. Furthermore, a study by Rosenburg, et al. (2012) proved that, in the presence of antiscalant, the nucleation phase as well as the crystal growth phase accelerated with a decrease in pH. These studies by Rahardianto, et al. (2007) and Rosenburg, et al. (2012) showed that the efficiency of the antiscalant

is a function of the pH. It can therefore be said that when the pH is lowered, the efficiency of the antiscalant decreases, thus degrading the antiscalant.

It was also found that antiscalants could be degraded by an advanced oxidation process (AOP). The AOP accomplishes high levels of oxidation by using highly reactive hydroxyl radicals (-OH) to drive the oxidation reaction (Andreozzi, et al., 1999). When AOP is applied to antiscalants, it removes the phosphates from the antiscalant molecules, and thus degrades the antiscalant, leaving it ineffective (Frost, et al., 1987). A study by Yang, et al. (2004) showed that the electro-Fenton process, which produces hydroxyl radicals through the reaction between hydrogen peroxide and Fe^{2+}, fully degrades the antiscalant and thus renders it useless.

Recent studies are looking at peroxone treatment, the combination of ozonation and hydrogen peroxide, to produce more hydroxyl radicals (Lawler, et al., 2010). The instability of the ozone in water is accelerated by the presence of the hydrogen peroxide and this instability increases the rate of the hydroxyl radical formation (von Gunten, 2003).

A study by Shih et al. (2006) found that aluminum at concentrations as low as 100 µg/l could reduce the efficiency of antiscalant by up to 20%. In some cases total inhibition of the antiscalant was observed. It is proposed that the aluminum ions in the solution compete with the calcium ions to preferentially bind with the antiscalant, subsequently preventing the adsorption of the antiscalant onto the crystal surface (Shih, et al., 2006).

2.7 Coagulation and flocculation

The coagulation-flocculation process is used to separate suspended solids from water by means of sedimentation. These suspended solids vary in particle shape, size, source, density and charge. Suspended solids in water have a negative charge and repel one another when they get close. This makes it impossible for the solids to increase in size in order to settle out and be removed, thus keeping the solids in suspension. Coagulation and flocculation make it possible for the suspended solids to form flocs that are larger in size in order to be able to settle out and be removed from the solution. However, coagulation and flocculation occur in successive steps. If coagulation is unsuccessful, flocculation will also be unsuccessful. Chemicals such as aluminum sulphate, aluminum chloride, sodium aluminate, ferric sulphate, ferrous sulfate, ferric chloride, hydrated lime and magnesium carbonate are regularly used as coagulation and flocculation chemicals. The flocs formed during coagulation and flocculation help with crystallisation since the larger flocs allow for better contact between the molecules, which is beneficial for crystal growth (Bratby, 2016; Degremont, 2007).

2.7.1 Coagulation

The aluminum and iron based coagulants can form multi-charged polynuclear complexes with adsorption characteristics. These multi-charged polynuclear complexes have an opposite charge to that of the suspended solids and, when added to the water, neutralise the negative charges in the solids. This change in charge allows the small suspended particles to stick together, forming microflocs. These microflocs are however not visible to the eye (Bratby, 2016; Degremont, 2007).

Factors influencing coagulation include temperature, chemical addition sequence, residual and rapid mixing. Temperature significantly affects the coagulation process, since the temperature shifts the optimum pH. The chemical addition sequence is usually first a pH adjustment chemical, then the metal coagulant and lastly the flocculant aid. However, there are systems where other sequences were found to be more effective. Rapid mixing allows the coagulant to have more effective destabilisation, since the most important destabilisation occurs within the first second the chemical is added and rapid mixing facilitates mixing of the chemical with the solution during this short time frame (Bratby, 2016; Degremont, 2007).

2.7.2 Flocculation

The microflocs formed during the coagulation process increase from submicroscopic size into visible particles during the flocculation process. The increase in the floc size is due to the microflocs colliding with one another due to an induced velocity gradient. The collisions cause the microflocs to bond and produce the larger flocs. The size of the flocs will increase as the collisions continue until an optimum size is reached and then the water is ready for sedimentation (Bratby, 2016; Degremont, 2007).

The two main factors that influence flocculation are the velocity gradient and the time of flocculation. If the velocity gradient increases or the process continues for longer, more collisions will occur leading to an increase in the particle size. There are numerous ways to increase the velocity gradient, namely baffled chambers or diffused air and mixing. There is, however, also a maximum velocity gradient to prevent the flocs from tearing apart. The velocity gradient usually is tapered with the increase in the particle size to prevent the flocs from tearing (Bratby, 2016).

2.8 Re-use and treatment of seed crystals

A study done by Tait et al. (2009) found that crystals can become compromised by impurities in the wastewater, which render the crystals ineffective and thus unfit for re-use as seed crystals. Some experimental work done by Tait et al. (2009) investigated the use of the crystal product as seed crystals instead of using new synthetic seed crystals. They found no significant difference in the crystal growth rates when the crystals were re-used as seed crystals in wastewater treatment (Tait, et al., 2009).

Another study by Rautenbach & Habbe (1991) investigated the treatment of seed crystals using air bubble injection. This treatment was done to clean a stack of seeding material in a "zero-discharge" process that was adapted for electrodialysis. However, it was found to be insufficient due to the distribution of the air. It was found that when using air bubble injection as a treatment method, it is crucial to have an even distribution of the air (Rautenbach & Habbe, 1991).

In the presence of antiscalant, the antiscalant adsorb onto the crystal (Kucera, 2015) to reduce crystal growth. It is expected that crystal treatment such as mixing and air scouring would cause attrition between the crystals and that the attrition would remove the antiscalant adsorbed onto the crystal. Thus, removing the antiscalant from the growth sites should restore the growth sites to be active for crystal growth once again.

From the studies into the degrading of antiscalant by Shih, et al. (2006) as well as Lawler, et al. (2010) it was found that the antiscalant can be degraded or inhibited by adding chemicals. If the antiscalant can be degraded or inhibited to avoid them adsorbing onto the crystals, the seeding efficiency of the crystals could possibly be maintained, so that they can be re-used effectively.

No other studies could be found that investigated the re-use of gypsum crystals as seed crystals or the treatment of the seed crystals.

2.9 Statistics

2.9.1 Uncertainty

Uncertainty is defined as the difference between observed or measured values and the true or specified value.

2.9.1.1 Uncertainty parameter

The uncertainty parameter can only be calculated for data points obtained from experimental work and gives a range containing the actual value. To do this calculation, the number of data points obtained should be less than 30. If there are more than 30 data points, an alternative approach and equations should be used (Hughes & Hase, 2010). The uncertainty parameter is primarily calculated by using the Excel statistic functions shown in Table 2.12.

Table 2.12: *Uncertainty parameter calculation.*

	Abbreviation	Excel function
Number of cells	n	count
Average	$\bar{x}$	average
Standard dev	s	stdev
Standard error	sn	s/sqrt(n)
Significance level	α	0.05

	Abbreviation	Excel function
Student's t-statistics	t(α, n-1)	t.inv.2t(α, n-1)
Uncertainty parameter	Δ_x	t(α, n-1)*sn

2.9.1.2 Uncertainty propagation

Uncertainty propagation is defined as the effect of a variable uncertainty on a function, where equation 2.25 shows the function y dependent on multiple variables (Hughes & Hase, 2010).

$$y = f(x_1, \dots, x_m) \quad [2.25]$$

The uncertainty parameter can then be defined as a function of the derivative y and the uncertainty parameter of the variables in function y (Equation 2.26) (Hughes & Hase, 2010).

$$\Delta_y = \sqrt{\left(\sum_{i=1}^{m} \left(\frac{\partial f}{\partial x_i}\right) \Delta_{xi}\right)^2} \quad [2.26]$$

2.10 Literature summary

Crystallisation plays a very important role in the water treatment industry. Over the last few years the crystallisation of gypsum was the topic of various studies, but crystallisation is such an extensive field of study that there are still some areas that have not been investigated.

There are seven main factors that significantly influence crystallisation, namely supersaturation, pH, agitation, temperature, ionic strength, impurities and seed crystals. Concerning these factors, literature indicates the following:

- The level of supersaturation increases the level of crystallisation in the absence of seed crystals. Higher levels of supersaturation reduce the induction time.
- In the absence of additives and inhibitors, pH has no significant impact on gypsum crystallisation. However, in the presence of inhibitors it was found that faster spontaneous crystallisation occurs at a lower pH.
- Slow mixing is preferred to generate crystals since the collisions increase the crystallisation rate. With vigorous mixing the collisions are too strong and break down the crystals, slowing down the crystallisation rate.
- The crystal growth rate increases significantly with an increase in temperature. Even a change such as 10°C has a drastic impact on crystallisation.
- The presence of metal ions, such as Mg^{2+}, Fe^{3+}, Cu^{2+} and Cd^{2+}, was found to inhibit crystal growth, but low concentrations of Al^{3+} was found to increase gypsum crystallisation.
- In experiments where impurities were present, it was found that the crystal growth rate decreased as the concentration of the impurities increased.

- Seeding is used to eliminate the nucleation phase, and thus increase crystallisation by providing active growth sites. The concentration, shape and size of the seed crystals have an influence on the effectivity of the seed crystals.
    - The crystal growth rate increases as the concentration of seed crystals increases, since more active growth sites are introduced into the system.
    - It was found that gypsum crystals that are plate-shaped delivered higher growth rates than crystals that are needle/tubular shaped.
    - Smaller crystals and crystals that are near nuclear size grow at a prolonged rate compared to bigger crystals.

One of the biggest problems with crystallisation as the water recovery process is the presence of antiscalants in the waste water, which inhibits the precipitation of gypsum and other salts. The antiscalant either affects the formation of crystals, modifies the crystals or is adsorbed onto the crystal, which reduces the number of active growth sites to prevent crystallisation. One method to overcome this problem is to make use of seed crystals. In industry it is expensive to use fresh seed crystals every time. Therefore, the crystals are recycled as seed crystals. However, due to the antiscalant that adsorbed onto the crystals, the efficiency of the seed crystals decreases with every re-use cycle. Very few studies have looked at the re-use of seed crystals and few, if any, looked at the treatment of the seed crystals or the conditions of re-use.

From the literature study, the following parameters were found for this investigation (Table 2.13).

Table 2.13: *Parameters for investigation.*

	Parameter
Seed crystals	2000 mg/l
pH	Uncontrolled
Temperature	25°C
Impurities	9 ppm antiscalant (3 ppm per level of saturation)
Slow mixing	G-factor of 0 -100 s^{-1}
Medium mixing	G-factor of 100 - 400 s^{-1}
Rapid mixing	G-factor above 500 s^{-1}
Aluminum concentration	0 - 2%
Hydrogen peroxide concentration	10 mg per mg of antiscalant

Chapter 3: Materials, methods and design

The materials, the methodology followed including the experimental setup and procedure, the analysis, data processing, uncertainty, experimental conditions, experimental design and the accuracy of the experiments are discussed in this chapter.

3.1 Materials

The chemicals used for the study with their purity and suppliers are detailed in Table 3.1.

Table 3.1: *Chemicals used in the study.*

Chemical	Purity	Supplier
Calcium chloride dihydrate	$\geq 99.0\%$	Sigma Aldrich
Sodium sulphate anhydrous	$\geq 99.0\%$	Sigma Aldrich
Flocon 260	-	FMC Corporation
Hydrogen peroxide	30%	KIMIX
Aluminum chloride	98%	Sigma Aldrich
Aluminum sulphate	$\geq 99.0\%$	KIMIX

3.2 Theoretical experimental conditions

3.2.1 Conditions and constraints

The following experimental conditions were used for experiments as determined and used by Gerber (2011) and Bock (2017): a constant temperature of 25˚C, unadjusted pH, a constant initial calcium and sulphate concentration above saturation, a constant amount of antiscalant (9 ppm, 3 ppm per level of saturation), and a constant amount of seed crystals ($\pm$ 2000 ppm).

All analysis was done with a sample that had been filtered through a 0.22 µm filter, which is normally used as a standard in water analysis. Thus, all the results are based on a 0.22 µm particle removal.

3.2.2 Saturation

The saturation concentration of pure gypsum was determined using PHREEQC® (Version 3.3.3) software that is freely available. PHREEQC® was designed to perform a range of low-temperature, aqueous, geochemical calculations. The program is based on an ion-association aqueous model and has the capability for speciation and saturation-index calculations as well as batch reaction and one-dimensional transport calculations involving reversible reactions and irreversible reactions (Parkhurst & Appelo, 1999).

The saturation concentration was determined by the saturated concentration of pure calcium sulphate, which was modelled using calcium and sulphate ions in pure water at a temperature and pH of 25°C and 7, respectively. The saturation index of gypsum was set to 0 to determine the saturation concentration. This was done using multiple different databases (Table 3.2) available on PHREEQC.

Table 3.2: *PHREEQC databases.*

Database in PHREEQC	Description
Wateq4f	Bases on the WATEQ4F database. Suited for the analysis of large amounts of water.
PHREEQC	Similar to *wateq4f.dat* but contain a smaller set of aqueous species and elements.
Pitzer	Suited for specific ion interaction, derived from the database of the PHRQPITZ program.
Amm	Similar to *phreeqc.dat* but the ammonia redox state has been altered.
Minteq / Minteq.v4	The database derived from the databases of the Minteq / MinteqV4 program.

The different saturation concentrations as calculated by PHREEQC utilizing the different databases is shown in (Table 3.3).

Table 3.3: *Saturation concentration of gypsum by different PHREEQC databases at 25°C and equimolar calcium and sulphate.*

Database in PHREEQC	Saturation concentration $CaSO_4$ (mol/L)
Wateq4f	0.01565
PHREEQC	0.01508
Pitzer	0.01505
Amm	0.01508
Minteq	0.01498
Minteq.v4	0.01597

The saturation concentration of gypsum as determined by the different databases was found to be different. Therefore, literature was used to determine the most accurate saturation concentration, as listed in Table 3.4.

Table 3.4: *Saturation concentration of gypsum at 25°C from literature.*

	Saturation concentration $CaSO_4$ (mol/L)	Reference
1	0.01520	(Bock, 1961)
2	0.01510	(Marshall & Slusher, 1966)
3	0.01540	(Power, et al., 1964)

On comparing the different literature values (Table 3.4) and the values obtained by simulation (Table 3.3), it was found that the PHREEQC and Amm databases have the same value and correspond well with the literature value of Marshall and Slusher (1966). Thus, a $CaSO_4$ saturation concentration of 0.01508 mol/L at 25°C was used in the calculations for this project.

3.2.3 Supersaturation ratio

A solution that is at thermodynamic equilibrium at a given temperature is a saturated solution, and a solution containing a higher concentration of the dissolved solute than the equilibrium saturation value is said to be super-saturated. The super-saturation ratio (Equation 3.1), developed from equation 2.13 as used by Bock (2017) for solutions of equimolar calcium and sulphate, is defined as the following relationship:

$$S = \frac{[Ca^{2+}]_i}{[Ca^{2+}]_s} \qquad [3.1]$$

where S is the supersaturation ratio and $[Ca^{2+}]_i$ is the concentration of free calcium ions in the solution. $[Ca^{2+}]_s$ is the saturation concentration of calcium with respect to the saturation of calcium sulphate, and in this case at *equimolar* calcium and sulphate concentrations. The saturation concentration of calcium sulphate (calculated with PHREEQC® in this case) also depends on the temperature and the ionic strength of the solution (reflected by the total dissolved solids, TDS, in solution). Therefore, the super-saturation factor (1, 2 and 3, in this case) is affected by the ionic strength of the solution, and therefore refers to the saturation level *at a specific ionic strength*.

The following chemical reactions were used to perform a species balance to determine the species concentration in the feed solution to the reactors as well as the working solution in the reactors for the saturated, 2 x saturated and 3 x saturated solutions (Table 3.5):

$$CaSO_4(aq) \rightleftharpoons Ca^{2+}(aq) + SO_4^{2-}(aq)$$

$$CaCl_2 \cdot xH_2O \rightleftharpoons Ca^{2+}(aq) + 2Cl^{-}(aq) + xH_2O$$

$$Na_2SO_4(aq) \rightleftharpoons 2Na^{+}(aq) + SO_4^{2-}(aq)$$

Table 3.5: *Concentration in the feed solution to the reactors and the working solution in the reactors for the saturated, 2 x saturated and 3 x saturated solutions as calculated by Phreeqc.*

		Feed solution		Working solution	
Chemical	Molar Mass (g/mol)	$C \times 10^3$ (mol/L)	C (mg/l)	$C \times 10^3$ (mol/L)	C (mg/l)
Saturation (SS1)					
Na_2SO_4	142.04	30.2	4283.9	15.1	2142.0
$CaCl_2.2H_2O$	147.02	30.2	4434.1	15.1	2217.1
Theoretical species and water concentration @ Saturation (SS1)					
Ca^{2+}	40.078	30.2	1208.7	15.1	604.4
Cl^-	35.453	60.3	2138.5	30.2	1069.3
H_2O	18.015	60.3	1086.7	30.2	543.3
Na^+	22.99	60.3	1386.8	30.2	693.4
SO_4^{2-}	96.06	30.2	2897.2	15.1	1448.6
2 x Saturation (SS2)					
Na_2SO_4	142.04	76.14	10814.9	38.07	5407.5
$CaCl_2.2H_2O$	147.02	76.14	11194.1	38.07	5597.1
Theoretical species and water concentration @ 2 x Saturation (SS2)					
Ca^{2+}	40.078	76.14	3051.5	38.07	1525.8
Cl^-	35.453	152.28	5398.8	76.14	2699.4
H_2O	18.015	152.28	2743.3	76.14	1371.7
Na^+	22.99	152.28	3500.9	76.14	1750.5
SO_4^{2-}	96.06	76.14	7314.0	38.07	3657.0
3 x Saturation (SS3)					
Na_2SO_4	142.04	96.3	13671.4	48.1	6835.7
$CaCl_2.2H_2O$	147.02	96.3	14150.7	48.1	7075.3
Theoretical species and water concentration @ 3 x Saturation (SS3)					
Ca^{2+}	40.078	96.3	3847.5	48.1	1928.8
Cl^-	35.453	192.5	6824.7	96.3	3412.4
H_2O	18.015	192.5	3467.9	96.3	1733.9
Na^+	22.99	192.5	4425.6	96.3	2212.8
SO_4^{2-}	96.06	96.3	9245.8	48.1	4622.9

3.3 Methodology

The study followed a five-step experimental approach for the physical treatment experiments as listed below. Upon completion of the experimental procedure, steps two to five were repeated twice for a total of three experimental crystallisation runs, as illustrated in Figure 3.1.

1. Seed crystal generation
2. Liquid removal
3. Seed crystal treatment
4. Seed crystal introduction
5. Crystallisation with seed crystals

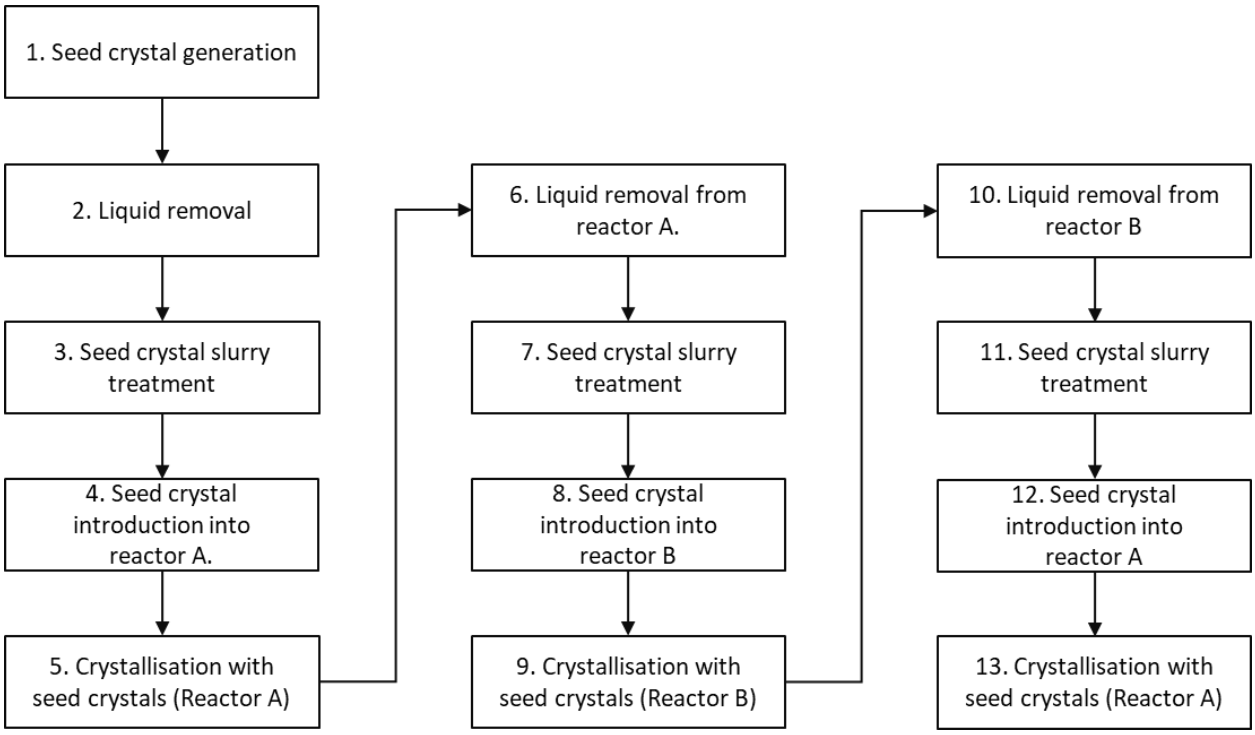

Figure 3.1: *Block flow diagram of the experimental path followed for the physical treatment experiments.*

A five-step approach was also followed for the chemical dosing experiments as listed below. Upon completion of the experimental procedure, steps two to five were repeated twice for a total of three experimental crystallisation runs, as illustrated in Figure 3.2.

1. Seed crystal generation
2. Liquid removal
3. Seed crystal introduction
4. Crystallisation with seed crystals
5. Chemical dosing

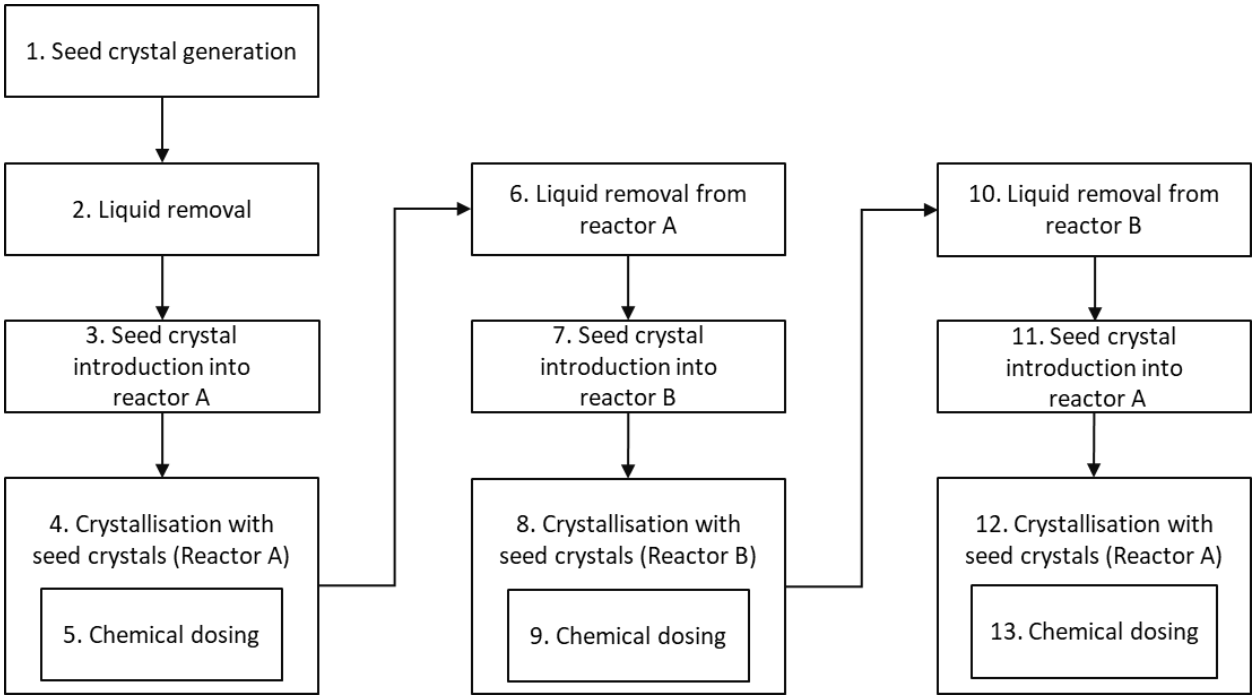

Figure 3.2: *Block flow diagram of the experimental path followed for the chemical dosing experiments.*

3.3.1 Experimental setup

The various experimental setups for the experimental stages are detailed and discussed in this section.

3.3.1.1 Crystal preparation and seed crystal generation

Both the crystal preparation and seed crystal generation processes were performed using a DLAB MS-H280-Pro magnetic stirrer plate at a constant stirrer speed (rpm) with a 50mm x 8mm magnetic stirrer bar. A 2L A-grade glass beaker was used for crystal production and preparation, while a 1L A-grade glass beaker was used for the seed crystal generation. A schematic of this setup is illustrated in Figure 3.3.

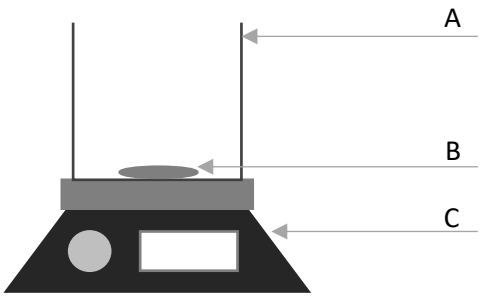

Figure 3.3: *Experimental setup for crystal preparation and seed crystal generation. A) 1L/2L A-grade glass beaker; B) Magnetic stirrer bar; C) DLAB MS-H280-Pro magnetic stirrer plate.*

3.3.1.2 Liquid removal

The liquid removal setup (Figure 3.4) consisted of a PVC pipe with a fixed-length going into the reactor (or beaker). This pipe was connected to a SEKO dosing pump that transported the liquid at a constant flow rate into a waste container for disposal. Thus, a constant volume of 120 ml gypsum crystals slurry was left in the reactor or beaker.

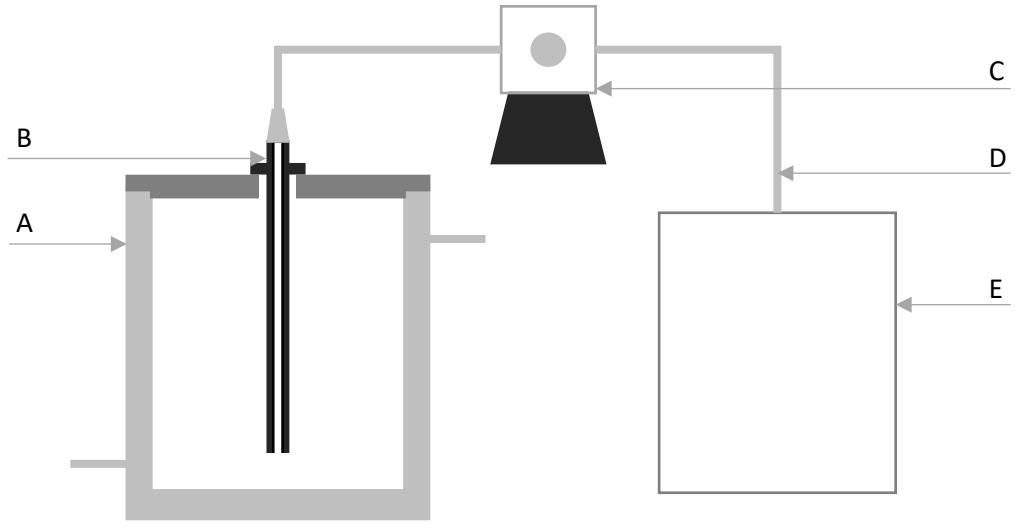

Figure 3.4: *Experimental setup for liquid removal. A) Reactor (1.8L); B) PVC pipe; C) SEKO dosing pump; D) Piping; E) Waste container.*

3.3.1.3 Seed crystal treatment

Different experimental setups were used for the mixing and air treatment systems and these will be detailed in this section. The physical treatment was performed on the 120 ml of seed crystal slurry that remained after the liquid removal.

3.3.1.3.1 Mixing

All the mixing treatments were performed in a 250 ml A-grade glass beaker using a 30 mm x 6 mm magnetic stirrer bar, a DLAB MS-H280-Pro magnetic stirrer plate and a stopwatch to time the duration of the treatment. This mixing setup was arranged as shown in Figure 3.5.

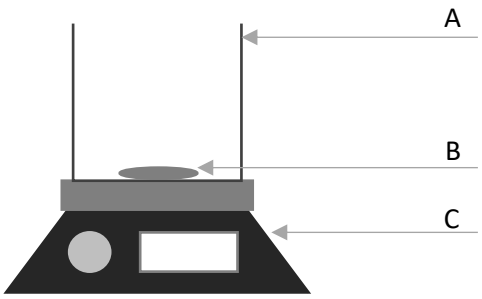

Figure 3.5: *Experimental setup for mixing as seed crystal treatment. A) 250 ml A-grade glass beaker; B) Magnetic stirrer bar; C) DLAB MS-H280-Pro magnetic stirrer plate.*

3.3.1.3.2 Air treatment

The air treatment setup discussed below as well as a stopwatch to time the duration of the treatment was used for all the air treatment experiments.

The air treatment setup (Figure 3.6) was built to sparge air through a liquid mixture (120 ml) in a 250 ml A-grade glass beaker. The air used in the treatment was obtained from the Stellenbosch Mechanical Engineering Department and contained some impurities such as oils and water. Thus, the air was firstly sent through a 30 cm cylindrical filter filled with activated carbon, to adsorb the organic contaminants. After that, the air was filtered through an STNC air filter to ensure that all remaining contaminants were removed. Once the air was considered clean, it went through a needle valve to ensure a constant pressure at the end of the line in the case of small pressure fluctuations. The pressure in the line was measured using a WIKA pressure gauge. Two gas flow meters calibrated at STP (AQUA 0.5-5 lpm and NBGF 5-50 lpm) were used to make sure the correct flow rate of air was sparged through the solution.

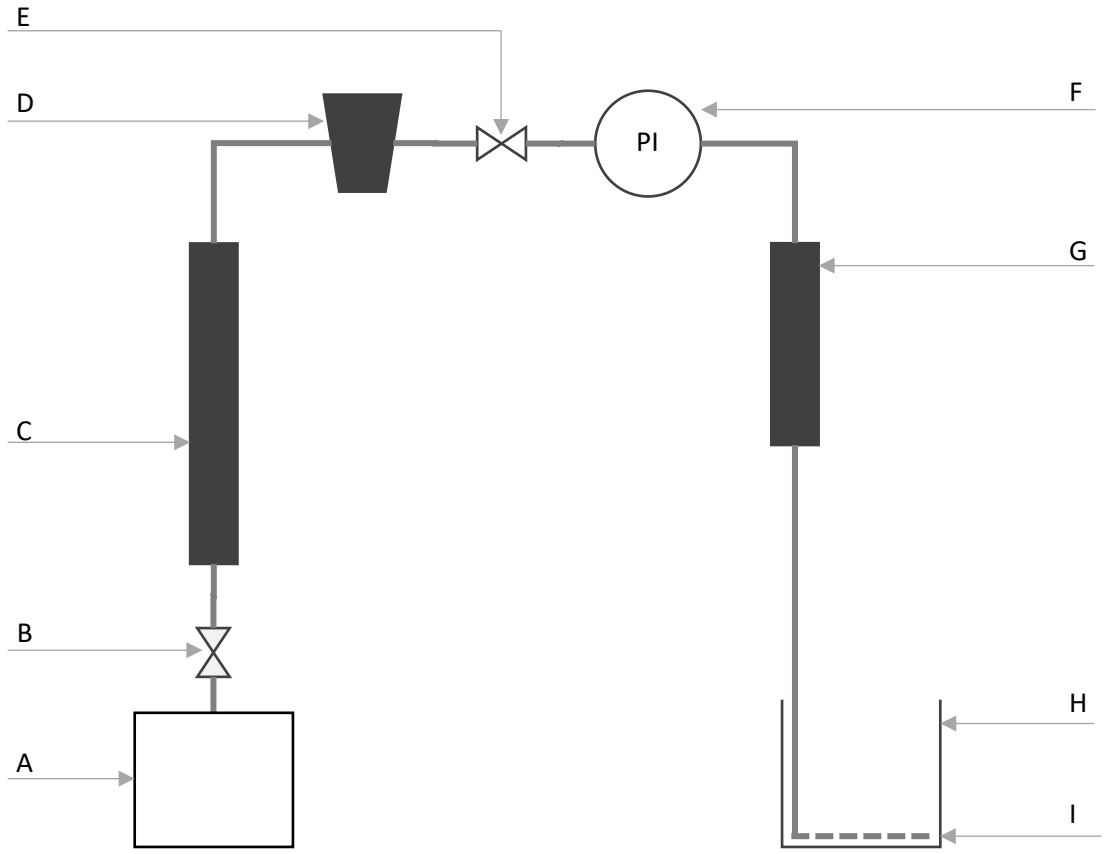

Figure 3.6: *Experimental setup for air scouring as seed crystal treatment.*

Table 3.6: *Legend for Figure 3.6.*

Tag	Component
A	Compressed air supply
B	Inlet control valve
C	Activated carbon filter
D	STNC air filter
E	Needle valve
F	WIKA pressure gauge
G	Air flow meters (AQUA 0.5-5 lpm and NBGF 5-50 lpm)
H	250 ml A-grade glass beaker
I	Air sparger

The circular sparger (Figure 3.7) with an outer diameter of 60 mm was constructed to fit into the 250 ml glass beaker, and was used to sparge the air through the seed crystal slurry. It was constructed from 5 mm piping that is typically used for irrigation. Ten 1.3 mm holes were drilled through the pipe,

resulting in holes at the top as well as at the bottom of the sparger. The holes at the bottom were to ensure that the crystals did not settle underneath the sparger at lower air flow rates.

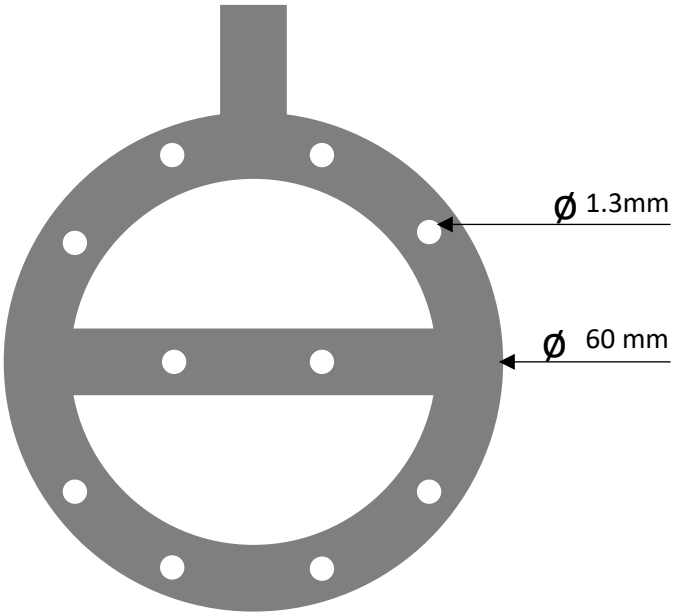

Figure 3.7: *Air sparger used during air scouring as seed crystal treatment.*

3.3.1.4 Crystallisation with seed crystals

The crystallisation with seed crystals was done in a reactor with an approximate volume of 1.8 L (inside diameter of 120 mm and a height of 160 mm) constructed from A-grade glass with a heating jacket constructed from PVC. The temperature in the reactor was controlled by circulating heating fluid through the heating jacket. Water was used as a heating fluid and was kept in a water bath at a constant temperature with an accuracy of ± 0.1˚C using a Delta® temperature controller. The temperature and pH inside the reactor were measured using a ThermoScientific pH and temperature meter. A DragonLab OS40-Pro overhead stirrer, using a four bladed Teflon impeller with a diameter of 60 mm, was used to agitate the mixture in the reactor at a constant stirring rate. The reactor was covered by a PVC lid with four holes allowing entrance for the temperature probe, pH probe, overhead stirrer, and one hole for sampling purposes. A schematic of the complete experimental crystallisation setup is shown in Figure 3.8.

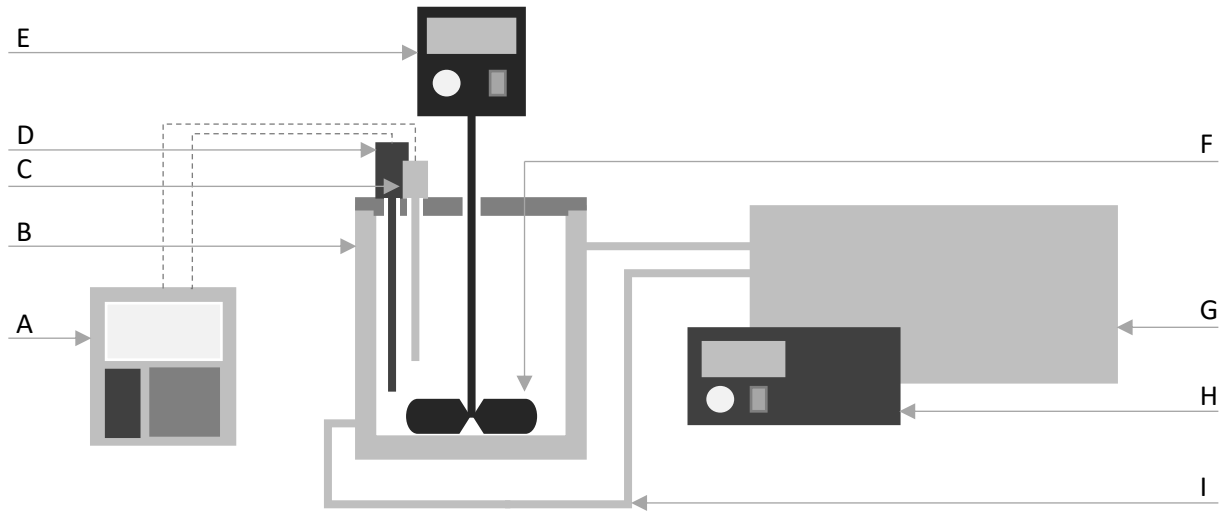

Figure 3.8: *Experimental setup for seeded gypsum crystallisation.*

Table 3.7: *Legend for Figure 3.8.*

Tag	Component
A	ThermoScientific pH and temperature meter
B	Reactor (1.8 L)
C	Temperature probe
D	pH probe
E	DragonLab OS40-Pro overhead stirrer
F	Four bladed Teflon impeller
G	Heating bath
H	Heating bath temperature controller
I	Heating fluid pipes

Two crystallisation reactors (Figure 3.9) were constructed for the experiments and designed similarly to the reactors used by Bock (2017). The reactor volume was increased to 1.8 L to ensure that enough gypsum crystals, needed for use as seed crystals in the following experiment, were formed during the experimental procedure. The dimensions of the reactor were determined by the availability of the glass pipe sizes.

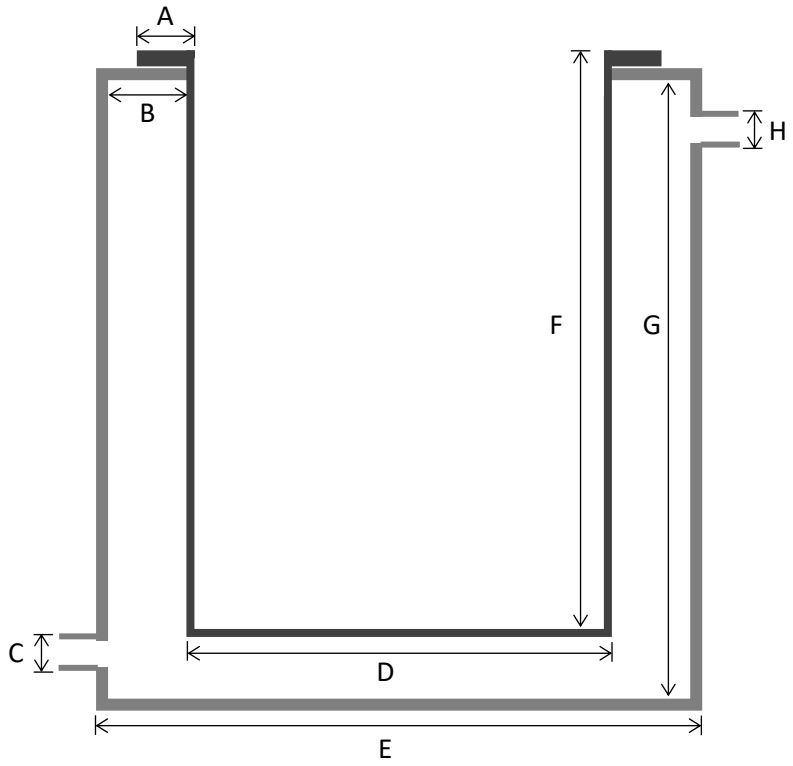

Figure 3.9: *Reactor vessel used in the experimental setup*

Table 3.8: *Legend for Figure 3.9.*

Tag	Component	Dimensions (mm)
A	Reactor flange	15
B	Heating jacket flange	10
C	Heating fluid inlet	6
D	Reactor diameter	120
E	Heating jacket diameter	150
F	Reactor height	160
G	Heating jacket height	180
H	Heating fluid outlet	6

Both the new reactors were validated by repeating an experimental run done by Bock (2017). As illustrated in Figure 3.10, the desupersaturation curve generated from the new reactor has a similar trend to the desupersaturation curve generated by Bock using the smaller reactors.

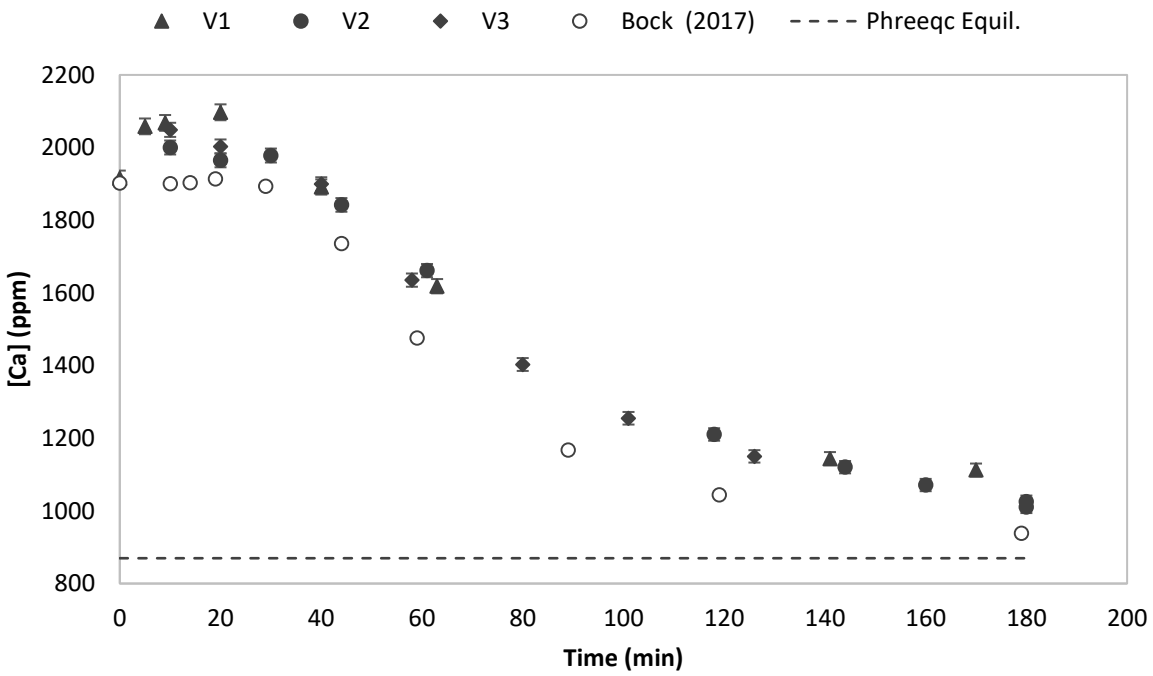

Figure 3.10: *Verification (V) of gypsum crystallisation experiment against experimental results generated by Bock (2017).*

The desupersaturation curves generated by the two new reactors were also compared to one another to ensure that the experiments were repeatable regardless of which reactor was used (Figure 3.11). Two experiments were done using reactor 1, generating two desupersaturation curves, Reactor1 and Reactor1', where Reactor1' was simply a repeat of Reactor1. The data show the same trend, although the values differ. This is due to the variation of the initial calcium concentration.

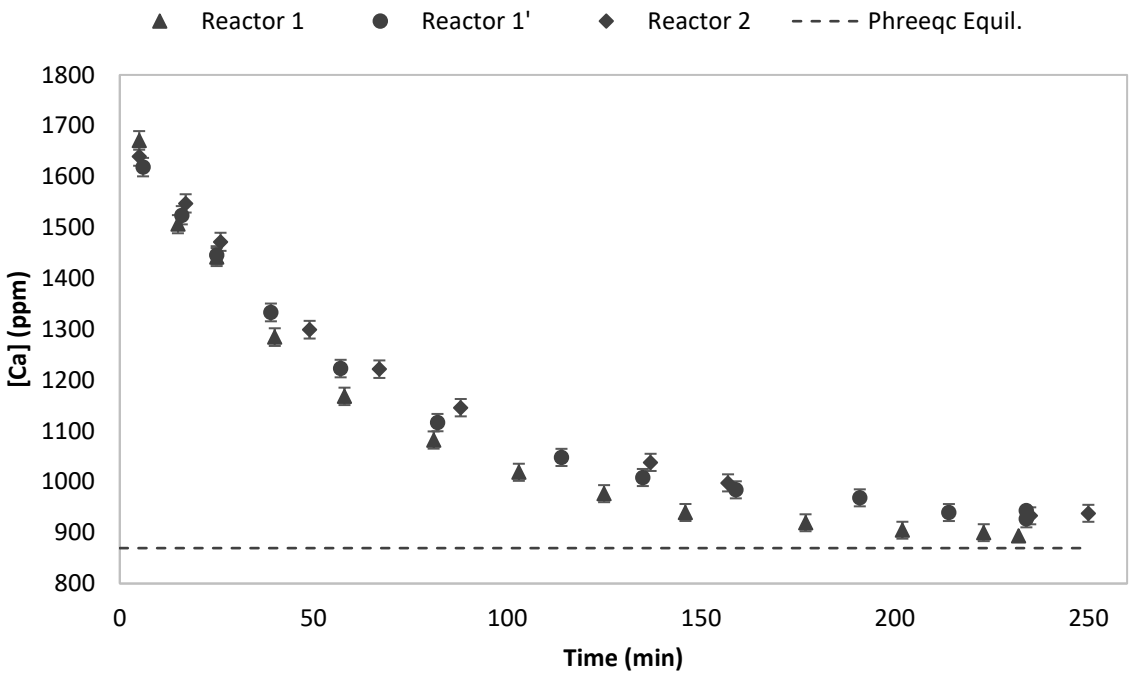

Figure 3.11: *Experimental results of SS3 in the presence of 2000 ppm (dry base) seed crystals to compare the results obtained from two different reactors.*

3.3.2 Experimental procedure

The five-step experimental approach is detailed in this section; full experimental protocols are provided in Appendix A.

3.3.2.1 Solution and fresh crystal preparation

Bulk solutions of 10 L each of the 0.09 molar sodium sulphate and 0.09 molar calcium chloride were prepared using RO water, sodium sulphate anhydrous and calcium chloride dihydrate. The RO water that was used to dissolve the sodium sulphate, was heated by placing the glass beaker containing the RO water into a bigger beaker containing boiling water. This was done since heat is needed for the sodium sulphate to dissolve in water.

Pure gypsum crystals were generated to use as seed crystals for the first seed crystal generation. These crystals were generated by spontaneous crystallisation by adding 1 L of 0.09 molar sodium sulphate solution and 1 L of 0.09 molar calcium chloride solution into a 2 L glass beaker and leaving it stirring overnight at 188 s^{-1} using a magnetic stirrer.

3.3.2.2 Seed crystal generation

The first gypsum seed crystals were prepared by mixing 500 ml of 0.09 molar sodium sulphate solution, 500 ml of 0.09 molar calcium chloride solution and the desired amount (9 ppm) of antiscalant in a 1 L

glass beaker. Two grams of pure gypsum crystals were mixed with 10 ml of RO-water to make a slurry and added to the mixture as seed crystals. The mixture was then stirred at 400 rpm using the magnetic stirrer. This was done the day prior to the experimental run and left overnight to be used as seed crystals the next day.

The water bath was set to heat up overnight to the desired temperature so that experiments could commence first thing the next day.

3.3.2.3 Liquid removal

The stirrer was switched off, and the crystals were left to settle for 3 minutes. This was the time it took to visually see a volume of settled crystals with a clear solution above it. The heating jacket of the reactor was drained during this settling time. After the crystals had settled, the liquid above the crystals was removed using the pump, and the remaining solution (120 ml) was transferred into a 250 ml glass beaker.

3.3.2.4 Physical seed crystal treatment

Two physical treatment methods were performed in different experiments. The treatment was only performed on the seed-crystal mixture obtained from the crystallisation experiment.

Mixing treatment: The seed crystal mixture was mixed using the magnetic stirrer at various mixing speeds and for various durations.

Air treatment: Air was sparged through the seed crystal mixture by placing the sparger at the bottom of the 250 ml glass beaker. The air was sparged through the solution at various air flow rates for various durations.

When the treatment was completed, 50 ml of the crystal slurry was extracted using a 60 ml syringe and weighed. This mass was recorded to ensure that a constant amount of crystals were used during the different experiments. These crystals were used as seed crystals in the next experiment. If no physical treatment was performed on the crystals, they were extracted directly from the 250 ml glass beaker using the syringe and weighed after the liquid was removed. The accuracy of this method was tested and is discussed in section 3.5.2.

In some cases, after the 50 ml of the solution had been extracted, the remaining crystals were filtered using a Bügner-filter and sampled for analysis.

3.3.2.5 Chemical dosing

In the case of chemical dosing, the chemical was added into the reactor during the crystallisation experiment in the reactor. Various concentrations of hydrogen peroxide or aluminum were added directly to the reactor two and a half minutes into the experimental run. It was added at two and a half minutes into the experiment to alow time get the chemicals ready as well as insuring a consistent dosing time.

3.3.2.6 Crystallisation with seed crystals

During the liquid removal time and the time allowed for the crystals to settle, the reactor jacket was connected to the water bath and filled. Using a measuring cylinder, 500 ml of both 0.09 molar sodium sulphate solution and 0.09 molar calcium chloride solution were measured for the experimental run. These concentrations were verified with ICP analysis and are discussed in section 3.5.

As soon as the seed crystals were ready, 500 ml of the sodium sulphate solution was added into the reactor, followed by the desired amount of antiscalant (9 ppm) using a micropipette. The 50 ml seed crystals in the syringe were added to the reactor together with 500 ml of calcium chloride solution. The overhead stirrer was set to 180 rpm and was started as well as a timer. The pH and temperature probes were submerged into the reactor to stabilize in time for the first sample.

Centrifugal tubes (36 x 15 ml) were prepared and labelled for the dilution of samples for analysis by filling the tubes with 7.5 ml of RO-water using a micropipette.

In the case of chemical dosing, the desired amount of hydrogen peroxide or aluminum was added two and a half minutes after the start of the experiment using a micropipette.

At 5 minutes, a 2.5 ml sample was taken from the reactor using a micropipette and was discharged into a 5 ml syringe. The sample was then filtered into a 4 ml glass vial using a 0.22 µm syringe filter. From that sample, 400 µL was taken with a micropipette and added to a prepared centrifugal tube containing 7.5 ml of RO-water. The time of the sample, temperature and pH were recorded. This sampling procedure was repeated at 15, 25, 40, 55, 70, 90, 110, 130 and 150 minutes respectively. Duplicate samples were taken at 55 minutes as well as at 150 minutes.

Upon completion of the crystallisation experiment, the stirrer was switched off, and the temperature probe as well as the pH probe were removed. This procedure and those of sections 3.2.2.3 and 3.2.2.4 were repeated twice more so that a total of three experimental crystallisation runs were completed.

3.3.2.7 Cleaning

All the glassware was rinsed five times with RO-water immediately after use to ensure that they were clean and dry in time for the next experimental run. The glassware was not washed or dried with any material to prevent scratches on the glass that could affect the crystallisation.

3.3.3 Analysis

The diluted samples taken during the experimental process were analysed using the Thermo-Fisher ICAP 6000 Series Inductively Coupled Plasma Optical Emission Spectrometer (ICP-OES) to determine the calcium and, in some cases, aluminum concentrations in the samples.

Some dried seed crystals were also physically analysed using a Zeiss MERLIN Scanning Electron Microscope (SEM).

The crystal size of the dried seed crystals was determined using a Saturn DigiSizer 5200 V1.12 Micromeritics® Particle size analyser.

The results were statistically analysed using the data package in Excel. These analyses included analysis of variance (ANOVA) and T-test analysis.

3.3.4 Data processing

Once the samples had been analysed, the data obtained from the ICP-OES were processed to calculate various values to be able to discuss the results.

First, the concentration values obtained from the ICP-OES had to be converted to the actual concentrations of the samples, since the samples had been diluted for ICP analysis. This was done by using the dilution equation (Equation 3.2).

$$c_{Ca} 2V_{sample} = c_{ICP} V_{diluted} \quad [3.2]$$

$$c_{Ca} = c_{ICP}\left(1 + \frac{V_{RO}}{2V_{sample}}\right) \quad [3.3]$$

$$V_{diluted} = V_{RO} + V_{sample} \quad [3.4]$$

Where c_{Ca} in ppm is the actual concentration of the sample that was taken from the reactor, V_{sample} is the volume of the sample taken from the reactor that was used in the dilution (2 x 0.2 ml = 0.4 ml), c_{ICP} is the concentration measured by the ICP-OES in ppm, and V_{RO} is the volume of RO water in the dilution (7.5 ml).

Now that the actual concentrations of the samples were known, the percentage calcium that had been removed by means of precipitation during the experimental run could be calculated (Equation 3.5).

$$\%\, Ca_{removed} = \left(1 - \frac{C_{Ca-final}}{C_{Ca-initial}}\right) 100 \qquad [3.5]$$

Where $Ca_{removed}$ is the percentage calcium removed during the experimental run, $c_{Ca-initial}$ is the calcium concentration at the beginning of the experiment, and $c_{Ca-final}$ is the calcium concentration after the experiment was completed.

The calcium removal was calculated for three of the experiments in the experimental run, and then the average calcium removal between the three experiments was calculated (Equation 3.6).

$$\%Ca_{Average} = \frac{\%Ca_{removed,1} + \%Ca_{removed,2} + \%Ca_{removed,3}}{3} \qquad [3.6]$$

Where $Ca_{Average}$ is the average calcium removal between the three experiments in the experimental run and $Ca_{removed,n}$ is the percentage calcium removed from the different experiments as calculated above using equation 3.5.

Lastly, the growth rate constant was calculated for each experiment. This was calculated by a second-order rate equation from literature on gypsum crystallisation (Liu & Nancollas, 1970; Smith & Sweett, 1971).

$$-\frac{d[Ca^{2+}]}{dt} = k'\left([Ca^{2+}] - [Ca^{2+}]_{eq}\right)^2 \qquad [3.7]$$

Where k' is the growth rate constant in L/mol.min. From the units of the growth rate constant, it can be seen that the calcium concentrations should be in mol/L. The integration of equation 3.7 gives equation 3.8, which gives the growth rate constant as a function of the final and initial calcium concentrations as well as the equilibrium concentration of calcium.

$$k' = \left(\frac{1}{C_{Ca} - C_{Ca-eq}} - \frac{1}{C_{Ca,i} - C_{Ca-eq}}\right).\frac{1}{t} \qquad [3.8]$$

The equilibrium concentration of calcium was calculated by PHREEQC® to be 0.0217 mol/l for a solution that is three times saturated (SS3) and 0.0231 mol/l for a solution that is four times saturated (SS4).

3.3.5 Uncertainty

3.3.5.1 Calcium concentration

The measured calcium concentration was dependent on several factors that can cause some uncertainty in the measurement. The main contributions to the uncertainty were identified as the analysis method and the dilution method. The effects of the temperature, pH and time were negated. Thus, the calcium concentration can be defined by equation 3.2 (simplified as equation 3.3) as a function of the ICP-OES measured value and the dilution volumes.

Both the volume terms (V_{RO} and V_{Sample}) have uncertainty parameters (ΔV_{Ro} and ΔV_{Sample}) that propagate because the two volumes were measured with different micropipettes. In addition, the concentration measured by the ICP (C_{ICP}) also has an uncertainty parameter (ΔC_{ICP}). These uncertainty parameters were calculated using the method detailed in Table 2.12 in section 2.9.

From these three parameters, the propagated uncertainty of the calcium concentration was calculated using equation 3.9, which had been derived from equation 2.23 and 3.3. The full derivation is detailed in Appendix C.

$$\Delta c_{Ca} = \sqrt{\left[\left(1 + \frac{V_{RO}}{2V_{Sample}}\right)\Delta C_{ICP}\right]^2 + \left[\frac{C_{ICP}}{2V_{Sample}}.\Delta V_{RO}\right]^2 + \left[-\frac{C_{ICP}V_{RO}}{2V_{Sample}^2}.\Delta V_{Sample}\right]^2} \qquad [3.9]$$

3.3.5.2 Percentage calcium removed

The percentage calcium removed during the experimental run was calculated using the calcium concentrations (C_{Ca}) at the start ($C_{Ca-initial}$) and on completion ($C_{Ca-final}$) of an experimental run, as defined in equation 3.5.

The calcium concentration had propagated uncertainty parameters for both the final ($\Delta C_{Ca-final}$) and initial ($\Delta C_{Ca-initial}$) concentration that were calculated as described in section 3.5.2.1. This uncertainty will propagate to the uncertainty of the percentage calcium removed. The propagated uncertainty of the percentage calcium removed was calculated by equation 3.10, which had been derived from equation 2.23 and equation 3.5. The full derivation is detailed in Appendix C.

$$\Delta\%Ca_{removed} = \sqrt{\left[\frac{100}{-C_{Ca-inital}}.\Delta C_{Ca-final}\right]^2 + \left[\frac{100\ C_{Ca-final}}{C_{Ca-inital}^2}.\Delta C_{Ca-inital}\right]^2} \qquad [3.10]$$

The average calcium removal percentage was calculated for all three runs using the percentage calcium removed (Equation 3.6). However, the average percentage is only a function of the percentage calcium removed, and thus the only propagation parameter that was taken into account was that of

the percentage calcium removed. The propagated uncertainty of the average percentage removed was calculated by equation 3.11. The full derivation is detailed in Appendix C.

$$\Delta\%Ca_{Average} = \sqrt{\left[\frac{\Delta\%Ca_{removed,1}}{3}\right]^2 + \left[\frac{\Delta\%Ca_{removed,2}}{3}\right]^2 + \left[\frac{\Delta\%Ca_{removed,3}}{3}\right]^2} \quad [3.11]$$

3.3.5.3 Growth rate constant

The growth rate constant is a function of the initial and final calcium concentration as well as the time, as shown in equation 3.8. The uncertainty of the calcium concentration propagate through to the growth rate as well, and thus the propagated uncertainty of the growth rate constant was calculated using equation 3.12. The full derivation of this equation can be seen in Appendix C.

$$\Delta k' = \sqrt{\left[\frac{\Delta C_{Ca}}{t.\left(C_{Ca}-C_{Ca-eq}\right)^2}\right]^2 + \left[\frac{-\Delta C_{Ca,i}}{t.\left(C_{Ca,i}-C_{Ca-eq}\right)^2}\right]^2} \quad [3.12]$$

3.4 Experimental design

The experiments conducted were designed to reach the 5 objectives stated in Chapter 1.

3.4.1 Baseline experiments

Before the experiments were performed, baseline experiments were done to determine the behaviour of crystallisation under these specific circumstances (Table 3.9). This included the effects of supersaturation, seeding as well as antiscalant on gypsum crystallisation.

Table 3.9: *Baseline experiments.*

Experiment	Conditions
B1 – SS3	Supersaturation 3
B2 – SS4	Supersaturation 4
B3 – SS3+S	Supersaturation 3 + Seeding
B4 – SS3+A	Supersaturation 3 + Anti-scalant
B5 – SS3+S+A	Supersaturation 3 + Seeding + Anti-scalant

3.4.2 Control experiments

Control runs without treatments were preformed to compare the results of these control experiments with those obtained from the treatment experiments. This comparison was done in order to

determine if the treatment was effective. Two sets of control experiments were conducted where the seed crystals were re-used: one in the presence of antiscalant and one in the absence of antiscalant. The control experiments were also used to assess the effect of seed crystal re-use.

3.4.3 Physical treatment of the seed-crystal mixture

The physical treatment of the seed-crystal mixture can be divided into two sets of experiments: mixing as seed crystal treatment and air scouring as seed crystal treatment.

3.4.3.1 Mixing as seed crystal treatment method.

Initially, the experiments for mixing as seed crystal treatment were designed based on a 3 X 3 full factorial design with two factors, namely the G-factor (mixing speed) and the duration of the treatment. Both factors had three levels. However, after completion of the experiments and analysis of the initial results, it was decided to add another level for the mixing time. The experiments for mixing as a seed crystal treatment method are detailed in Table 3.10. No known research with mixing as a seed crystal treatment method has been done before. Thus, there were no literature values to follow as guidelines for the mixing speeds or durations. The values were chosen according to Degremont (2007), where mixing speed was represented by the G-factor: slow speed (G-factor 0-100 s^{-1}), medium speed (G-factor 100 – 400 s^{-1}) and rapid mixing (G-factor above 500).

Table 3.10: *Experiment numbers for mixing as seed crystal treatment.*

	G-factor (s^{-1})		
Time (min)	**93**	**188**	**533**
1	1.1 - 1.3	4.1 - 4.3	7.1 -7.3
5	2.1 - 2.3	5.1 - 5.3	8.1 - 8.3
10	3.1 - 3.3	6.1 - 6.3	9.1 - 9.3
15	26.1 – 26.3	27.1 - 27.3	-

3.4.3.2 Air scouring as seed crystal treatment method

The experiments for air scouring as seed crystal treatment were also based on a 3 x 3 full factorial design with two factors, namely the air flux through the seed-crystal mixture and the duration of the treatment. Both factors had three levels. These experiments are detailed in Table 3.11. The minimum flow rate of air needed was based on the calculated minimum air flow rate required to cause a fluidised bed.

Table 3.11: *Experiment numbers for air scouring as seed crystal treatment with the flux at STP.*

	Air flux (m/h)		
Time (min)	15.6	62.4	155.9
1	10.1 - 10.3	13.1 - 13.3	16.1 - 16.3
5	11.1 - 11.3	14.1 -14.3	17.1 - 17.3
10	12.1 - 12.3	15.1 -15.3	18.1 - 18.3

3.4.4 Chemical dosing

The chemical dosing can be divided into two sets of experiments: in the presence of hydrogen peroxide (H_2O_2) and in the presence of aluminum (Al).

3.4.4.1 Gypsum crystallisation in the presence of hydrogen peroxide.

A factorial design was used for the experiments conducted in the presence of hydrogen peroxide (the factor), and there were three levels within this factor. Lawler, et al. (2010) found that the optimum amount of ozone was 10 mg ozone per milligram of antiscalant. Since both hydrogen peroxide and ozone produce hydroxyl radicals, a similar dosage was used. The dosage was also halved for the lower bound and doubled for the upper bound. The experiments done in the presence of hydrogen peroxide are detailed in Table 3.12.

Table 3.12: *Experiment numbers in the presence of hydrogen peroxide.*

Concentration H_2O_2 (ppm)	**Experiment**
45 ppm (5 mg/mg antiscalant)	19.1 - 19.3
90 ppm (10 mg/mg antiscalant)	20.1 - 20.3
135 ppm (15 mg/mg antiscalant)	21.1 - 21.3

3.4.4.2 Gypsum crystallisation in the presence of aluminum

A factorial design was used for the experiments conducted in the presence of aluminum (the factor), and there were three levels within this factor. The amount of aluminum to be added was based on the amount of antiscalant in the system. The optimum amount was taken as 1 mg of aluminum per milligram of antiscalant. The dosage was then also halved for the lower bound, and doubled for the upper bound. Since aluminum can not be dosed in pure form, the aluminum was dosed by means of aluminum chloride. However, different forms of aluminum dosage were tested, and one experiment was done where the aluminum was dosed by means of aluminum sulphate to compare to the results that were obtained from aluminum chloride. The experiments performed in the presence of aluminum are detailed in Table 3.13.

Table 3.13: *Experiment numbers in the presence of aluminum ions.*

Concentration Al (ppm)	Experiment	Source of Al
4.5 ppm (0.5 mg/mg antiscalant)	22.1 - 22.3	$AlCl_3$
9 ppm (1 mg/mg antiscalant)	23.1 - 23.3	$AlCl_3$
18 ppm (2 mg/mg antiscalant)	24.1 - 24.3	$AlCl_3$
4.5 ppm (0.5 mg/mg antiscalant)	25.1 - 25.3	$Al_2(SO_4)_3$

3.4.4.3 Gypsum crystallisation in the presence of both hydrogen peroxide and aluminum

An additional experiment was conducted in the presence of 90 ppm hydrogen peroxide [the optimum according to Lawler, et al. (2010)] and 4.5 ppm aluminum in the form of aluminum chloride. This was the minimum amount of aluminum chloride that was used to determine if the combination of aluminum and hydrogen peroxide yields better results.

3.5 Experimental accuracy

Based on the experimental procedure detailed in section 3.3.2, the accuracy of concentrations in the stock solutions and the seeding procedure was investigated in this section.

3.5.1 Stock solution

Various samples of the different calcium stock solutions were taken and analysed by means of ICP-OES analysis to determine the calcium concentration (Figure 3.12). The average calcium concentration was found to be 3601 ppm (0.090mol/l) ± 42 ppm. According to calculations, the desired concentration of calcium in the solution was 3847.5 ppm (0.096 mol/l). The average calcium concentration was found to deviate 0.69% form the preferred concentration.

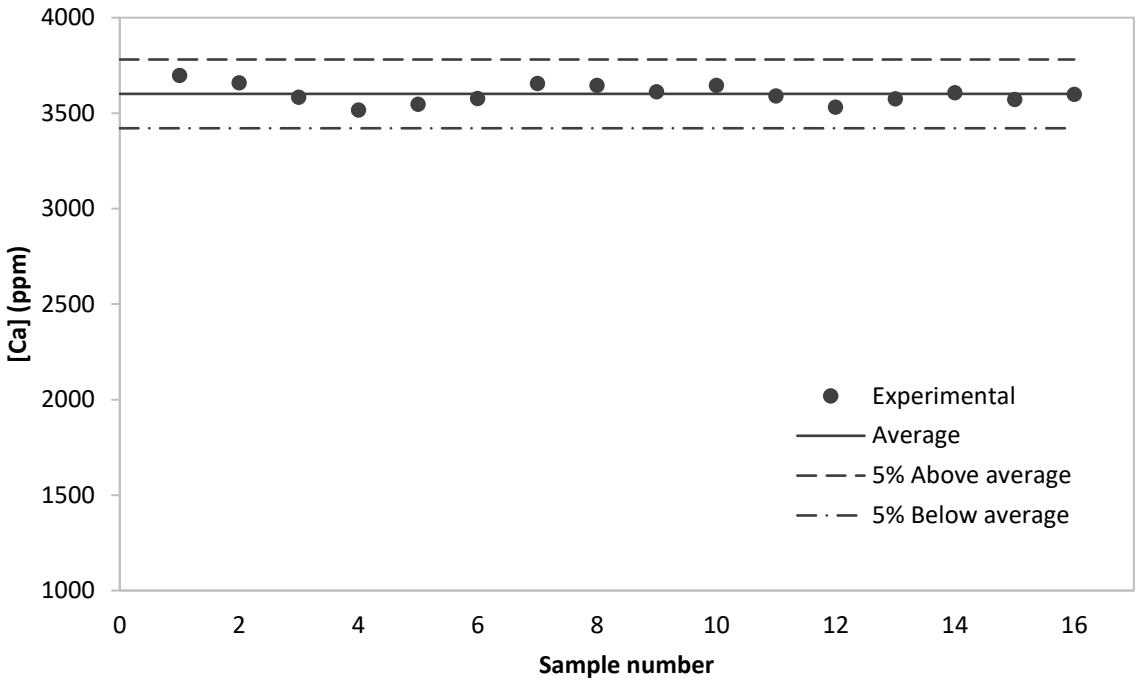

Figure 3.12: *Analytical results for stock solutions used for approximately three times the supersaturation of gypsum solutions.*

The calcium stock solution was analysed by means of ICP-OES analysis, and the sulphate stock solution was analysed by means of ion chromatography (IC) at the Process Engineering analytical laboratory of Stellenbosch University. The amount of calcium and the amount of sulphate should be equal to ensure an equimolar mixture when added together. According to theoretical calculations, the desired concentration of calcium as well as sulphate is 0.090 mol/l. Six different samples were analysed, and the average calcium concentration was found to be 0.09086 mol/l ± 0.00092 mol/l and the average sulphate concentration was found to be 0.092 mol/l ± 0.0015 mol/l (Figure 3.13). This indicates that the average calcium concentration and the average sulphate concentration deviate by 0.42% and 1.65%, respectively from the theoretically calculated concentration.

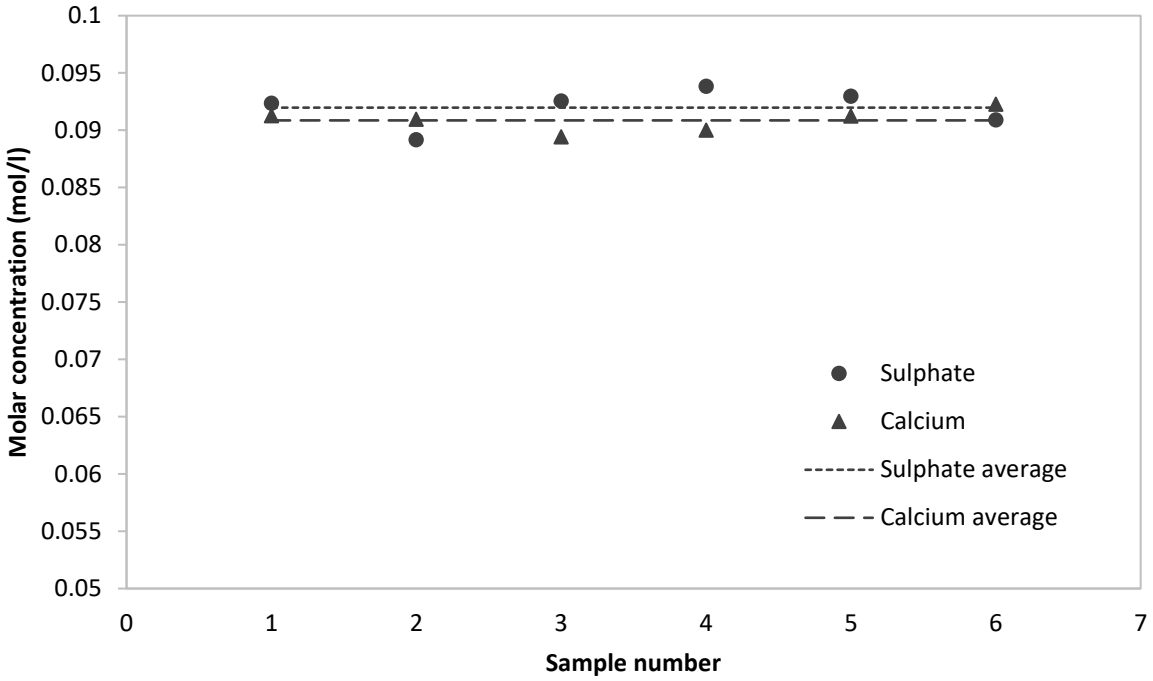

Figure 3.13: *Analytical results for stock solution concentrations of sulphate and calcium.*

3.5.2 Seeding

The procedure to transfer the seed crystals in solution to the reactor was tested numerous times to ensure that the amount of seeding stays constant. The seed crystals were added to the reactor using a syringe, as detailed in section 3.3.2.4. A constant volume of 50 ml of the seed-crystal mixture was measured, using the syringe, and weighed to ensure a minimal difference in the amounts of seed crystals. For these tests, the seed crystal mixture was filtered, dried and weighed in order to determine if the 50 ml delivers a constant amount of seed crystals (Figure 3.14). The average dried crystal mass delivered by the seven test runs of 50 ml seed crystal mixture each was found to be 1.97 g ± 0.03 g (1.5% variation). The average mass of the syringe and the 50 ml seed crystal mixture was found to be 85.55 g ± 0.19 g.

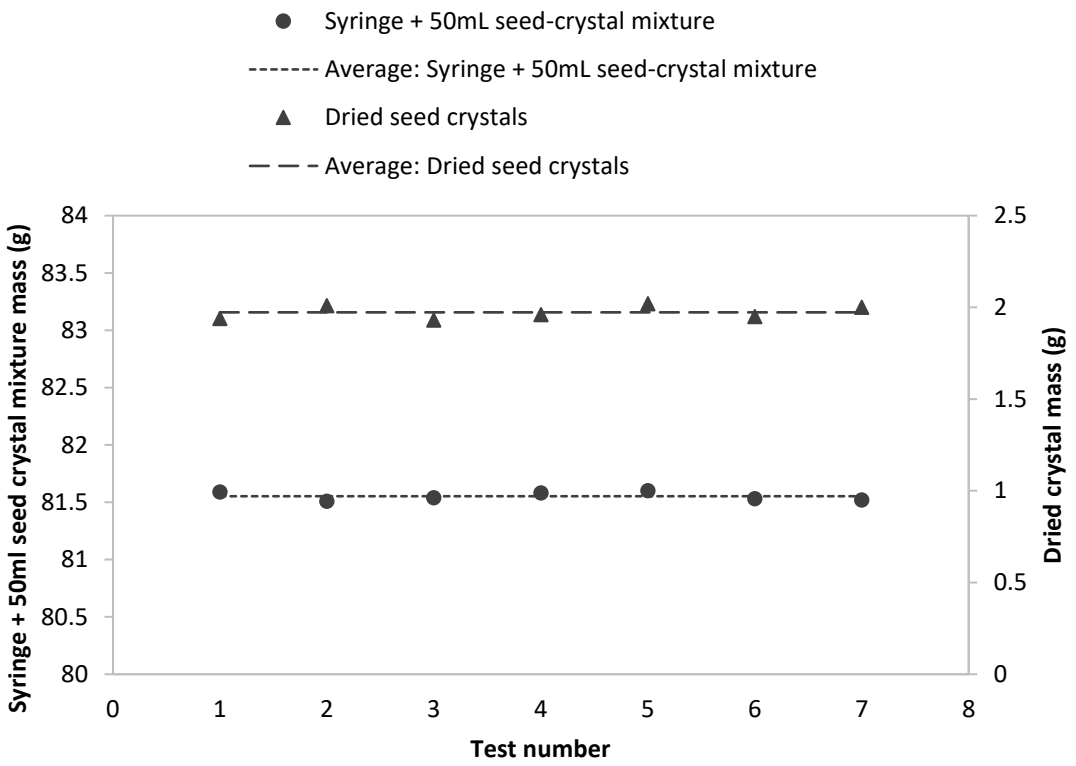

Figure 3.14: *The syringe mass including 50 ml of seed crystal mixture and the resulting mass of dried crystals produced.*

Chapter 4: Results and Discussion

All analysis was done with a sample that had been filtered through a 0.22 µm syringe filter, which is normally used as a standard in water analysis. Thus, all the results are based on a 0.22 µm particle removal.

4.1 Baseline results

Baseline data was generated to determine the behaviour of the crystallisation process under specific conditions. These conditions included supersaturation, seeding and the presence of antiscalants.

4.1.1 Effect of supersaturation

To determine the effect of supersaturation, crystallisation experiments were performed at three times gypsum saturation (supersaturation 3, SS3) as well as four times gypsum saturation (supersaturation 4, SS4) for approximately 2 hours and 40 minutes.

As expected and also indicated in literature, the induction time decreased as the supersaturation increased (Figure 4.1). This indicates that the nucleation rate of the crystallisation process was faster at a higher supersaturation. Additionally, it was observed that the crystal growth rate was increased at higher supersaturation, as it took longer to reach the equilibrium concentration at the lower supersaturation. This was confirmed by the reaction kinetics calculated from the start up to ~160 minutes for supersaturation experiments, as detailed in Table 4.1.

Table 4.1: *The initial and final concentrations of calcium and the growth rate constants for SS3 and SS4 at 25°C and a G-factor of 188 s^{-1}.*

Supersaturation condition	Start		At ~160 min		Growth rate constant	
	Time (min)	Ca Conc. (ppm)	Time (min)	Ca Conc. (ppm)	k't (l/mol)	k' ($l.mol^{-1}.min^{-1}$)
SS3	5	1719.25	160	1061.84	161.41	1.041
SS4	5	2371.32	167	1000.20	512.03	3.154

The growth rate constant at SS4 is ~3 times that of the growth rate constant of SS3. Thus, an increase in the rate constants was observed with the increase in supersaturation.

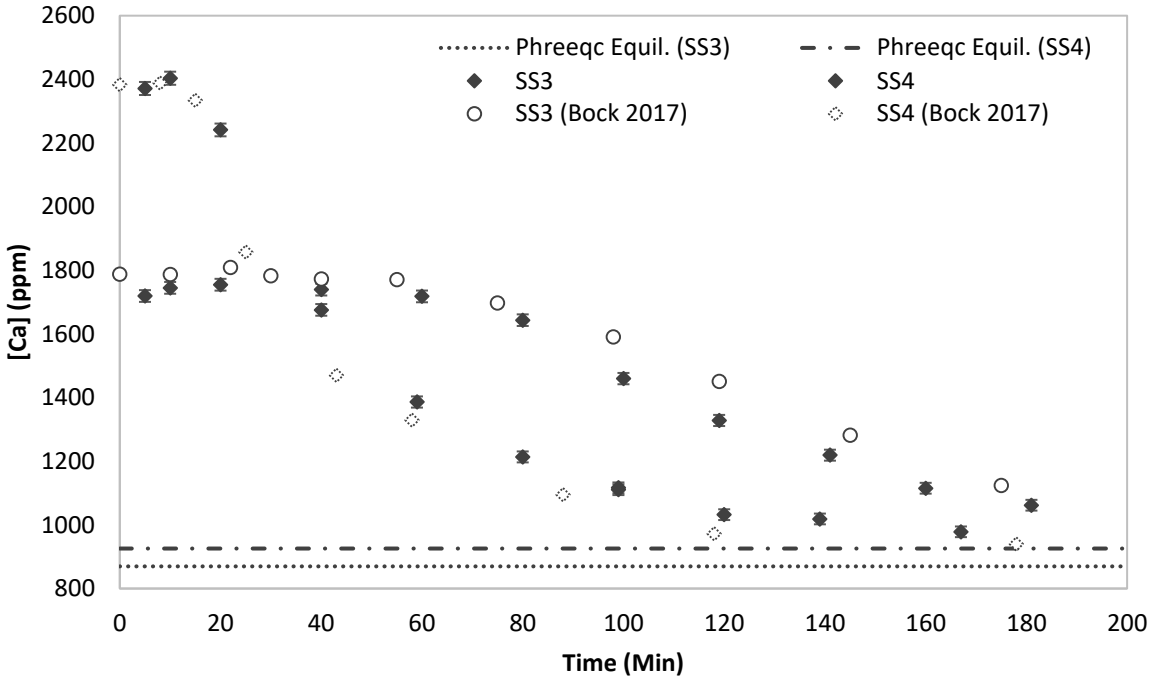

Figure 4.1: *Desupersaturation curve for SS3 and SS4 at 25°C and a G-factor of 188 s^{-1}, including the equilibrium concentrations of SS3 and SS4 calculated by Phreeqc as well as data from literature (Bock, 2017).*

The rate of nucleation is dependent on the level of supersaturation. Therefore, at a higher supersaturation, the nucleation phase would be quicker. This would lead to a shorter induction time that in the end produces a faster crystal growth. Since the nucleation phase is faster, the nucleoids that form are formed faster. Because the concentration is higher, more nucleoids were formed that increased the number of active growth sites, allowing for faster cyrstallisation (Mullin, 1972).

4.1.2 Effect of seeding

To verify the effect of seeding, two experiments were performed at the three times gypsum saturation (SS3). However, 2000 ppm of pure gypsum seed crystals were added to the one experiment compared to no seeding crystals present in the other.

Figure 4.2 indicates that the addition of the seed crystals removed the lag time. This is due to the nucleation phase being negated when seed crystals were added, since active growth sites were then readily available for crystallisation. In contrast, in the absence of seed crystals, active growth sites first need to be formed by the nucleation phase (Mullin, 1972). Due to the lack of lag time, overall crystallisation was faster when seed crystals were added resulting in equilibrium being reached faster. This was supported by the reaction kinetics that were calculated for the overall processes, from the start up to ~140 minutes (Table 4.2).

Table 4.2: *The initial and final concentrations of calcium and the growth rate constants for SS3 and SS3 + seed crystals at 25°C and a G-factor of 188 s^{-1}.*

Supersaturation condition	Start		At ~140 min		Growth rate constants	
	Time (min)	Ca Conc. (ppm)	Time (min)	Ca Conc. (ppm)	k't (l/mol)	k' ($l.mol^{-1}.min^{-1}$)
SS3	5	1719.25	141	1219.10	67.53	0.497
SS3+S	5	1668.60	143	927.38	644.54	4.671

This confirmed that the growth rate in the presence of seed crystals is much higher than in the absence of seed crystals, as described in literature (Amjad, 1988; Amjad & Hooley, 1986). The overall growth rate constant in the presence of seeding crystals was found to be ~10 times that of the growth rate constant in the absence of seed crystals.

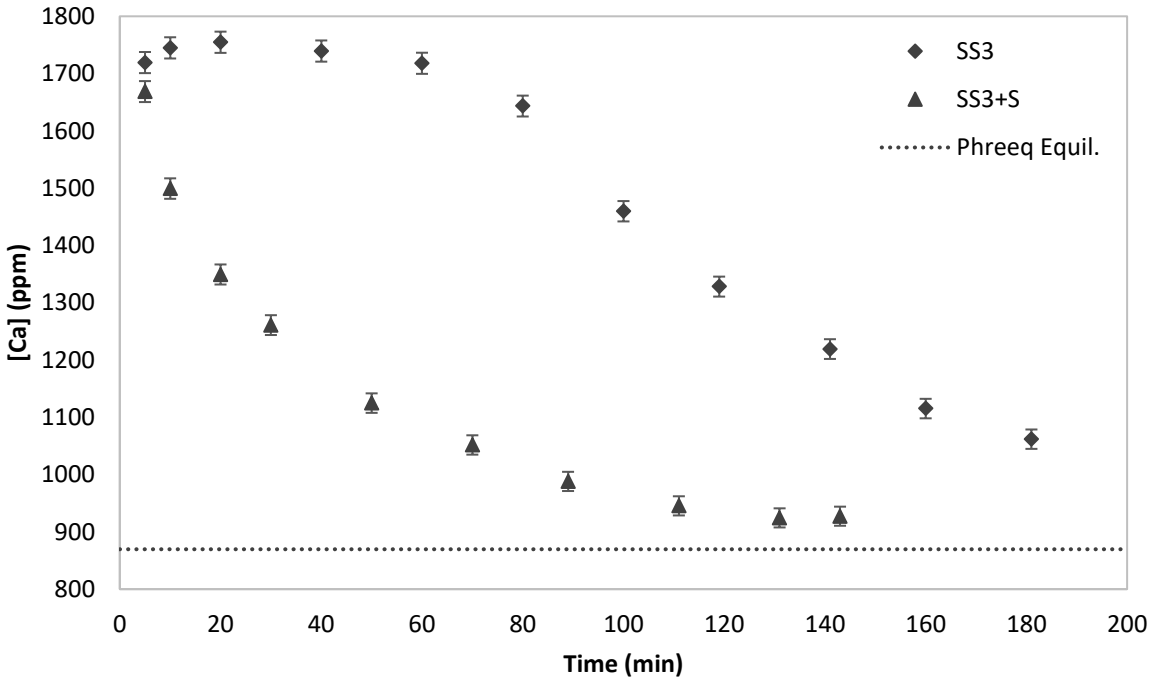

Figure 4.2: *Desupersaturation curve for SS3 and SS3 + seed crystals at 25°C and a G-factor of 188 s^{-1}, including the equilibrium concentration of SS3.*

Comparison of the growth rates of the overall process (Table 4.2) with or without seed crystals, confirmed that the use of seed crystals increased the overall growth rate. However, when the growth rate constants of only the growth phase were compared, thus not taking the nucleation phase into account, the difference was found to be much smaller (Table 4.3). The growth rate of the pure SS3 experiment was calculated from 100 minutes, when the nucleation phase was considered complete, up to 181 minutes (~80 minutes). This calculated growth rate for the pure SS3 experiment was compared to the growth rate in the presence of seed crystals for the same duration.

Table 4.3: *The initial and final concentrations of calcium and the growth rate constants for SS3 excluding the nucleation phase and SS3 + seed crystals at 25°C and a G-factor of 188 s^{-1}.*

Supersaturation condition	Start of growth phase		After 80 min		Growth rate constants	
	Time (min)	Ca Conc. (ppm)	Time (min)	Ca Conc. (ppm)	k't (l/mol)	k' ($l.mol^{-1}.min^{-1}$)
SS3 (Excl. nucleation)	100	1718.00	181	1061.84	161.34	1.992
SS3+S	5	1668.60	89	988.09	288.33	3.432

In the presence of seed crystals, the growth rate increased during the growth phase. This could mainly be due to the amount of seed crystals added, as the amount of active growth sites were increased by seeding compared to the growth sides provided by the nucleation phase. It could also be due to the crystal size, as the crystals that were constructed by the nucleation phase, were near-nucleic size. In comparison, the added seed crystals were much more prominent and, as supported by Mullin (1972), smaller crystals of near-nucleic size grow at a slower rate.

4.1.3 Effect of antiscalant

The effect of antiscalant was determined by adding 9 ppm of polycarboxylic acid-based antiscalant to the three times gypsum saturated solution, 3 ppm per gypsum saturation. It was expected that the crystallisation rate would decrease or that no crystallisation would take place with the addition of antiscalant as it is a crystal inhibitor. In the presence of 9 ppm polycarboxylic acid-based antiscalant, no crystallisation took place; thus, the antiscalant inhibited the crystal growth completely (Figure 4.3). The calcium concentration stayed almost constant during the run of 185 minutes.

Seed crystals were used to determine if they could supersede the inhibiting effect of the antiscalant. It was found that the seed crystals neutralised the effect of the antiscalant up to a point. However, the effect of the antiscalant could still be seen to some extent when compared to the seeding in the absence of antiscalant (Figure 4.4). Figure 4.4 shows that, in the presence of antiscalant and seed crystals, the equilibrium was reached later than in the presence of only seed crystals and the absence of antiscalant.

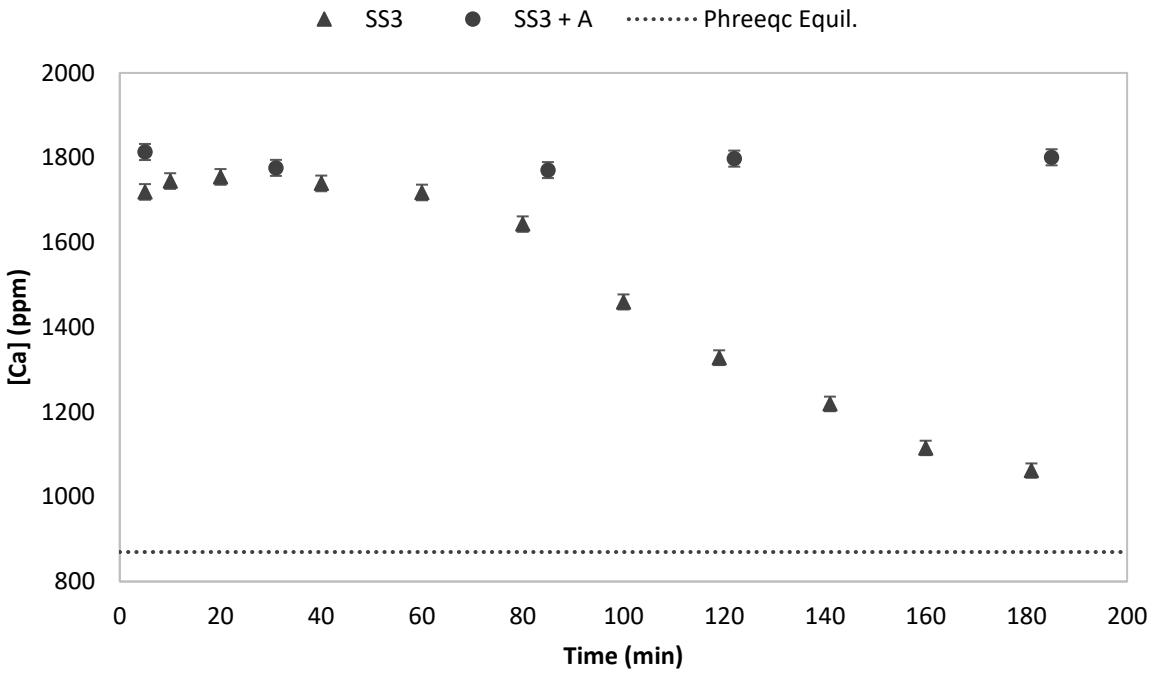

Figure 4.3: *Desupersaturation curve for SS3 and SS3 + antiscalant at 25°C and a G-factor of 188 s^{-1}, including the equilibrium concentration of SS3.*

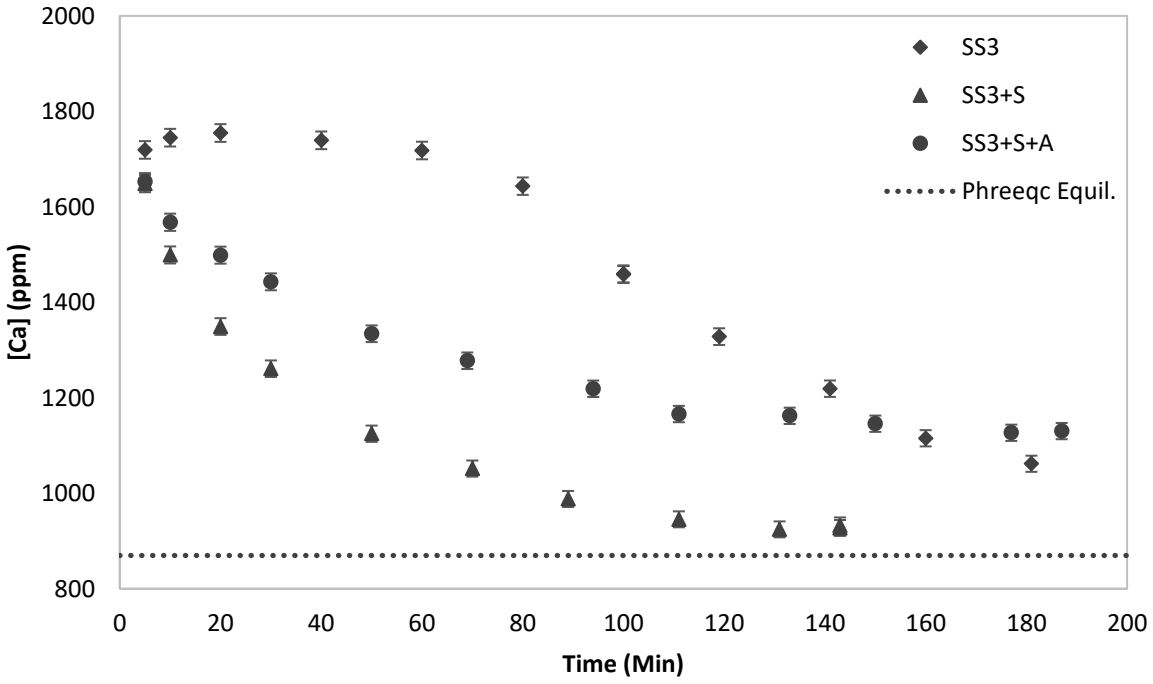

Figure 4.4: *Desupersaturation curve for SS3, SS3 + seed crystals and SS3 + seed crystals + antiscalant at 25°C and a G-factor of 188 s^{-1}, including the equilibrium concentration of SS3 calculated by Phreeqc.*

The growth rate constants (Table 4.4) confirmed that slower crystal growth occurred in the presence of antiscalant and seed crystals than in the absence of antiscalant. However, this was still faster than in the absence of both seed crystals and antiscalant. In addition, the growth rate constant confirmed that hardly any crystallisation occurred in the presence of antiscalant and the absence of seed crystals.

Table 4.4: *The initial and final concentrations of calcium and the growth rate constants for SS3, SS3 + seed crystals, SS3 + antiscalant and SS3 + seed crystals + antiscalant at 25°C and a G-factor of 188 s^{-1}.*

Supersaturation condition	Start		At ~150 min		Growth rate constants	
	Time (min)	Ca Conc. (ppm)	Time (min)	Ca Conc. (ppm)	k't (l/mol)	k' ($l.mol^{-1}.min^{-1}$)
SS3	5	1719.25	141	1219.10	67.53	0.497
SS3+S	5	1668.60	143	927.38	644.54	4.671
SS3+A	5	1813.47	150	1797.82	0.72	0.006
SS3+S+A	5	1652.49	150	1145.68	94.02	0.648

4.2 Effect of re-used seed crystals

To act as a control of the different seed crystal treatment methods, experiments were performed where seed crystals were re-used in both the absence and presence of antiscalants.

The desupersaturation curve for the re-use of seed crystals in the absence of antiscalant (Figure 4.5) shows that the three curves were similar, as the conditions were identical and no impurities or inhibitors were present. Therefore, the re-use of pure gypsum seed crystals in the absence of antiscalant appears not to affect the precipitation rate.

The calcium removal was also determined for each run, and it was found that all three runs had similar calcium removal (Figure 4.6).The first re-use of the seed crystals removed 42.5% of the calcium in the system, followed by 42.5% and 43.3% removal during the second and third seed crystal re-use, respectively. Therefore, this confirmed that the re-use of seed crystals in the absence of antiscalant and impurities does not affect the gypsum precipitation notably.

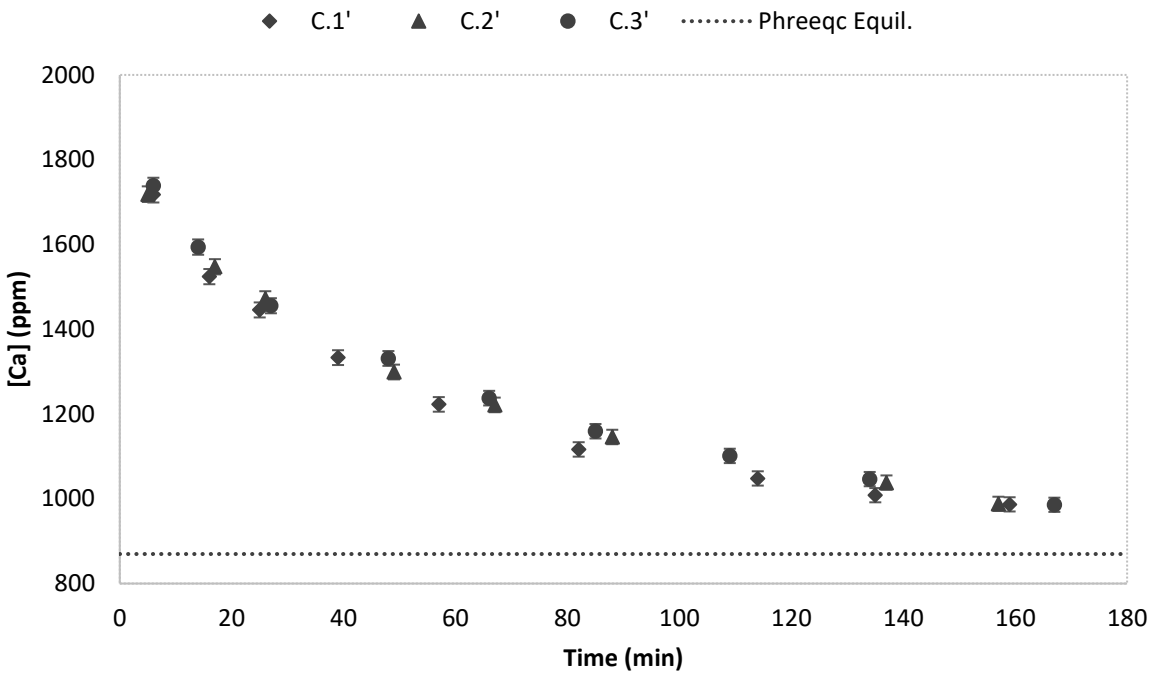

Figure 4.5: *The desupersaturation curve for the control run in the absence of antiscalant (C') at three times gypsum saturation, with 2000 ppm seeding. C.1' was the first re-use of seed crystals, C.2' the second and C.3' the third re-use of seed crystals, at 25°C, including the equilibrium concentration of SS3 calculated by Phreeqc.*

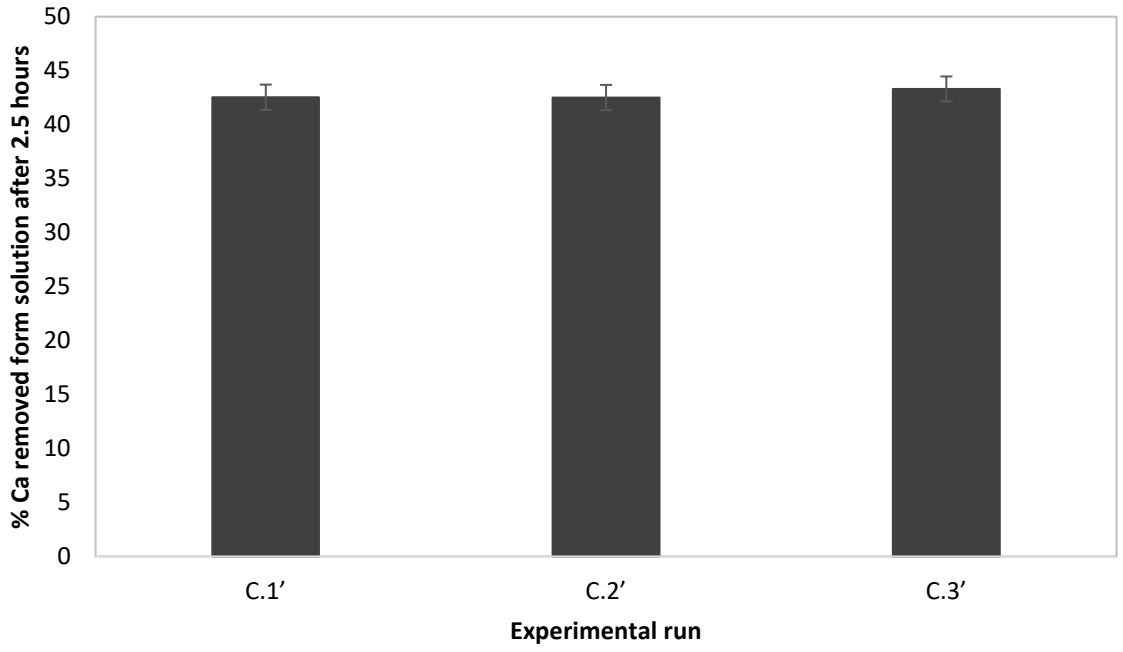

Figure 4.6: *The percentage calcium removed from solution (SS3) after 2.5 hours of the control run in the absence of antiscalant (C'), with 2000 ppm seeding. C.1' was the first re-use of seed crystals, C.2' the second and C.3' the third re-use of seed crystals, at 25°C.*

However, the re-use of seed crystals was found to affect the precipitation process when crystallisation took place in the presence of 9 ppm polycarboxylic acid-based antiscalant. The desupersaturation curves for the three runs, where seed crystals were re-used in the presence of antiscalant, were clearly different from one another (Figure 4.7). After each 2.5 hour experimental run, a higher final calcium concentration was found than in the experiment before, resulting in lower calcium removal.

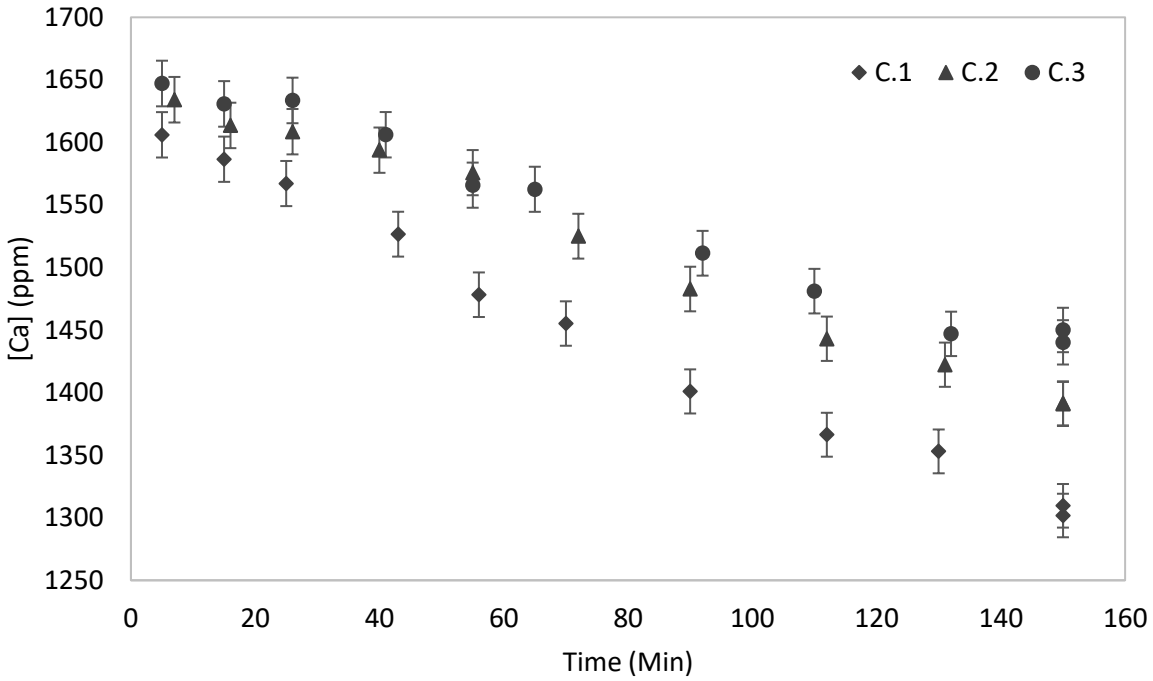

Figure 4.7:*The desupersaturation curve for the control run in the presence of 9 ppm antiscalant (C) at three times gypsum saturation, with 2000 ppm seeding where C.1 was the first re-use of seed crystals, C.2 the second and C.3 the third re-use of seed crystals, at 25°C. (The equilibrium calcium concentration of SS3 calculated by Phreeqc = 869.7 ppm).*

The calcium removal of each run (Figure 4.8) confirmed that the more the seed crystals were re-used, the less effective they became, leading to a decrease in calcium removal with each run. The first re-use of the seed crystals removed 18.7% of the calcium in the system, followed by only a 14.9% calcium removal for the second re-use. When the crystals were re-used for the third time, it only yielded a 12.3% calcium removal. A significant decrease in the calcium removal with every re-use of the seed crystals was therefore observed.

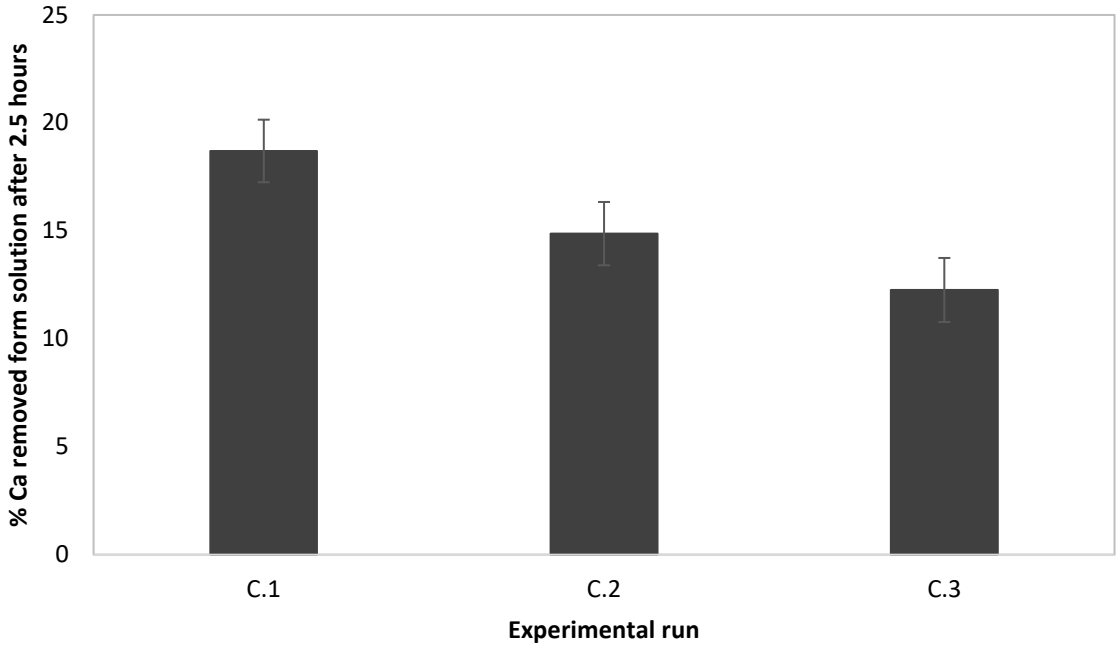

Figure 4.8: *The percentage calcium removed from solution (SS3) after 2.5 hours of the control run in the presence of 9 ppm antiscalant (C) with 2000 ppm seeding, where C.1 was the first re-use of seed crystals, C.2 the second and C.3 the third re-use of seed crystals at 25°C.*

Figure 4.7 and Figure 4.8 show that the effectiveness of the seed crystals decreased with the re-use of the seed crystals in the presence of 9 ppm polycarboxylic acid-based antiscalant. This is because the antiscalant inhibits precipitation by reducing the number of active growth sites available for crystallisation. This reduction in growth sites takes place by adsorption of the antiscalant onto the growth site, which renders the growth site unsuitable for further growth and therefore makes the crystal less efficient as a seed crystal (Kucera, 2015). By re-using these seed crystals with fewer growth sites, the seeding is made less effective. The amount of active growth sites is then reduced even further in successive re-use cycles by more adsorption of the antiscalant, which reduces the effectiveness of the seeding even more. The decrease in active growth sites leads to a decrease in the crystal growth rate, which leads to a decrease in the overall precipitation.

There is a large difference (27.5%) between the percentage of calcium removed in 2.5 hours when the crystals were re-used as seed crystals in the absence of antiscalant compared to re-use in the presence of antiscalant (Table 4.5). In the absence of antiscalant, the calcium removal is more than double that of the calcium removal in the presence of antiscalant.

Table 4.5: *The percentage of calcium removed from the solution for the control experiments in the presence of 2000 ppm re-used gypsum seed crystals.*

Run	% Ca removed from the solution after 2.5 hours	
	Absence of antiscalant	Presence of antiscalant
1	42.5	18.7
2	42.5	14.9
3	43.3	12.3
Average	**42.8**	**15.3**

The crystals formed in these experiments were investigated by means of SEM analysis (Figure 4.9). The results of SEM analysis for the control experiment in the absence of antiscalant is shown in Figure 4.9 (a), (c) and (e), and the results for the control run in the presence of antiscalant is shown in Figure 4.9 (b), (d), and (f).

Figure 4.9 shows that the crystals in the absence of antiscalant (Figure 4.9 [a], [c] and [e]) have a different crystal shape compared to the crystals of the control experiment in the presence of antiscalant (Figure 4.9 [b], [d], and [f]). In the absence of antiscalant, the crystals were found to be more plate-shaped compared to the more needle/tubular shape in the presence of antiscalant. The difference in the shape of the seed crystal is the reason for the difference in the average calcium removal, since it was found by Lui & Nancollas (1970) that plate-shaped crystals cause higher crystal growth rates. The difference in the crystal shapes is due to the absence or presence of the antiscalant that can change the crystal shape (Mullin, 1972).

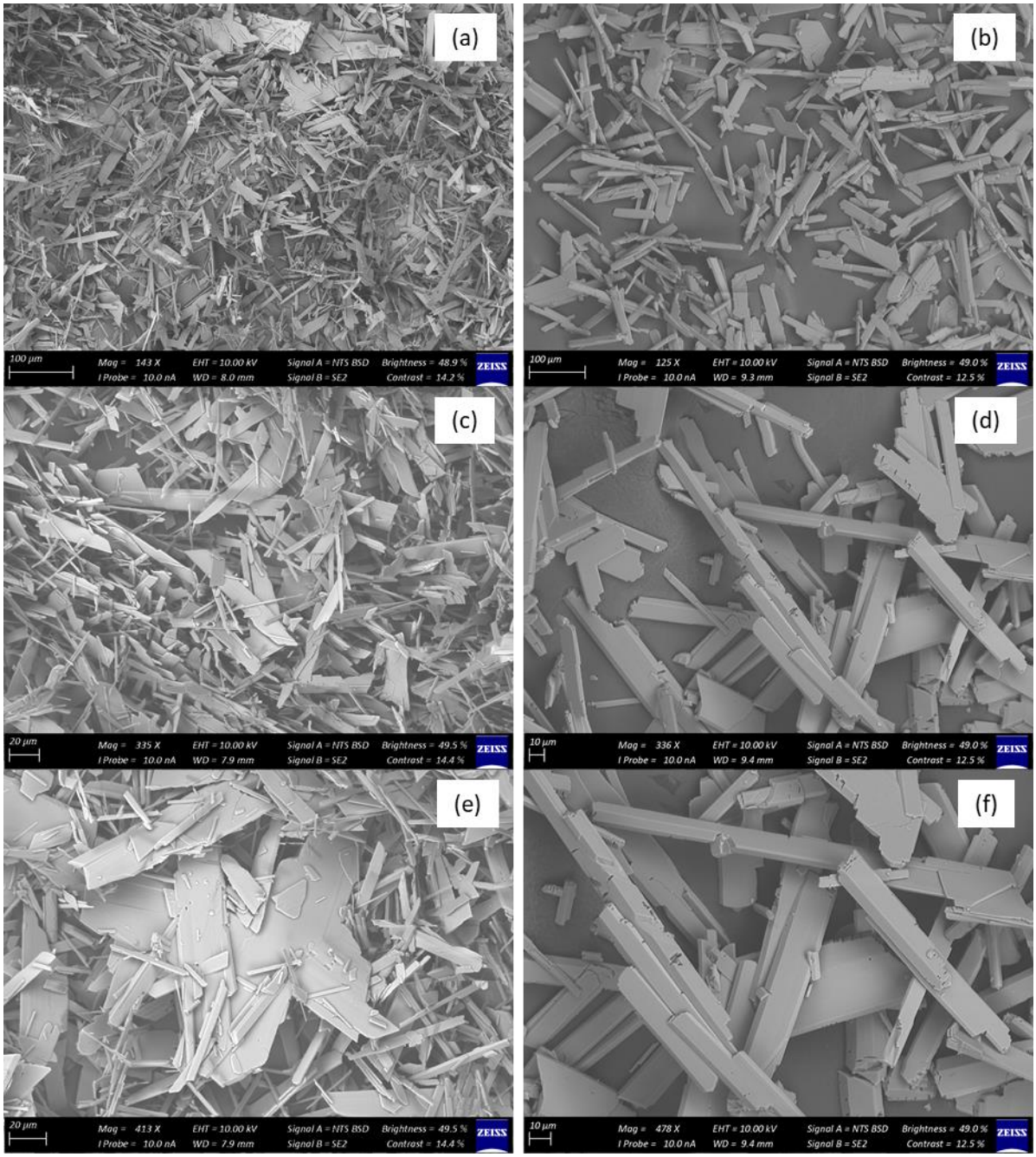

Figure 4.9: *SEM analysis of pure gypsum crystals formed in the absence of antiscalant (a, c and e) and gypsum crystals formed in the presence of antiscalant (b, d and f), where c, d, e and f are at larger magnification than (a) and (b).*

4.3 Effect of physical seed crystal treatment methods

4.3.1 Mixing as seed crystal treatment method

Mixing as a seed crystal treatment method was evaluated by eleven experimental runs as detailed in Table 4.6. All of these experiments were performed at a controlled temperature of 25˚C and an uncontrolled pH around 4.9 in the presence of 2000 ppm (dry base) seeding. The experiments were done at different G factors and for different durations, resulting in different specific G-factors (G*), reported as $G^* = G \times t \times 10^{-5}$.

Table 4.6: *Experiment numbers for mixing as seed crystal treatment.*

	G-factor (s^{-1})		
Time (min)	**93**	**188**	**533**
1	1.1 - 1.3	4.1 - 4.3	7.1 -7.3
5	2.1 - 2.3	5.1 - 5.3	8.1 - 8.3
10	3.1 - 3.3	6.1 - 6.3	9.1 - 9.3
15	27.1 - 27.3	26.1 - 26.3	-

The efficiency of mixing as a treatment method was determined by the amount of calcium removed, assuming an equimolar sulphate removal. The growth rate constant and the average calcium removal for the three runs were also calculated. A summary of the data is detailed in Table 4.7. The table shows the G-factor and duration of the mixing treatments, the initial and final calcium concentrations, the percentage calcium removed, the average percentage calcium removed for the three runs where seed crystals were re-used, and the growth rate constant of the control experiments and the experiments performed with mixing as seed crystal treatment. The full set of experimental data is provided in Appendix B.

Table 4.7: *Experimental data for evaluation of mixing as a crystal treatment method.*

Exp.	Crystal treatment		Calcium conc. (ppm) @ 5 min	Calcium Conc. (ppm) @ 150 min	% Calcium removed	Average Calcium Removal %	k' ($l.mol^{-1}.min^{-1}$)
	G-factor (s^{-1})	Time (min)					
C.1'	No antiscalant		1717.51	986.84	42.5	42.8	1.927
C.2'			1718.67	988.08	42.5		1.917
C.3'			1738.99	985.88	43.3		1.856
C.1	9 ppm antiscalant		1606.10	1305.68	18.7	15.3	0.259
C.2			1634.14	1391.21	14.9		0.168
C.3			1647.09	1445.15	12.2		0.125
1.1	93	1	1658.14	1328.68	19.9	14.2	0.252
1.2			1696.96	1497.04	11.8		0.106
1.3			1739.91	1550.57	10.9		0.088
2.1	93	5	1657.23	1164.87	29.7	23.5	0.585
2.2			1698.82	1307.78	23.0		0.298
2.3			1681.84	1384.22	17.7		0.197
3.1	93	10	1683.40	1091.02	35.2	25.7	0.909
3.2			1707.19	1262.60	26.0		0.373
3.3			1725.68	1454.57	15.7		0.150
27.1	93	15	1695.71	1262.57	25.5	19.4	0.369
27.2			1753.13	1442.73	17.7		0.169
27.3			1732.81	1473.45	15.0		0.138
4.1	188	1	1628.71	1140.17	30.0	22.1	0.626
4.2			1661.45	1351.16	18.7		0.270
4.3			1718.44	1415.44	17.6		0.181
5.1	188	5	1626.54	1108.21	31.9	26.5	0.852
5.2			1626.15	1206.88	25.8		0.454
5.3			1633.25	1278.10	21.7		0.315
6.1	188	10	1707.37	1014.73	40.6	31.4	1.576
6.2			1670.50	1209.06	27.6		0.469
6.3			1687.65	1251.01	25.9		0.387
26.1	188	15	1740.94	1294.42	25.7	21.8	0.334
26.2			1734.63	1373.82	20.8		0.229
26.3			1739.92	1410.23	19.0		0.194
7.1	533	1	1647.64	1137.39	31.0	24.5	0.626
7.2			1606.65	1267.87	21.0		0.353
7.6			1702.84	1324.04	22.3		0.269
8.1	533	5	1729.78	1176.47	32.0	26.3	0.580
8.2			1696.98	1245.39	26.6		0.402
8.3			1695.68	1349.34	20.4		0.242
9.1	533	10	1665.45	1275.92	23.4	20.6	0.357
9.2			1746.16	1411.38	19.2		0.195
9.3			1762.34	1421.36	19.4		0.191

*The control experiment and experiments 6 and 9 were repeated to verify repeatability and to increase the confidence in the data.

From Table 4.7 and Figure 4.10 it is clear that the calcium removal decreased every time the crystals were re-used, similar to the control run when no seed crystal treatment was done in the presence of antiscalant. A maximum of 40.6% of calcium was removed during the first run of experiment 6, where the seed crystal mixture was mixed for 10 minutes at 188 s^{-1}. However, the calcium removal decreased to 27.6% and 25.9% with the second and third runs, respectively. Thus, the removal decreased by 13% from the first run to the second run and then again by 1.7% (which is within the uncertainty) from the second to the third run. Therefore, the amount of calcium removed decreased over each run and would probably have reached an equilibrium where it would not have decreased further. The decreasing effectiveness of the seed crystals could be the result of the antiscalant inhibiting the growth by reducing the number of active growth sites, as discussed in section 4.2 (Kucera, 2015). The same observation can be made from the data of the growth rate constant (k') in Table 4.7, supporting the theory that the effectiveness of the seed crystals decreases with their re-use, even when the seed crystal mixture was treated by vigorous mixing.

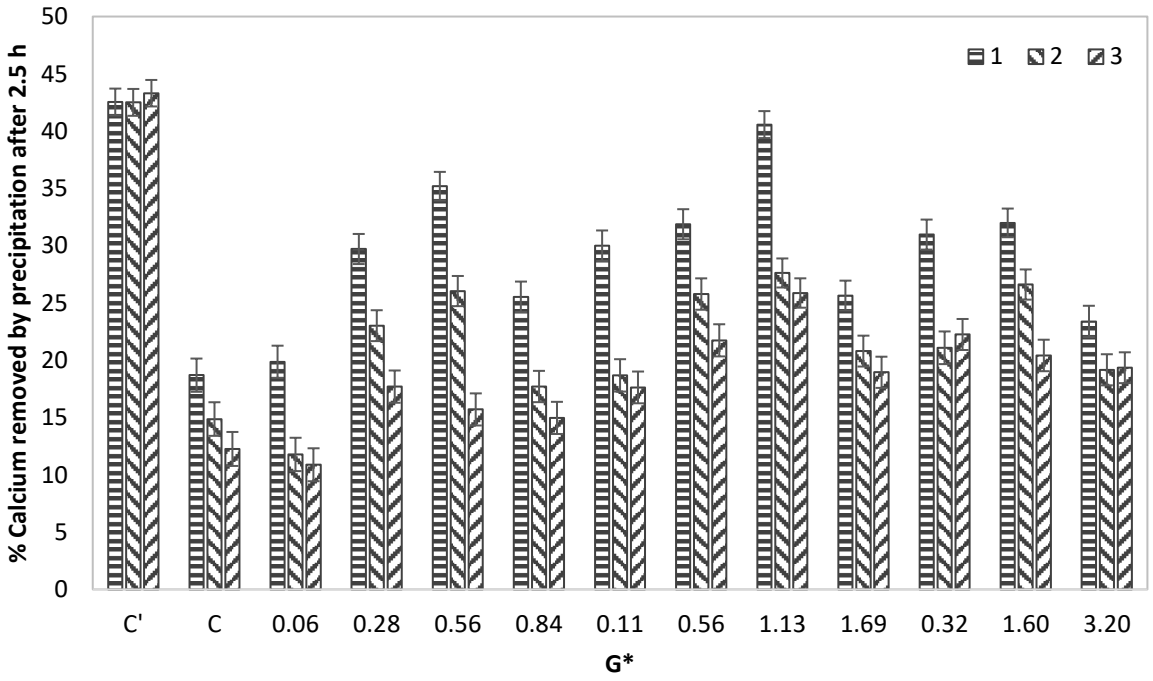

Figure 4.10: *The percentage calcium removed from solution (SS3) by means of precipitation after 2.5 hours of the control runs and the 11 experiments performed with mixing as treatment method, in the presence of 9 ppm antiscalant, with 2000 ppm seeding where (1) was the first re-use of seed crystals, (2) the second and (3) the third re-use of seed crystals.*

The average percentage calcium removed for the three runs of each experiment was compared to both control runs, where no treatments were done in the presence and absence of antiscalant (Figure 4.11). When mixing as treatment was applied, the average calcium removal of all but one experiment was higher than the average calcium removal of 15.3% of the control run in the presence

of antiscalants. The calcium removal of experiment 1 (G* = 0.56) was found to be lower than the calcium removal of the control run in the presence of antiscalant, but it is still within the experimental uncertainty range. The average calcium removal of all the runs where mixing as a treatment method was applied, was however found to be lower than the 42.8% average of calcium removed in the absence of antiscalant. The highest average calcium removal was found to be 31.4% (more than double that of the control run) for experiment 6 (G* = 1.13), when the seed-crystal mixture was treated for 10 minutes of mixing at a G-factor of 188 s^{-1}.

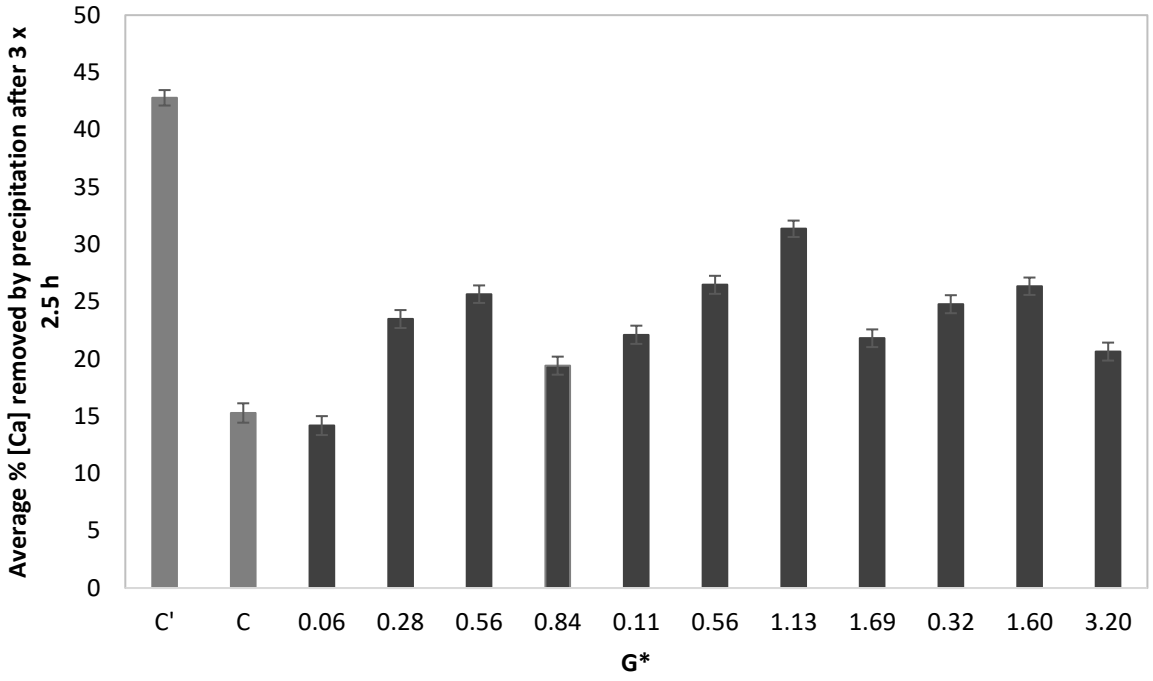

Figure 4.11: *The average percentage calcium removed from solution (SS3) after 2.5 hours by means of precipitation for the control runs and the 11 experiments performed with mixing as treatment method (in the presence of 9 ppm antiscalant, with 2000 ppm re-used seeding crystals).*

The increase in the average calcium removal in the presence of antiscalant when mixing was used as a seed crystal treatment compared to the control was further investigated by means of SEM analysis. For the control experiment and experiment 6 (G* = 1,13), the SEM analysis produced Figure 4.12. From these images, it is clear that the seed crystals of the control run (Figure 4.12 [a]) as well as the seed crystals where mixing was applied (Figure 4.12 [b]), show no structural difference and have similar tube shapes. However, physically it can be seen that the seed crystals from the control run (Figure 4.12 [a]) are smooth with some cavities. However, the seed crystals from experiment 6 (G* = 1.13), where the seed crystal mixture was mixed before it was re-used (Figure 4.12 [b]), were found to have substantially more cavities. This shows that attrition had had an effect.

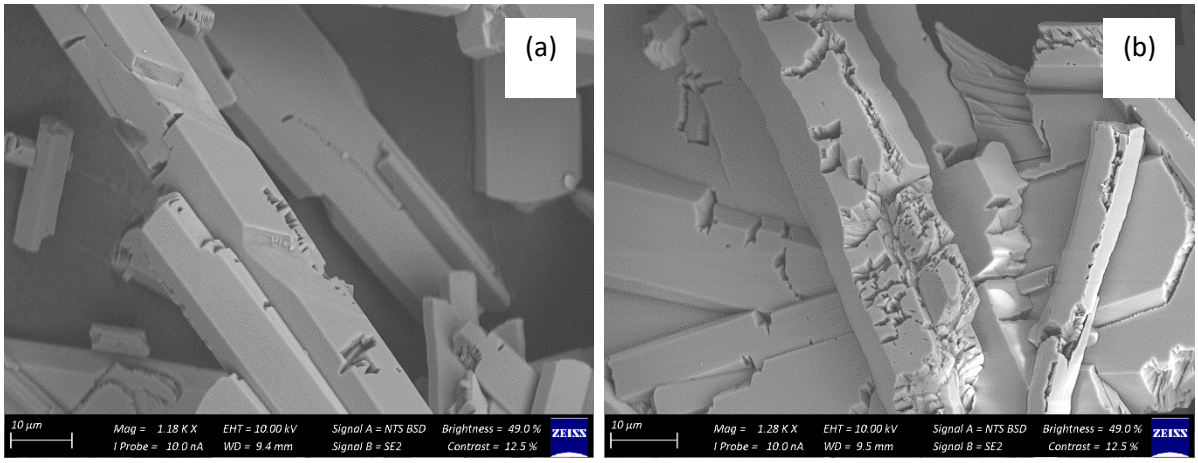

Figure 4.12: *SEM analysis of gypsum crystals formed during the control run in the presence of antiscalant (a) and gypsum crystals formed during experiment 6 when 188 s^{-1} mixing as seed crystal treatment was done for 10 minutes (G* = 1.13).*

The small cavities observed on the crystals after the mixing treatment could be due to two possible causes. Firstly, the cavities could have been formed when the attrition removed the antiscalant that was adsorbed onto the active growth site, leaving a cavity on the crystal where it was removed. Secondly, the cavities could possibly be due to attrition. By creating these cavities, the surface area of the crystals was enhanced, possibly resulting in more active growth sites. The increase in the active growth sites could be the reason for the increase in the average calcium removal that was seen when mixing was applied as a treatment method compared to the control run. The cavities that were found on the seed crystals of the control run are most likely because of collisions between crystals when they were mixed in the reactor during the experimental run. These cavities were, however, still less than those on the crystals that were treated by mixing, since there was no extra mixing applied to the seed crystal mixture of the control.

Figure 4.13 illustrates the effect of the different mixing treatment conditions better than Figure 4.11, since the differences between the mixing speeds and the different mixing times are more evident.

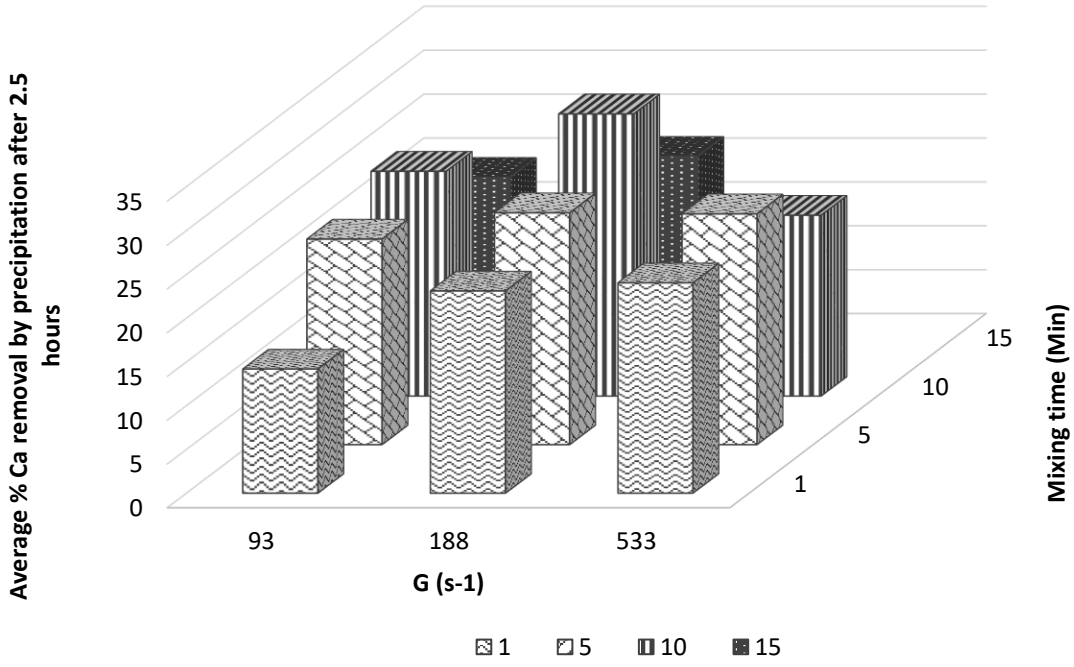

Figure 4.13: *The average percentage calcium removed from solution (SS3) by means of precipitation after 2.5 hours for the 11 experiments that was performed by mixing as treatment method. The effect of variation in mixing speed(rpm) and mixing duration(min) on calcium removal (in the presence of 9 ppm antiscalant and 2000 ppm re-used seeding crystals) is shown.*

It was found that mixing the seed-crystal mixture for 10 minutes at 188 s^{-1} gave the best average calcium removal of 31.4% over the three runs when re-using the seed crystals. However, after ten minutes of treatment a maximum was reached, and calcium removal decreased when the seed crystal mixture was mixed for a longer duration. The average calcium removal increased as the treatment duration increased for the other mixing rates as well, to a maximum at 10 minutes and 5 minutes for 93 s^{-1} and 533 s^{-1}, respectively, after which the average calcium removal decreased again.

It was found that the average calcium removal increased with increasing G-factor when the seed crystal mixture was treated for 1 minute. However, when the seed crystal mixture was treated for 5 minutes or 10 minutes, the average calcium removal increased between G-factors of 93 s^{-1} and 188 s^{-1}, but decreased for G-factors between 188 s^{-1} and 533 s^{-1}.

The findings above were further investigated by analysing the seed crystals to determine the size of the seed crystals after the mixing was applied. The mean crystal size of the unused seed crystals of the control experiment as well as experiment 6 (G* = 1.13) and 9 (G* = 3.20) was determined by means of a Micromeritics® Particle size analyser (Table 4.8).

Table 4.8: *The mean particle size and standard deviation of the seed crystals from the control run in the presence of antiscalant (C) and for experiment 6 (G* = 1.13) and experiment 9 (G* = 3.20).*

Sample	Control Run (C)	Experiment 6 (G* =1.13)	Experiment 9 (G* = 3.20)
Mean particle size (μm)	79.79	78.62	72.55
Standard deviation of 3 (μm)	6.128	6.473	4.975

The seed crystals from the control experiment had the largest mean particle size, followed closely by those from experiment 6 (G* = 1.13) and then, with a more substantial decrease in mean particle size, those from experiment 9 (G* = 3.20) (Table 4.8). According to Mullin (1972), crystal growth increases with an increase in the size of the seed crystals. The control run should have had the highest crystal growth rate and thus also the highest amount of calcium removal, as it had the largest mean particle size. However, from Figures 4.11 and 4.13, it is clear that experiment 6 (G* = 1.13) had the highest average percentage calcium removal, although the mean particle size was slightly lower than that of the control run. A substantial decrease in the mean particle size as well as in the average calcium removal was found between experiment 6 (G* = 1.13) and 9 (G* = 3.20). This shows that the particle size did affect the precipitation.

The particle size analysis showed a possible reason for the decrease in calcium removal when the seed crystal mixture was mixed for too long. The seed crystals can only handle a certain amount of time and intensity of the mixing treatment before breaking down into smaller crystals, at which point the crystal growth rate and calcium removal will decrease (Mullin, 1972). This could explain the decrease in the average calcium removal between experiments 3 (G* = 0.56) and 27 (G* = 0.84), experiments 6 (G* = 1.13) and 26 (G* = 1.69), and experiments 8 (G* = 1.60) and 9 (G* = 3.20). Furthermore, this could also explain the decrease in the calcium removal between experiments 5 (G* = 0.56) and 8 (G* = 1.60), and experiments 6 (G* = 1.13) and 9 (G* = 3.20), where the mixing speed was increased. This increase in mixing speed results in an increase in the intensity of the treatment, causing the crystals to break down.

The increase in the calcium removal between experiments 1 (G* = 0.06), 2 (G* = 0.28) and 3 (G* = 0.56), as well as between experiments 4 (G* = 0.11), 5 (G* = 0.56) and 6 (G* = 1.13), as well as between experiments 7 (G* = 0.32) and 8 (G* = 1.60), could be due to the increase in treatment time. Attrition increases with time, causing more of the cavities seen in Figure 4.12 to form. This could possibly increase the amount of crystal growth sites leading to an increase in calcium removal. The amount of cavities formed will increase with the increase in time until the duration of the treatment exceeded a point where the crystals will start to break down. The similar argument could be made for the increase in the calcium removal between experiments 1 (G* = 0.05),4 (G* = 0.11) and 7 (G* = 0.32),

as well as between experiments 2 (G* = 0.28) and 5 (G* = 0.56), and as well as between experiments 3 (G* = 0.56) and 6 (G* = 1.13), where the mixing speed was increased. This increase in mixing speed led to an increase in attrition intensity. As the intensity increased, the crystals collided more with one another, the impeller and the container walls, causing the cavities (Figure 4.12) to form. These cavities increased the amount of crystal growth sites, which resulted in more calcium removal. However, as is the case for mixing time, the mixing intensity also has a limit where it becomes too much for the crystals, and they start to break down.

Since the increase in calcium removal was possibly due to the collisions between the crystals when the seed crystal mixture was vigorously mixed, the force of the mixing was investigated by considering Relative Centrifugal Forces (RCF) as well as G-factors.

The RCF was calculated by using equation 2.20, based on the speed and size of the magnetic stirrer bar (r = 0.015 m), which generated the different mixing speeds that were used for the treatments (Table 4.9).

$$RCF = RPM^2 \times 1.118 \times 10^{-5} \times r \qquad [2.20]$$

Furthermore, the G-factors (s^{-1}) was investigated for the different treatments by using equation 2.21.

$$G = \sqrt{\frac{P}{V\mu}} \qquad [2.21]$$

Where G is the G-factor measured in s^{-1}, V is the volume of 0.12 L and μ the viscosity of the liquid. The impeller power (P) was calculated by using equation 2.22.

$$P = N_P \times \rho \times n^3 \times d^5 \qquad [2.22]$$

Where the power number (N_P) of the stirrer was found to be 0.5 (CerCell, 2019; Pandey, 2019) as the seed crystal mixture was mixed with the simplest axial mixer. The density (ρ) was calculated to be 1053 kg/m^3. The agitation speed (n) was measured in revolutions/second and the impeller diameter (d) in meters.

Using equation 2.21 and equation 2.22, the impeller power and the G-factors for the different treatments were calculated (Table 4.9).

Table 4.9: *The Relative Centrifugal Forces (RCF), power and G-factors for the different stirring speeds used during mixing as seed crystal treatment.*

rpm	250	400	800
RCF (x g)	0.01	0.03	0.11
P (mW)	0.9	3.8	30.3
G-factor (s^{-1})	93	188	533

The RCF of 0.01 times gravity that was experienced at 250 rpm was found to be less than half of the 0.03 times gravity experienced at a mixing speed of 400 rpm, and then the RCF of 0.11 times gravity at 800 rpm is almost five times that of the RCF at 400 rpm. Thus, the RFC increases drastically as the mixing speed increases.

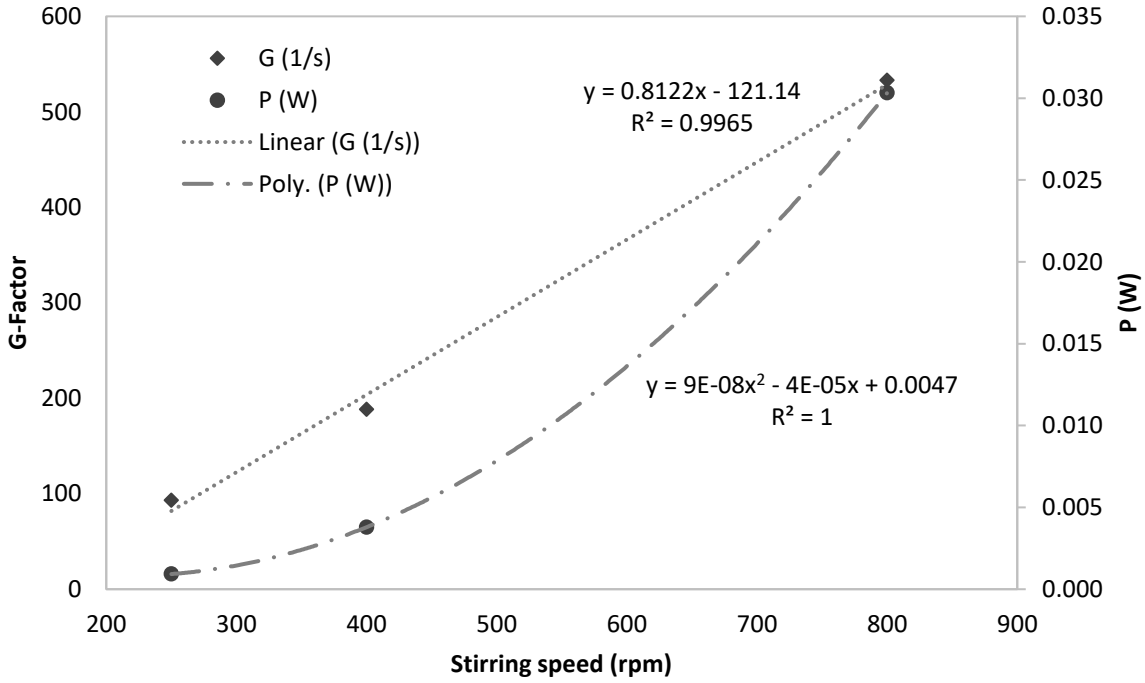

Figure 4.14: *The relation between the power and the stirring speed and between the G-factors and the stirring speed for the different stirring speeds used during mixing as seed crystal treatment.*

Figure 4.14 shows that the relation between impeller power (P) and the stirrer speed is of the second order, whereas the relation between the G-factor and the stirrer speed is linear with and R^2 value of 0.9965.

The relation between the specific G-factor (G*) and the average % calcium removed (Figure 4.15) shows that the average calcium removal percentage increased as the specific G-factor increased up until a G* value of 1.13. A further increase in the specific G-factor led to a decrease in average calcium removal.

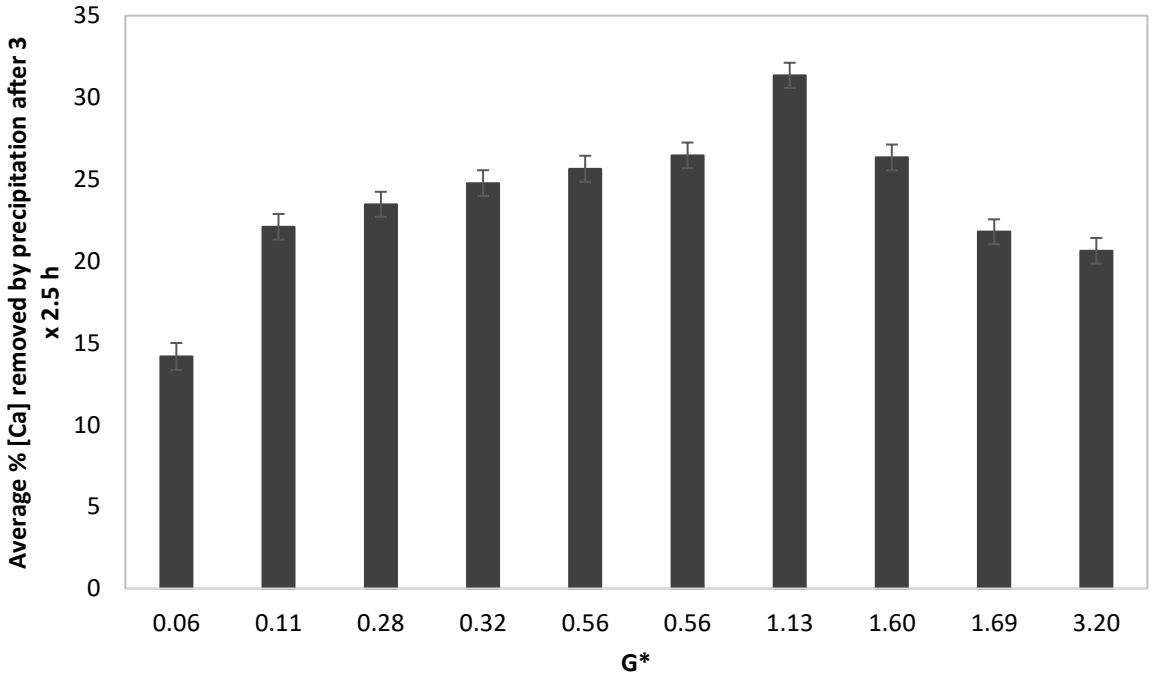

Figure 4.15: *Average calcium removal by means of precipitation after three 2.5 hour runs with physical treatments at different G* values.*

From the results (Figure 4.11 and Figure 4.15) the mixing treatment condition for optimum calcium removal was found to be mixing at a G-factor of 188 s^{-1} for 10 minutes, resulting in a specific G-factor (G*) of 1.13 for maximum average calcium removal over the three runs. This finding once again confirms that attrition did have an influence on the results of the evaluation of mixing as a treatment method.

4.3.1.1 Significant difference

An analysis of variance (ANOVA) was done on the average calcium removed values for the 11 runs as well as the control to determine if there is a significant difference between the values. The ANOVA table (Table 4.10) shows a p-value of 1.76 x 10^{-12}, which indicates that at least one significant difference was found between two values.

Table 4.10: *ANOVA results for the average percentage calcium removal of the control runs and the 11 experiments where mixing was performed as seed crystal treatment.*

Source of Variation	*SS*	*df*	*MS*	*F*	*P-value*	*F crit*
Between Groups	761.29	9	84.59	103.99	1.76 x 10^{-12}	2.54
Within Groups	13.02	16	0.81			
Total	774.30	25				

To specifically see if there is a significant difference between the control and the best result, a t-test was performed with a significance level of 0.05. The t-test had a p-value of 2.97×10^{-6}. This is smaller than 0.05, which confirms that there is a significant difference between the data obtained from the control experiment and experiment 6 (G* = 1.13). The full results of the t-test can be seen in Appendix D.

4.3.1.2 Repeatability of mixing as seed crystal treatment method

To increase confidence in the data obtained when mixing was applied as seed crystal treatment method, experiment 6 (G* = 1.13) was repeated. The percentage calcium removal of each experimental run, as well as the average calcium removal, were compared (Table 4.11). The data obtained from this repeat run showed that the data were repeatable within 3% accuracy.

Table 4.11: *The stirrer speed and duration of the mixing treatment, initial and final calcium concentrations, percentage calcium removed and the average percentage calcium removed for the three runs where seed crystals were re-used for experiment 6 (G* = 1.13) and the repeat of the experiment (experiment 6').*

Run	Crystal treatment		Calcium conc. (ppm) @ 5 min	Calcium Conc. (ppm) @ 150 min	% Calcium removed	Average % Calcium removal
	G-factor (s^{-1})	Time (min)				
6.1			1707.37	1014.73	40.6	
6.2	188	10	1670.50	1209.06	27.6	31.3
6.3			1687.65	1251.01	25.9	
6.1'			1740.35	1036.93	40.4	
6.2'	188	10	1738.94	1225.85	29.5	32.2
6.3'			1757.63	1290.21	26.6	

The desupersaturation curves of the three different runs for each of the experiments were also compared (Figure 4.16). This shows that the experiment is repeatable since all the results of the repeat experiment were within the uncertainty of the first experiment.

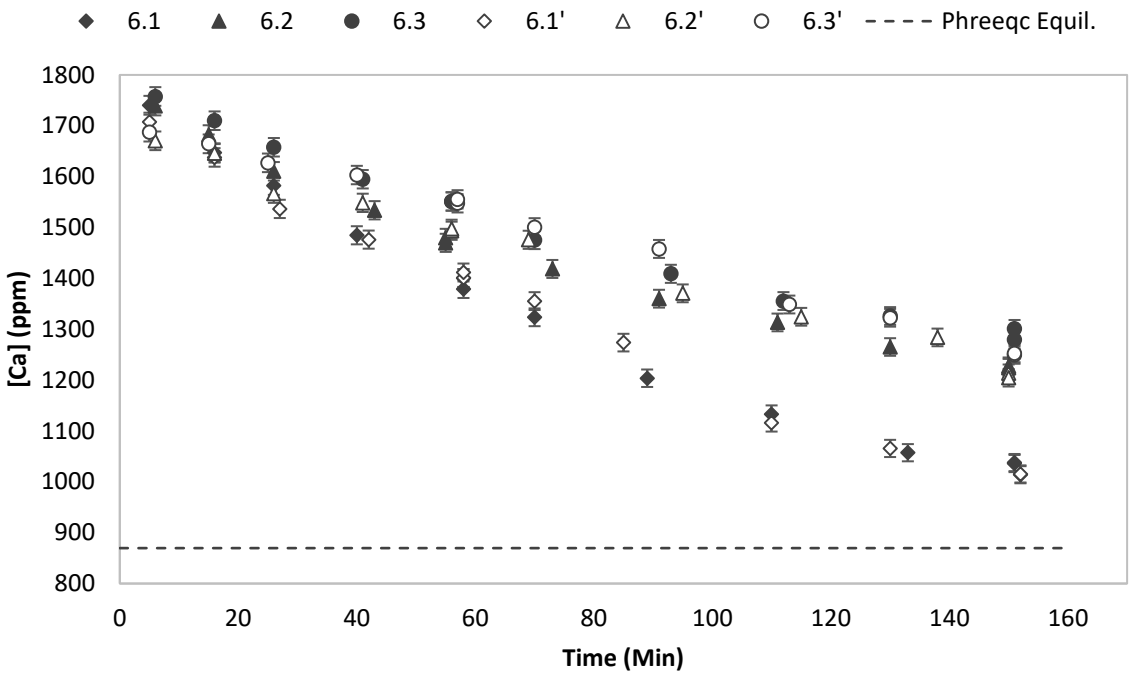

Figure 4.16:*The desupersaturation curve for experiment 6 and the repeat of the experiment (6') at three times gypsum saturation, with 2000 ppm seeding. The numbers (1), (2) and (3) are the number of seed crystal re-uses, treated at 188 s^{-1} for 10 minutes, including the equilibrium concentration (SS3) as calculated by Phreeqc.*

4.3.2 Air scouring as seed crystal treatment method

Air scouring as a seed crystal treatment method was evaluated by nine experimental runs as detailed in Table 4.12. All of these experiments were performed at a controlled temperature of 25˚C and an uncontrolled pH around 4.9 in the presence of 2000 ppm (dry base) seeding. The experiments were done at different air fluxes (F) and for different durations, resulting in different specific air fluxes (F*) reported as F* = F x t.

Table 4.12: *Experiment numbers for air scouring as seed crystal treatment with the flux at STP.*

	Air flux (m/h)		
Time (min)	15.6	62.4	155.9
1	10.1 - 10.3	13.1 - 13.3	16.1 - 16.3
5	11.1 - 11.3	14.1 -14.3	17.1 - 17.3
10	12.1 - 12.3	15.1 -15.3	18.1 - 18.3

The efficiency of air scouring as a treatment method was determined by the amount of calcium removed, assuming an equal sulphate removal. The growth rate constant and the average calcium

removal for the three runs were also calculated. A summary of the data is detailed in Table 4.13, which shows the air flux and duration of the air scouring treatments, initial and final calcium concentrations, percentage calcium removed, as well as the average percentage calcium removed for the three runs where seed crystals were re-used. Furthermore, the growth rate constant of the control experiments and the experiments performed with air scouring as seed crystal treatment is also shown. The full set of experimental data is provided in Appendix B.

Table 4.13: *Summary of the experimental data for the evaluation of air scouring as seed crystal treatment.*

Exp.	Crystal treatment		Calcium conc. (ppm) @ 5 min	Calcium Conc. (ppm) @ 150 min	% Calcium removed	Average % Calcium removal	k' ($l.mol^{-1}.min^{-1}$)
	Air flux (m/h)	Time (min)					
C.1'	No antiscalant		1717.51	986.84	42.5	42.8	1.927
C.2'			1718.67	988.08	42.5		1.917
C.3'			1738.99	985.88	43.3		1.856
C.1	9 ppm antiscalant		1606.10	1305.68	18.7	15.3	0.259
C.2			1634.14	1391.21	14.9		0.168
C.3			1647.09	1445.15	12.3		0.125
10.1	15.6	1	1614.92	1273.77	21.1	16.2	0.313
10.2			1655.51	1398.75	15.5		0.171
10.3			1667.90	1469.14	11.9		0.115
11.1	15.6	5	1677.33	1276.52	23.9	17.8	0.337
11.2			1640.06	1374.89	16.2		0.188
11.3			1638.44	1421.45	13.2		0.141
12.1	15.6	10	1699.74	1347.49	20.7	16.1	0.245
12.2			1718.82	1448.13	15.8		0.152
12.3			1720.73	1516.60	11.9		0.102
13.1	62.4	1	1639.25	1250.05	23.7	17.6	0.368
13.2			1651.18	1360.97	17.6		0.209
13.3			1678.05	1484.49	11.5		0.108
14.1	62.4	5	1684.24	1305.68	22.5	18.6	0.295
14.2			1686.55	1407.40	16.6		0.176
14.3			1720.23	1433.86	16.7		0.165
15.1	62.4	10	1737.89	1348.68	22.4	16.5	0.259
15.2			1751.35	1485.81	15.2		0.135
15.3			1764.00	1555.55	11.8		0.094
16.1	155.9	1	1691.61	1384.78	18.1	15.45	0.200
16.2			1735.32	1461.54	15.8		0.148
16.3			1739.05	1521.06	12.5		0.106
17.1	155.9	5	1718.96	1307.84	23.9	15.8	0.305
17.2			1732.97	1489.58	14.0		0.126
17.3			1763.85	1597.38	9.4		0.071

Exp.	Crystal treatment		Calcium conc. (ppm) @ 5 min	Calcium Conc. (ppm) @ 150 min	% Calcium removed	Average % Calcium removal	k' ($l.mol^{-1}.min^{-1}$)
	Air flux (m/h)	Time (min)					
18.1			1801.64	1395.21	22.6		0.229
18.2	155.9	10	1769.51	1529.62	13.6	15.5	0.112
18.6			1795.22	1607.95	10.4		0.076

*The control experiment and experiment 13 were repeated to verify repeatability and to increase the confidence in the data.

Similar to the trends found with the control run and with mixing as seed crystal treatment method, Table 4.14 and Figure 4.17 show the decrease in the calcium removal when the crystals were re-used. The results were found to be very close to one another with all but experiment 12 (F* = 2.60 m) and 16 (F* = 2.60 m) being within the uncertainty of one another for the first run. A maximum of 23.9% calcium removal was found for experiment 17 (F* = 12.99 m) when air was sparged through the seed-crystal mixture at 155.9 m/hr for 5 minutes. However, the calcium removal then decreased to 14.0% and 9.4% for the second and third runs, respectively. This means a 10% decrease from the first to the second re-use and then a further 5% decrease from the second to the third time the crystals were re-used. Similar to when mixing was used as a treatment method, a drastic decrease in the calcium removal was found between the first and second re-use. However, unlike the mixing findings, the decrease between the second and the third re-use was also drastic. The decreasing effectiveness of the seed crystals could be the result of the antiscalant inhibiting the growth by reducing the number of active growth sites, as discussed in Section 4.2 (Kucera, 2015).

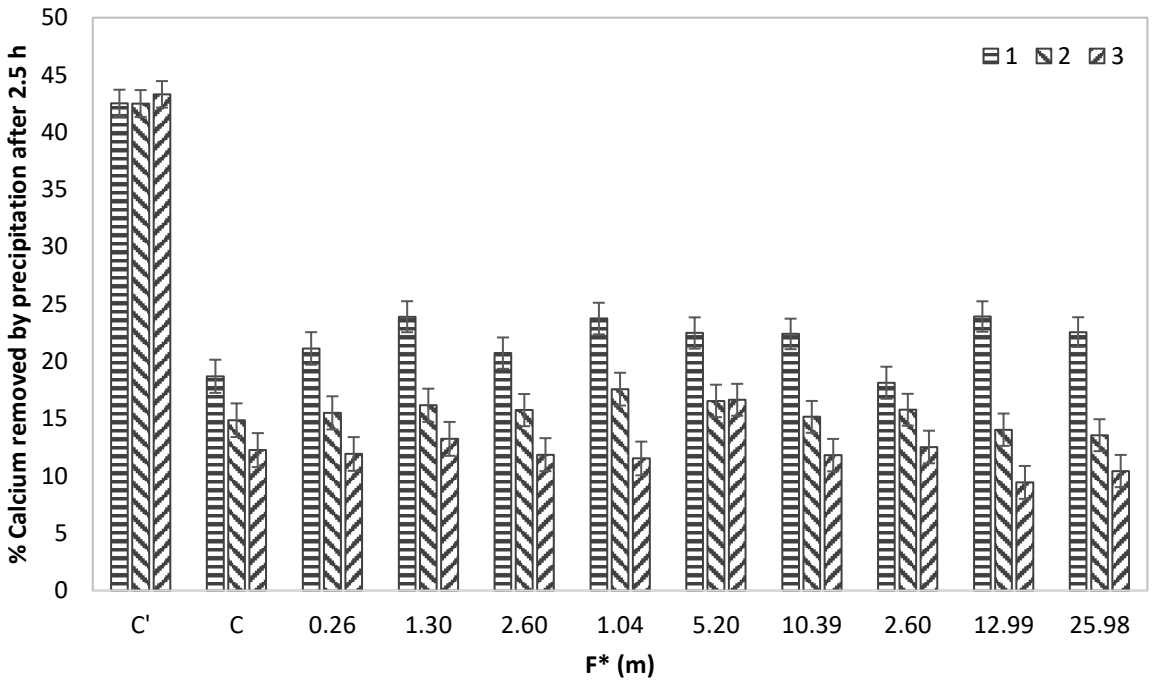

Figure 4.17:*The percentage calcium removed from solution (SS3) by means of precipitation after 2.5 hours of the control runs and the 9 experiments performed with air scouring as treatment method (in the presence of 9 ppm antiscalant, with 2000 ppm seeding) where (1) was the first re-use of seed crystals, (2) the second and (3) the third re-use of seed crystals.*

The average percentage calcium removed for the three runs done for each experiment was compared to both control runs, where no treatments were done in the presence and absence of antiscalant (Figure 4.18). It is clear that the average calcium removal for all the experiments where air scouring was applied as seed crystal treatment was found to be very similar to the 15.3% average calcium removed in the presence of antiscalants, showing little to no increase. All the experiments, except for experiments 11 (F* = 1.30 m), 13 (F* = 1.04 m) and 14 (F* = 5.20 m), were found to be within the uncertainty of the control run. The calcium removal of the experiments was also found to be much lower than the average calcium removal of 42.8% in the absence of antiscalant. From Figure 4.18 air scouring was found to be an unsuccessful seed crystal treatment method. When compared to the control, it increased the calcium removal by maximum 3%, and an increase in the calcium removal was only seen for experiments 11 (F* = 1.30 m), 13 (F* = 1.04 m) and 14 (F* = 5.20 m). The other experiments resulted in the same or less calcium removal than the control experiment in the presence of antiscalant.

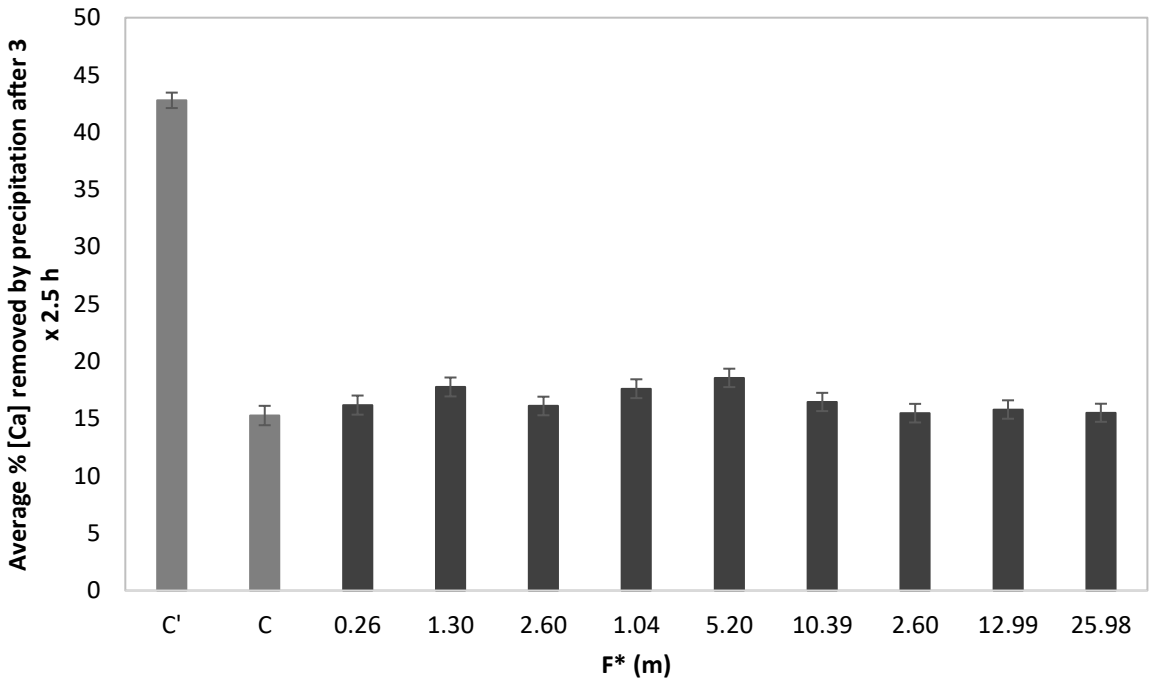

Figure 4.18: *The average percentage calcium removed from solution (SS3) by means of precipitation after 2.5 hours of the control runs and the 9 experiments performed with air scouring as treatment method (in the presence of 9 ppm antiscalant, with 2000 ppm re-used seeding crystals).*

When air scouring was used as a seed crystal treatment, the calcium removal neither increased nor decrease compared to the control experiment in the presence of antiscalant. This was further investigated by means of SEM analysis. For the control experiment and experiment 10 (F* = 0.26 m), the SEM analysis produced Figure 4.19. These images show that the seed crystals of the control run (Figure 4.19 [a]) as well as the seed crystals where air scouring was applied (Figure 4.19 [b]), show no structural difference and are similarly shaped tube-shaped crystals. Furthermore, no physical differences were observed either between the seed crystals from experiment 10 (F* = 0.26 m) and the seed crystals from the control experiment in the presence of antiscalant.

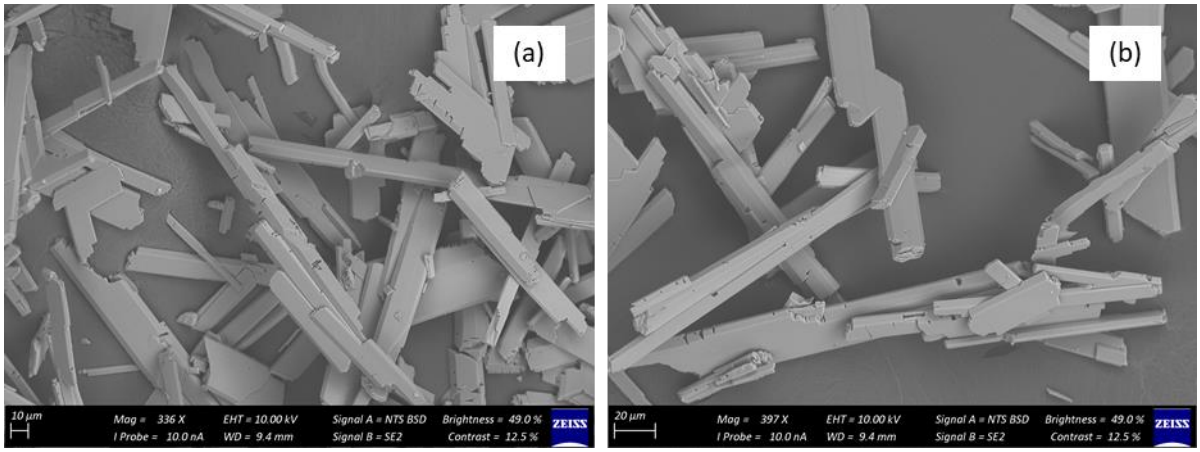

Figure 4.19: *SEM analysis of gypsum crystals formed during the control run in the presence of antiscalant (a) and gypsum crystals formed during experiment 10 (F* = 0.26 m) when 15.6 m/h of air was sparged through the seed crystal mixture for 1 minute (b).*

Cavities on the seed crystals of experiment 10 (F* = 0.26 m) were expected, since the air scouring may also cause some attrition. However, the amount of cavities that were seen in the photos of seed crystals of experiment 10 were very similar to that of the control run.

The SEM analysis did not provide more clarity on the results. Therefore, a further investigation was done into the seed crystal size. The mean crystal size of the unused seed crystals of the control experiment as well as experiment 10 (F* = 0.26 m) was determined by means of a Micromeritics® Particle size analyser (Table 4.14).

Table 4.14: *The mean particle size and standard deviation of the seed crystals from the control run in the presence of antiscalant (C) and experiment 10.*

Sample	Control Run	Experiment 10 (F* = 0.26 m)
Mean particle size (μm)	79.79	79.21
Standard deviation of 3 (μm)	6.128	5.188

The mean particle size of experiment 10 (F* = 0.26 m) was found to be very similar to the mean particle size of the control run, with the two values differing by 0.58 μm (Table 4.14).

From the findings above it can be concluded that the air treatment did not do anything to either decrease or increase the calcium removal and was unsuccessful as a seed crystal treatment.

4.3.2.1 Repeatability of air scouring as seed crystal treatment method

It was more difficult to repeat the results when air scouring was applied as seed crystal treatment method compared to when mixing was used as a seed crystal treatment method. The percentage calcium removal of both experimental runs, as well as the average calcium removal for experiment 13 (F* = 1.04 m) are compared (Table 4.15). Table 4.15 shows the air flow flux and duration of the air

scouring treatment, the initial and final calcium concentrations, the percentage calcium removed and the average percentage calcium removed for the three runs where seed crystals were re-used for experiment 13 (F* = 1.04 m) and the repeat of the experiment (experiment 13').

Table 4.15: *Experimental data for the evaluation of the repeatability of air scouring as a crystal treatment method.*

Run	Crystal treatment		Calcium conc. (ppm) @ 5 min	Calcium Conc.(ppm) @ 150 min	% Calcium removed	Average % Calcium removal
	Air flux (m/h)	Time (min)				
13.1	62.4	1	1639.25	1250.05	23.7	17.6
13.2			1651.18	1360.97	17.6	
13.3			1678.05	1484.49	11.5	
13.1'	62.4	1	1586.70	1179.66	25.7	20.8
13.2'			1647.17	1301.72	21.0	
13.3'			1680.03	1415.37	15.8	

The desupersaturation curves of the three different runs for each of the experiments were also compared (Figure 4.20). This shows some repeatability, but not as clear as it should be. There is a possibility that the slight lack in the repeatability is due to the air distribution during the treatment.

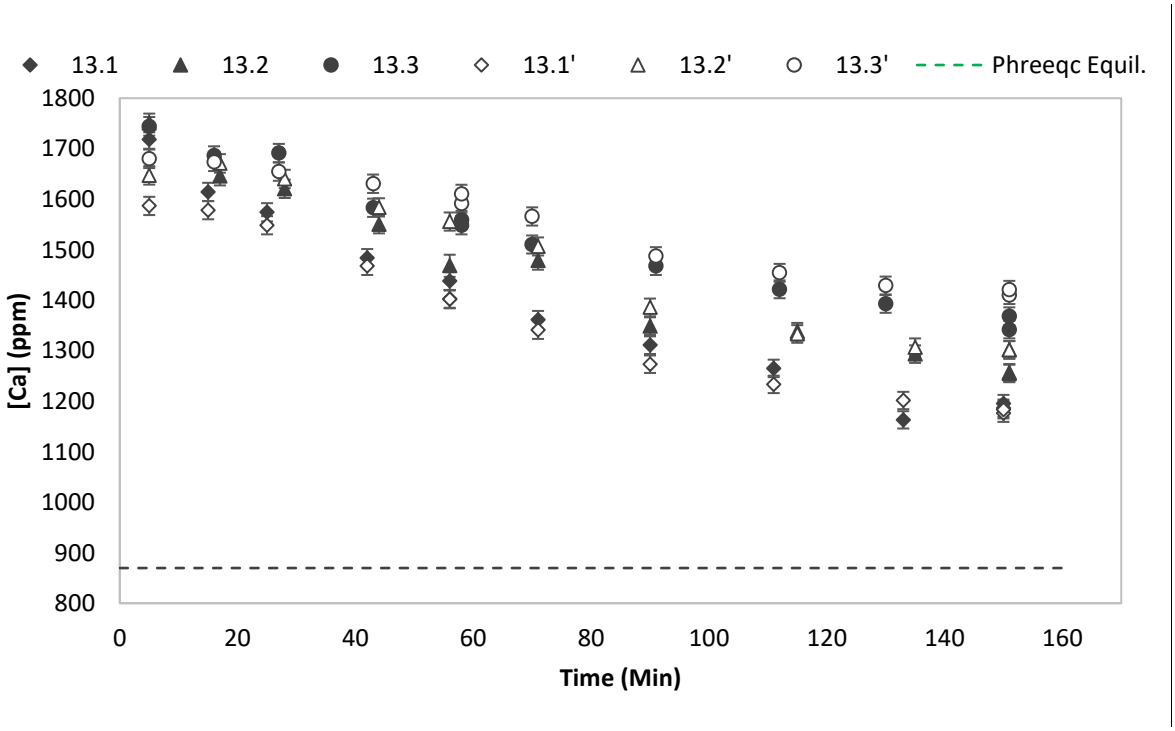

Figure 4.20: *The desupersaturation curve for experiment 13 and the repeat of the experiment (13') at three times gypsum saturation (with 2000 ppm seeding) where (1), (2) and (3) are the number of seed crystal re-uses that was treated at F = 62.4 m/h for 5 minutes, including the equilibrium concentration (SS3) calculated by Phreeqc.*

4.4 Effect of chemical dosing

4.4.1 In the presence of hydrogen peroxide

Gypsum crystallisation in the presence of hydrogen peroxide was evaluated by three experimental runs as detailed in Table 4.16. All of these experiments were performed at a controlled temperature of 25˚C and an uncontrolled pH around 4.8. All experiments were done in the presence of 2000 ppm (dry base) seeding crystals.

Table 4.16: *Experiment numbers in the presence of hydrogen peroxide.*

Concentration H_2O_2 (ppm)	
45 ppm (5 mg/mg antiscalant)	19.1 - 19.3
90 ppm (10 mg/mg antiscalant)	20.1 - 20.3
135 ppm (15 mg/mg antiscalant)	21.1 - 21.3

The influence of the presence of hydrogen peroxide was determined by the amount of calcium removed, assuming an equal sulphate removal. The growth rate constant and the average calcium removal for the three runs were also calculated. A summary of the data is detailed in Table 4.17. The table shows the concentration of hydrogen peroxide, the initial and final calcium concentrations, the percentage calcium removed, the average percentage calcium removed for the three runs where seed crystals were re-used, and the growth rate constant and pH of the control experiments and the experiments performed in the presence of hydrogen peroxide. The full set of experimental data is provided in Appendix B.

Table 4.17: *Experimental data for the determination of the influence of hydrogen peroxide on gypsum crystallisation.*

Exp.	Hydrogen peroxide addition	Calcium conc. (ppm) @ 5 min	Calcium Conc. (ppm) @ 150 min	% Calcium removed	Average % Calcium removal	k' ($l/mol^{-1}.min^{-1}$)	pH
C.1'	No antiscalant	1717.51	986.84	42.5	42.8	1.927	-
C.2'		1718.67	988.08	42.5		1.917	-
C.3'		1738.99	985.88	43.3		1.856	-
C.1	9 ppm antiscalant	1606.10	1305.68	18.7	15.3	0.259	4.9
C.2		1634.14	1391.21	14.9		0.168	4.9
C.3		1647.09	1445.15	12.3		0.125	4.9
19.1	45 ppm H_2O_2 (5 mg/mg antiscalant)	1718.01	1157.65	32.6	24.4	0.634	4.8
19.2		1719.04	1254.42	27.0		0.393	4.8
19.3		1722.53	1491.24	13.4		0.121	4.8
20.1	90 ppm H_2O_2 (10 mg/mg antiscalant)	1713.32	1165.52	32.0	25.3	0.607	4.7
20.2		1768.33	1311.03	25.9		0.319	4.7
20.3		1754.69	1436.09	18.2		0.176	4.7
21.1	135 ppm H_2O_2 (15 mg/mg antiscalant)	1737.10	1376.56	20.8	15.4	0.227	4.8
21.2		1757.25	1499.93	14.6		0.127	4.8
21.3		1750.00	1561.86	10.8		0.085	4.8

*The control experiment and experiment 20 were repeated to verify repeatability and to increase the confidence in the data.

Similar to the trends found from the physical treatments, Table 4.19 and Figure 4.21 show the decrease in calcium removal when the crystals were re-used. The maximum calcium removal of 32.6% was found for experiment 19 (45 ppm H_2O_2), when 5 mg hydrogen peroxide per milligram of antiscalant was added. Experiment 20 (90 ppm H_2O_2) was similar to experiment 19 (45 ppm H_2O_2), with a calcium removal of 32.0% when 10 mg hydrogen peroxide per milligram of antiscalant was added. For both experiments 19 (45 ppm H_2O_2) and 20 (90 ppm H_2O_2), the calcium removal decreased to 27.0% and 25.9%, respectively, when the crystals were re-used. For the third run, the calcium removal decreased once again, resulting in a removal of 13.4% and 18.2, respectively. The decreasing effectivity of the seed crystals could be the result of the antiscalant inhibiting the growth by reducing the number of active growth sites, as discussed in section 4.2 (Kucera, 2015). The lowest pH of 4.7 was found for experiment 20 (90 ppm H_2O_2) compared to the pH of 4.9 during the control run in the presence of antiscalant. The pH values of the experiments in the presence of hydrogen peroxide decreased by 0.2 compared to the pH of the control experiments.

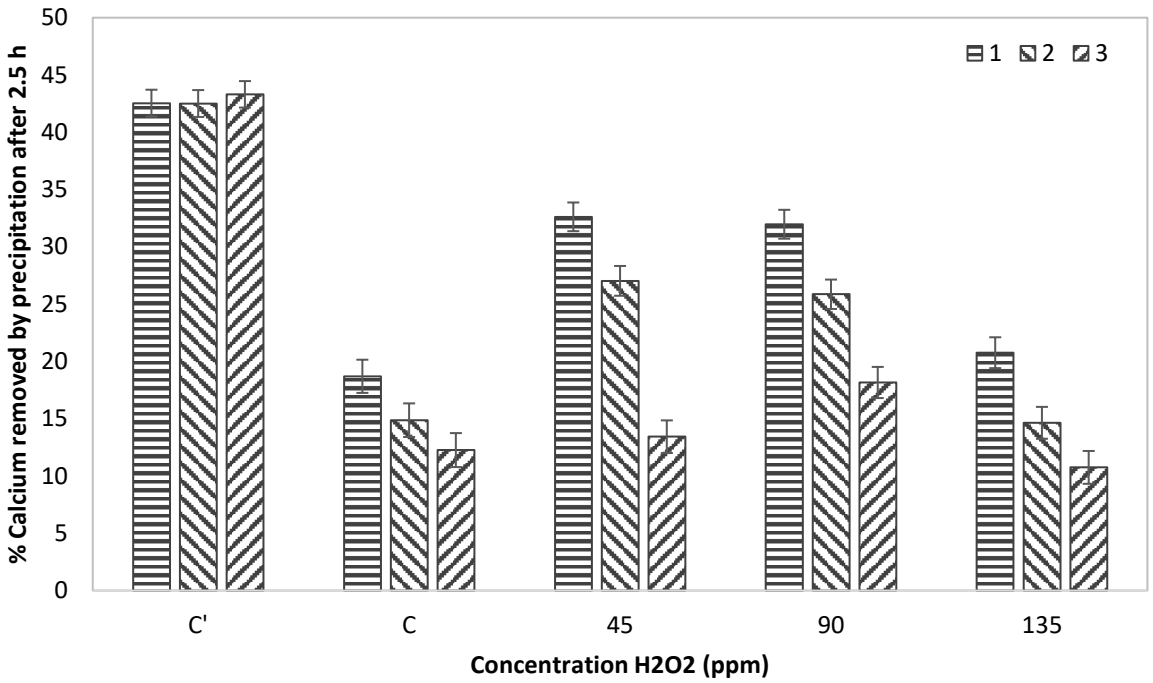

Figure 4.21: *The percentage calcium removed from solution (SS3) by means of precipitation after 2.5 hours of the control runs and the 3 experiments performed in the presence of hydrogen peroxide and 9 ppm antiscalant, with 2000 ppm seeding where (1) was the first re-use of seed crystals, (2) the second and (3) the third re-use of seed crystals.*

The average calcium removal for the three runs done for each experiment was compared to both control runs where no treatments were done in both the presence and absence of antiscalant (Figure 4.22). The average calcium removal in the presence of hydrogen peroxide for all three runs was found to be higher than the 15.3% average calcium removed in the presence of antiscalants, but still lower than the 42.8% average percentage calcium removed in the absence of antiscalant. The highest average calcium removal of 25.3% was found for experiment 20 (90 ppm H_2O_2), when 10 mg hydrogen peroxide per milligram of antiscalant was added. This is almost a 10% increase from the control.

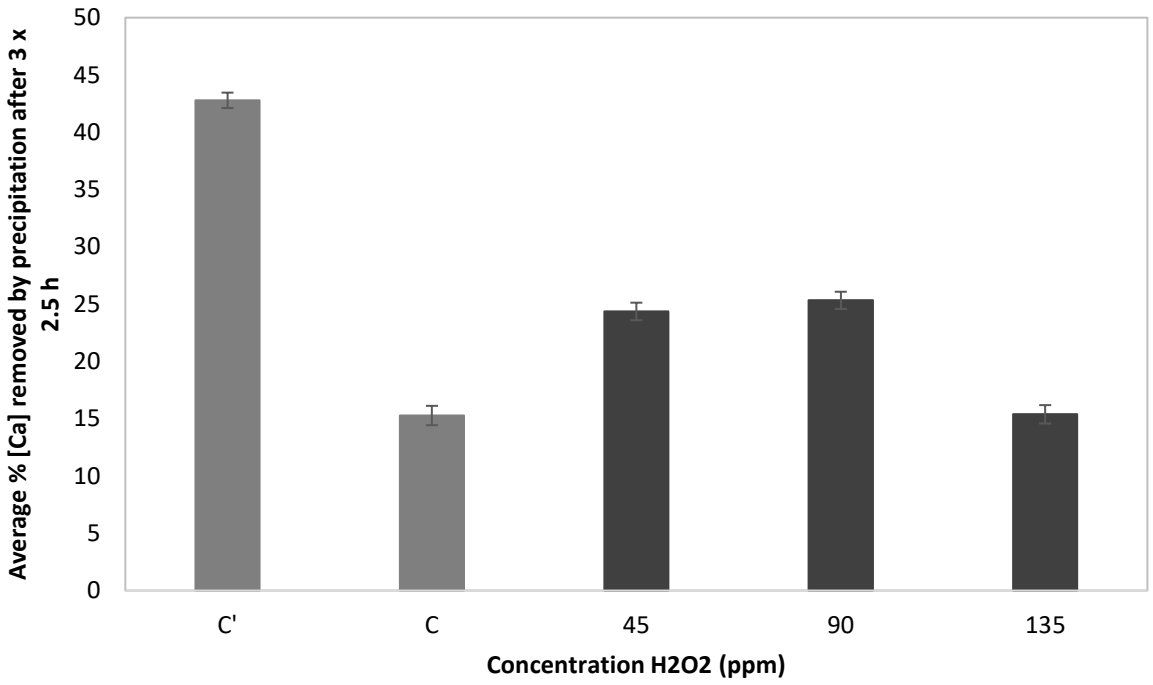

Figure 4.22:*The average percentage calcium removed from solution (SS3) by means of precipitation after 2.5 hours of the control runs and the 3 experiments performed in the presence of hydrogen peroxide and 9 ppm antiscalant, with 2000 ppm re-used seeding crystals.*

There is an increase in the average calcium removal in the presence of hydrogen peroxide compared to the calcium removal of the control in the presence of antiscalant. This could be due to the fact that hydrogen peroxide degrades the antiscalant, thereby allowing more crystallisation to take place, which increases calcium removal. The hydrogen peroxide could degrade the antiscalant in two different ways. Firstly, by lowering the pH in the solution. The effectiveness of the antiscalant is decreased with the decrease in pH (Rosenberg, et al., 2012). Secondly, the hydrogen peroxide could also degrade the antiscalant by undergoing homolytic cleavage, which produces two highly reactive hydroxyl radicals at a lower pH (around 4) and in the presence of sunlight (UV). These hydroxyl radicals drive the advanced oxidation process (AOP) (Lawler, et al., 2010; Jones, 2000). When this oxidation process is applied to an antiscalant, it removes the phosphates from the antiscalant molecules, and this causes the antiscalant to be ineffective (Frost, et al., 1987). It is also possible that a combination of the pH and the hydroxyl radicals can lead to antiscalant degradation since homolytic cleavage is dependent on the pH.

It was previously found that a combination of hydrogen peroxide and metal ions react to degrade the antiscalant completely (Lawler, et al., 2010). However, with the use of pure hydrogen peroxide, the antiscalant was not degraded completely. Better results might be obtained if the antiscalant could be degraded fully by designing the conditions of the experiment to be in favour of the homolytic cleavage process, including a lower pH.

The increase in calcium removal in the presence of hydrogen peroxide compared to the control run in the presence of antiscalant was further investigated by means of SEM analysis. For the control experiment and experiment 20 (90 ppm H_2O_2), the SEM analysis produced Figure 4.23. It can be seen that the seed crystals from the control run (Figure 4.23 [a]) had a different shape than that of the seed crystals in the presence of hydrogen peroxide (Figure 4.23 [b]). The control run seed crystals were found to be more tubular shaped, compared to the plate-shaped crystals of the seed crystals in the presence of the hydrogen peroxide.

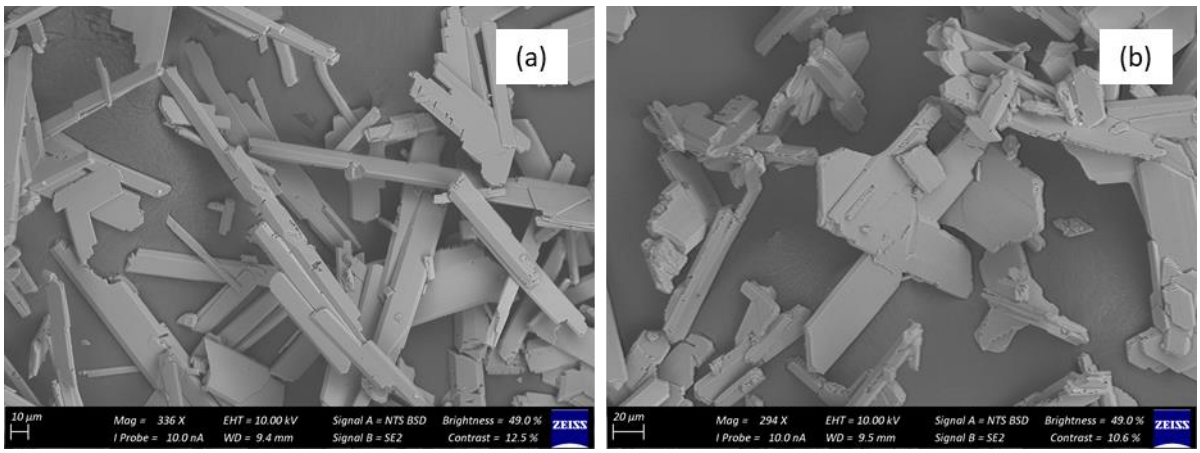

Figure 4.23: *SEM analysis of gypsum crystals formed during the control run in the presence of antiscalant (a) and gypsum crystals formed during experiment 20 (90 ppm H_2O_2) (b).*

A physical difference was found between the seed crystals of the control run in the presence of antiscalant and the seed crystals from experiment 20 (90 ppm H_2O_2) in the presence of hydrogen peroxide. The seed crystals of experiment 20 (90 ppm H_2O_2) were also compared to the seed crystals of the control run in the absence of antiscalant (Figure 4.24). The seed crystals in the absence of antiscalant (Figure 4.24 [a]) were more plate-shaped, similar to the seed crystals in the presence of hydrogen peroxide (Figure 4.24 [b]). Figure 4.24 (a) also shows some smaller and thinner crystals. However, they seem flat and plate-shaped and were possibly still growing.

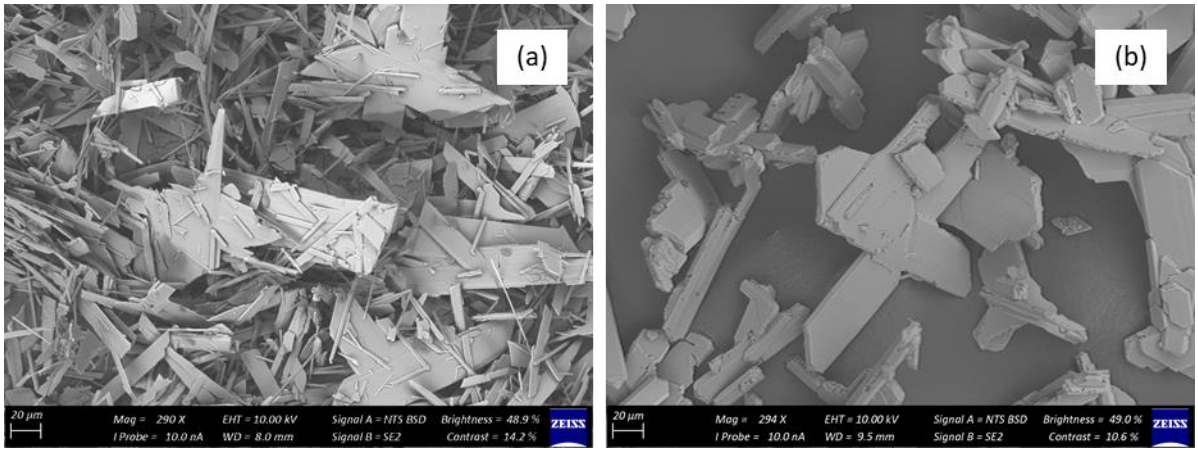

Figure 4.24: *SEM analysis of gypsum crystals formed during the control run in the absence of antiscalant (a) and gypsum crystals formed during experiment 20 in the presence of 90 ppm hydrogen peroxide (b).*

The similarity between the seed crystals in the absence of antiscalant and the seed crystals of experiment 20 (90 ppm H_2O_2) in the presence of hydrogen peroxide show that the antiscalant was degraded. It is however not possible to determine whether the degradation was due to the decrease in the pH of the solution or the formation of hydroxyl radicals.

A drastic decrease in the average calcium removal was seen between experiment 20 (90 ppm H_2O_2) and experiment 21 (135 ppm H_2O_2) (Figure 4.22 and Table 4.19), with calcium removal dropping from 25.3% to 15.4% with an increase in hydrogen peroxide concentration. The drastic decrease in the average calcium removal could be due to an overdose of hydrogen peroxide. The concentration of hydrogen peroxide influenced its efficiency in degrading the antiscalant. Similar results were found when a combination of hydrogen peroxide and ozone were used together. It was found that when the amount of hydrogen peroxide was increased above a certain level, it led to a decrease in the efficiency to degrade the antiscalant (Lawler, et al., 2010). Lawler et al. (2010) also tested the use of pure ozone to degrade antiscalant. A decrease in the degradation of the antiscalant was found when the presence of the ozone was increased from 10 mg of ozone per milligram of antiscalant to 20 mg of ozone per milligram of antiscalant, similar to what was found in experiment 21 (135 ppm H_2O_2).

4.4.1.1 Significant difference

An analysis of variance (ANOVA) was done on the average calcium removed during each of the three runs as well as the control, to determine if there is a significant difference between the values. The ANOVA table (Table 4.18) shows a p-value of 2×10^{-7}, which shows that at least one significant difference was found between 2 values.

Table 4.18: *ANOVA results for the average percentage calcium removal of the control runs and the 3 experiments in the presence of hydrogen peroxide.*

Source of Variation	*SS*	*df*	*MS*	*F*	*P-value*	*F crit*
Between Groups	285.99	3	95.33	155.05	2×10^{-7}	4.07
Within Groups	4.92	8	0.62			
Total	290.91	11				

To specifically see if there is a significant difference between the control and the best result, a t-test was performed at a significance level of 0.05. The t-test had a p-value of 7.04×10^{-4}, which is smaller than 0.05 and this confirms that there is a significant difference between the data obtained from the control experiment and that obtained from experiment 20 (90 ppm H_2O_2). The full results of the t-test can be seen in Appendix D.

4.4.1.2 Repeatability in the presence of hydrogen peroxide

To increase confidence in the data obtained in the presence of hydrogen peroxide, experiment 20 (90 ppm H_2O_2) was repeated. The percentage calcium removal of each experimental run, as well as the average calcium removal were compared (Table 4.19). Table 4.19 shows the concentration of hydrogen peroxide, the initial and final calcium concentrations, the percentage calcium removed and the average percentage calcium removed for the three runs where seed crystals were re-used for experiment 20 and the repeat of the experiment (experiment 20'). The data obtained from the repeat run of the experiment showed that there was a slight difference in the results of experiment 20 and its repeat, but this still falls within the uncertainty of the average calcium removal.

Table 4.19: *Experimental data for evaluation of repeatability in the presence of hydrogen peroxide*

Exp.	**Hydrogen peroxide addition**	**Calcium conc. (ppm) @ 5 min**	**Calcium Conc. (ppm) @ 150 min**	**% Calcium removed**	**Average % Calcium removal**
20.1	90 ppm H_2O_2 (10 mg/mg antiscalant)	1713.32	1165.52	32.0	25.3
20.2		1768.33	1311.03	25.9	
20.3		1754.69	1436.09	18.2	
20.1'	90 ppm H_2O_2 (10 mg/mg antiscalant)	1752.47	1089.31	37.8	26.8
20.2'		1724.25	1278.01	25.9	
20.3'		1766.56	1472.41	16.7	

The desupersaturation curves of the three different runs for each of the experiments were also compared (Figure 4.25). The data show fairly good repeatability for the second and third run, with the data falling within the uncertainty. Some deviation was found for the first experimental run. The

desupersaturation curve, as well as the calcium removal calculated for the different runs (Table 4.19) show a slight deviation.

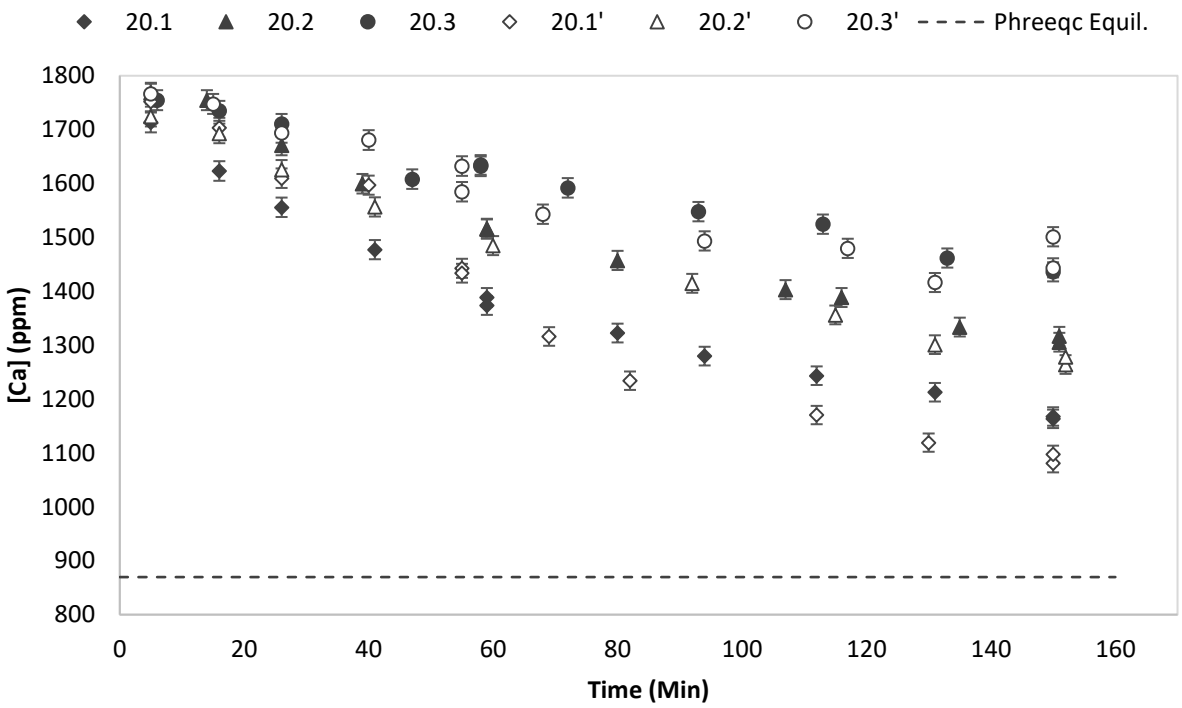

Figure 4.25: *The desupersaturation curve for experiment 20 and the repeat of the experiment (20') at three times gypsum saturation, with 2000 ppm seeding where (1), (2) and (3) are the number of seed crystal re-uses (in the presence of 90 ppm hydrogen peroxide, including the equilibrium concentration calculated by Phreeqc).*

4.4.2 In the presence of aluminum

Gypsum crystallisation in the presence of aluminum was evaluated by four experimental runs as detailed in Table 4.20. All of these experiments were performed at a controlled temperature of 25˚C and an uncontrolled pH around 4.4. All experiments were done in the presence of 2000 ppm (dry base) seeding.

Table 4.20: *Experiments in the presence of aluminum.*

Concentration Al (ppm)	Experiment	Source
4.5 ppm (0.5 mg/mg antiscalant)	22.1 - 22.3	$AlCl_3$
9 ppm (1 mg/mg antiscalant)	23.1 - 23.3	$AlCl_3$
18 ppm (2 mg/mg antiscalant)	24.1 - 24.3	$AlCl_3$
4.5 ppm (0.5 mg/mg antiscalant)	25.1 - 25.3	$Al_2(SO_4)_3 . nH_2O$

The influence of the presence of aluminum was determined by the amount of calcium removed, assuming an equal molar of sulphate removal according to the stoichiometry. The growth rate constant and the average calcium removal for the three runs were also calculated. A summary of the

data is provided in Table 4.21. The table shows the concentration of aluminum, the initial and final calcium concentrations, the percentage calcium removed, the average percentage calcium removed for the three runs where seed crystals were re-used, and the growth rate constant and pH of the control experiments and the experiments performed in the presence of aluminum. The full set of experimental data is provided in Appendix B.

Table 4.21: *Summary of the experimental data for evaluation of crystallisation in the presence of aluminum.*

Run	Aluminum	Calcium conc. (ppm) @ 5 min	Calcium Conc. (ppm) @ 150 min	% Calcium removed	Average % Calcium removal	k' ($l.mol^{-1}.min^{-1}$)	pH
C.1'		1717.51	986.84	42.5		1.927	-
C.2'	No antiscalant	1718.67	988.08	42.5	42.8	1.917	-
C.3'		1738.99	985.88	43.3		1.856	-
C.1		1606.10	1305.68	18.7		0.259	4.9
C.2	9 ppm antiscalant	1634.14	1391.21	14.9	15.3	0.168	4.9
C.3		1647.09	1445.15	12.3		0.125	4.9
22.1	4.5 ppm Al	1623.93	936.41	42.3		3.776	4.6
22.2	0.5 mg/mg antisc.	1639.39	955.40	41.7	41.2	2.866	4.6
22.3	$AlCl_3$	1645.34	992.91	39.7		1.887	4.5
23.1	9 ppm Al	1620.64	986.03	39.2		2.008	4.4
23.2	1 mg/mg antisc.	1628.42	1005.29	38.3	38.9	1.674	4.4
23.3	$AlCl_3$	1658.57	1006.72	39.3		1.667	4.4
24.1	18 ppm Al	1604.45	956.48	40.4		2.809	4.4
24.2	2 mg/mg antisc.	1587.28	974.79	38.6	38.6	2.245	4.4
24.3	$AlCl_3$	1617.84	1020.06	37.0		1.469	4.4
25.1	4.5 ppm Al	1686.13	957.51	43.2		2.809	4.4
25.2	0.5 mg/mg antisc.	1667.87	1016.82	39.0	39.3	1.532	4.4
25.3	$Al_2(SO_4)_3.nH_2O$	1647.80	1062.04	35.6		1.082	4.4

*The control experiment and experiment 23 were repeated to verify repeatability and to increase the confidence in the data.

Unlike the trends found with the physical treatment methods and in the presence of hydrogen peroxide, Table 4.21 and Figure 4.26 barely show any decrease in the calcium removal when the crystals were re-used compared to the control run in the presence of antiscalant. Most of the results lie within the experimental uncertainty range. The maximum calcium removed was found for experiment 25 when 43.2% of calcium was removed in the presence of 4.5 ppm aluminum. For this experiment 0.5 mg aluminum was added per milligram of antiscalant in the form of aluminum sulphate. However, experiment 22 delivered similar results by removing 42.3% calcium in the presence of 4.5 ppm aluminum, when 0.5 mg aluminum per milligram of antiscalant was added in the form of aluminum chloride. For both these experiments, the calcium removal barely decreased to

39.0% and 41.7% for the second run, respectively. For the third re-use of the seed crystals, the decrease was once again minimal, delivering a removal of 35.5% and 39.7%, respectively. The slight decrease in the effectiveness of the seed crystals could be the result of the antiscalant, as discussed in section 4.2 (Kucera, 2015). Since the decrease is so minimal, it is possible that the presence of aluminum ions caused the antiscalant to be ineffective. The same observation can be made from the data of the growth rate constant (k') in Table 4.26. This data shows that the effectiveness of the seed crystals decreases slightly with their re-use in the presence of aluminum ions. The lowest pH of 4.4 was found for experiment 23 (9 ppm Al) and experiment 25 (4.5 ppm Al) compared to the pH of 4.9 during the control run in the presence of antiscalant. The pH values of the experiments in the presence of aluminum decreased by 0.5 compared to the pH of the control experiment in the presence of antiscalant.

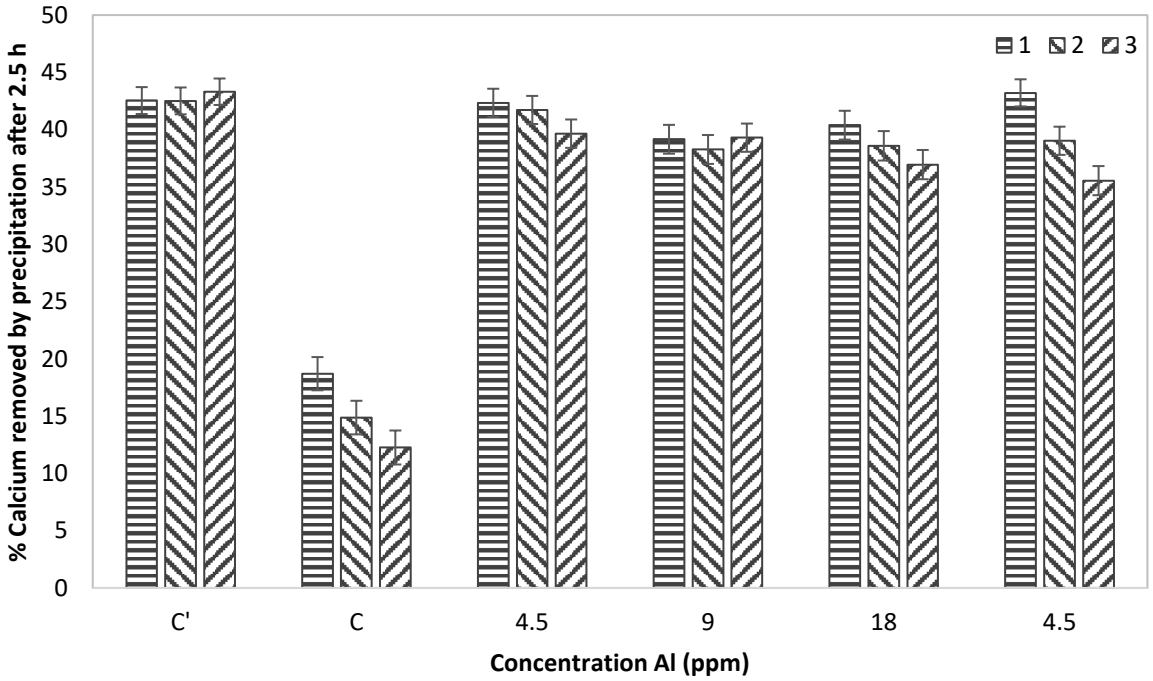

Figure 4.26: *The percentage calcium removed from solution (SS3) by means of precipitation after 2.5 hours of the control runs and the 4 experiments performed in the presence of aluminum and 9 ppm antiscalant (with 2000 ppm seeding) where (1) was the first re-use of seed crystals, (2) the second and (3) the third re-use of seed crystals.*

The average percentage calcium removed for the four runs of each experiment was compared to both control experiments where no treatments were done in the presence and absence of antiscalant (Figure 4.27). The calcium removal in the presence of aluminum for all four runs was found to be much higher than the 15.3% average calcium removal of the control run in the presence of antiscalants. However, this was still slightly lower than the 42.8% average calcium removal of the control run in the absence of antiscalant. The highest average calcium removal was found in experiment 22 (41.2%),

where 0.5 mg of Al per milligram of antiscalant was present in the form of aluminum chloride (4.5 ppm Al). This is only 1.6% less than the control in the absence of antiscalant.

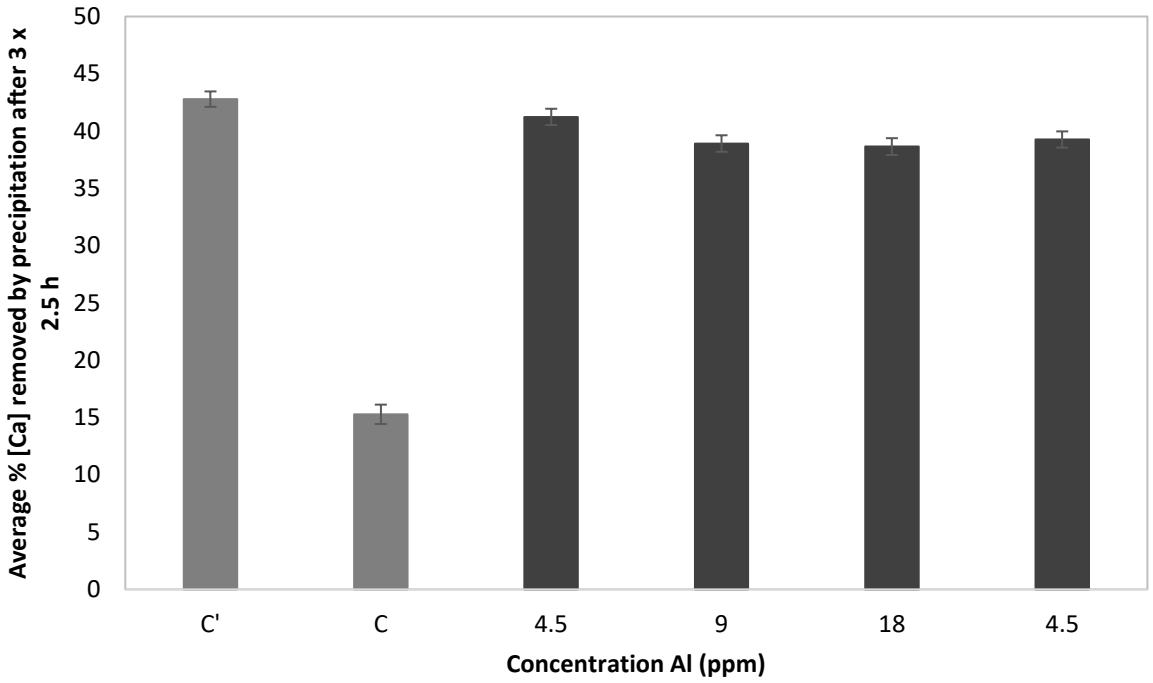

Figure 4.27:*The average percentage calcium removed from solution (SS3) by means of precipitation after 2.5 hours of the control runs and the 3 experiments performed in the presence of aluminum and 9 ppm antiscalant, with 2000 ppm re-used seeding crystals.*

The drastic increase in the average calcium removal in the presence of aluminum compared to the calcium removal of the control in the presence of antiscalant could be due to the aluminum, as found in the study by Rashed et al. (2004). It is possible that the aluminum chloride or aluminum sulfate acted as a flocculant forming flocs of larger size that led to better contact between molecules to benefit crystallisation, resulting in increased calcium removal. Another possibility is that the presence of the aluminum ions degrades the antiscalant by lowering the pH. This increases crystallisation and calcium removal, since the effectiveness of the antiscalant decreases with the decrease in pH (Rosenberg, et al., 2012). It is also possible that a combination of flocculation and antiscalant degradation resulted in the drastic increase in the calcium removal.

This increase was further investigated by means of SEM analysis. For the control experiment and experiment 23 (9 ppm Al), the SEM analysis produced Figure 4.28. The seed crystals from the control run (Figure 4.28 [a]) were found to have a different shape than that of the seed crystals in the presence of aluminum (Figure 4.28 [b]). The control run seed crystals were found to be more tubular shaped, compared to the plate-shaped seed crystals in the presence of aluminum. These plate-shaped seed

crystals in the presence of aluminum were found to have a similar shape to the seed crystals that were found in the presence of hydrogen peroxide.

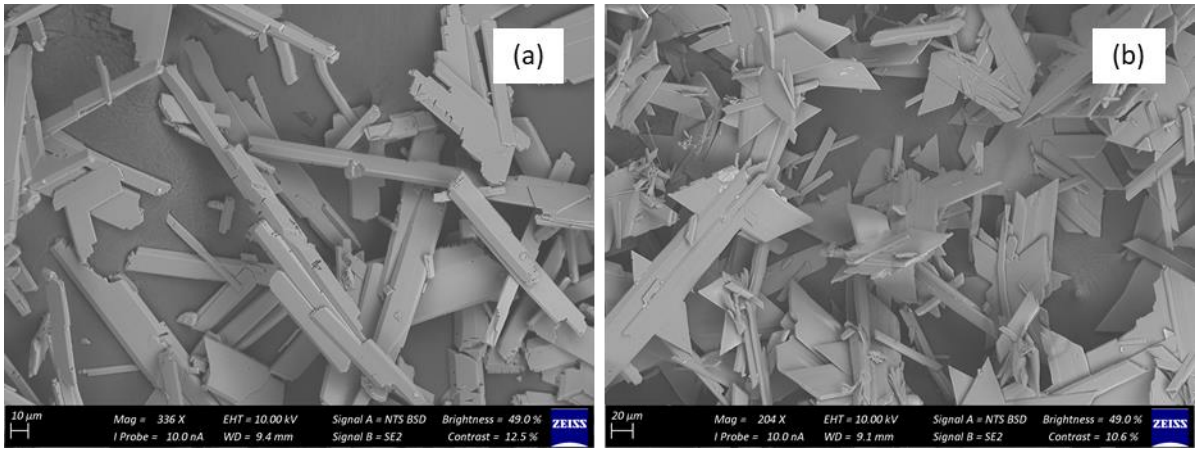

Figure 4.28: *SEM analysis of gypsum crystals formed during the control run in the presence of antiscalant (a) and gypsum crystals formed during experiment 23 in the presence of 9 ppm aluminum (b).*

The seed crystals of experiment 23 (9 ppm Al) were also compared to the seed crystals of the control run in the absence of antiscalant (Figure 4.29). This comparison was done because a physical difference was previously found between the seed crystals of the control run in the presence of antiscalant and the seed crystals from experiment 23 in the presence of 9 ppm aluminum. The seed crystals in the absence of antiscalant (Figure 4.29 [a]) are also more plate-shaped, similar to the seed crystals in the presence of aluminum (Figure 4.29 [b]). Figure 4.29 (a) also shows some smaller and thinner crystals. However, these are flat and plate-shaped and were possibly still growing.

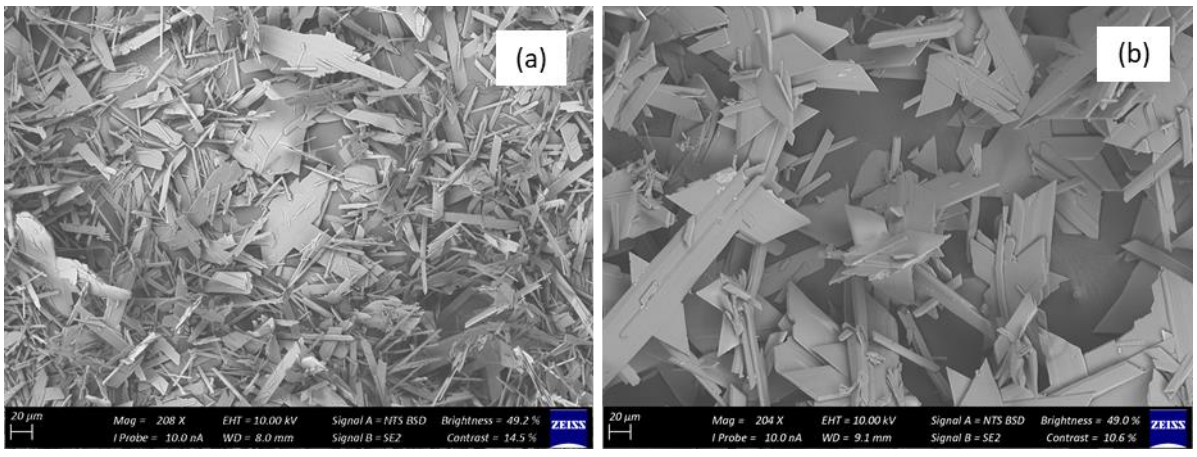

Figure 4.29: *SEM analysis of gypsum crystals formed during the control run in the absence of antiscalant (a) and gypsum crystals formed during experiment 23 in the presence of 9 ppm hydrogen peroxide (b).*

The similarity between the seed crystals in the absence of antiscalant and the seed crystals of experiment 23 in the presence of 9 ppm aluminum show that the antiscalant was degraded. This degradation might have taken place due to a decrease in pH as a result of the addition of aluminum.

Chemicals containing aluminum such as $AlCl_3$, $Al_2(SO_4)_3$, Polyaluminum chloride (PAC) and polyaluminum ferric chloride (PAFC) are widely used as a flocculant (Bratby, 2016). Therefore, flocculation behaviour was considered when SEM analysis was performed. The SEM analysis found flocs of small crystals (Figure 4.30), which shows that slight flocculation did occur. This flocculation behaviour can create larger flocs by removing the free-floating, small, slow-growing crystals from the solution by grouping them in the cluster to form a bigger floc that can deliver faster crystal growth.

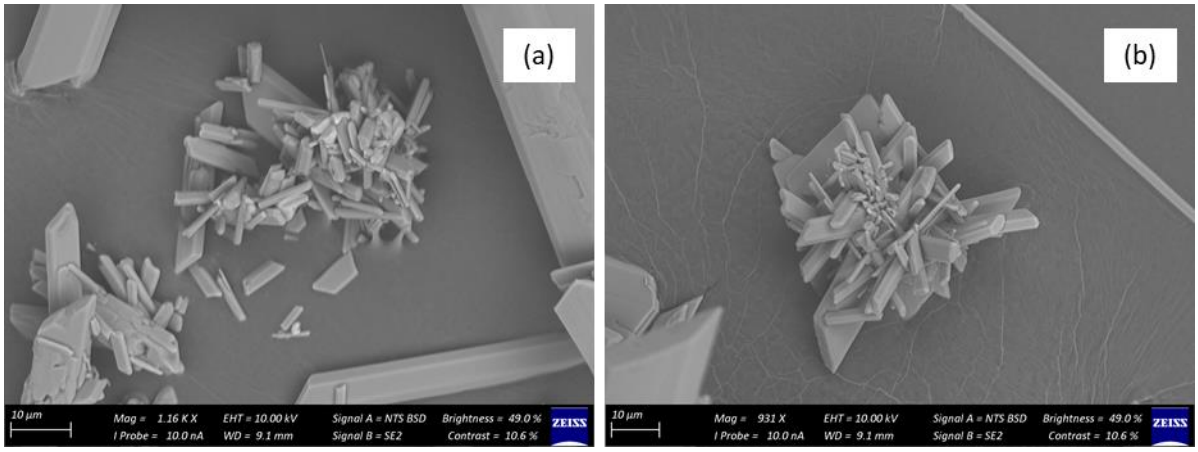

Figure 4.30: *SEM analysis of gypsum crystals formed during experiment 23 in the presence of 9 ppm aluminum, showing flocculation behaviour.*

After some flocculation behaviour was noted during the SEM analysis, the seed crystal size of the remaining seed crystals of experiment 22 and the control experiment was determined by means of a Micromeritics® Particle size analyser. The mean particle size of the seed crystals is detailed in Table 4.22.

Table 4.22: *The mean particle size and standard deviation of the seed crystals from the control run in the presence of antiscalant (C) and from experiment 22.*

Sample	Control Run (C)	Experiment 22 (9 ppm Al)
Mean particle size (μm)	79.79	87.70
Standard deviation of 3 (μm)	6.128	4.972

Table 4.23 shows that the seed crystals in the presence of aluminum are larger than the seed crystals from the control experiment, which confirms flocculation. The mean particle size in the presence of aluminum was found to be 7.91 μm bigger than that of the control run. This would, according to the

theory by Mullin, increase the crystal growth rate (Mullin, 1972), and would thus increase the calcium removal.

The aluminum concentration at the beginning and end of each run of experiment 23 (9 ppm Al) and experiment 24 (18 ppm Al) were measured by the ICP-OES when the samples were analyzed for calcium. Figure 4.31 shows a slight decrease in the aluminum concentration on comparing the concentration at the start of the experiment to aluminum concentration at the end of the experiment. However, this decrease falls within the uncertainty of the measurement. This indicates that the aluminum did not take part and therefore flocculation did not occur to its full potential. The slight decrease in the aluminum concentrations could be the reason for the traces of flocculation behaviour found with the SEM analysis.

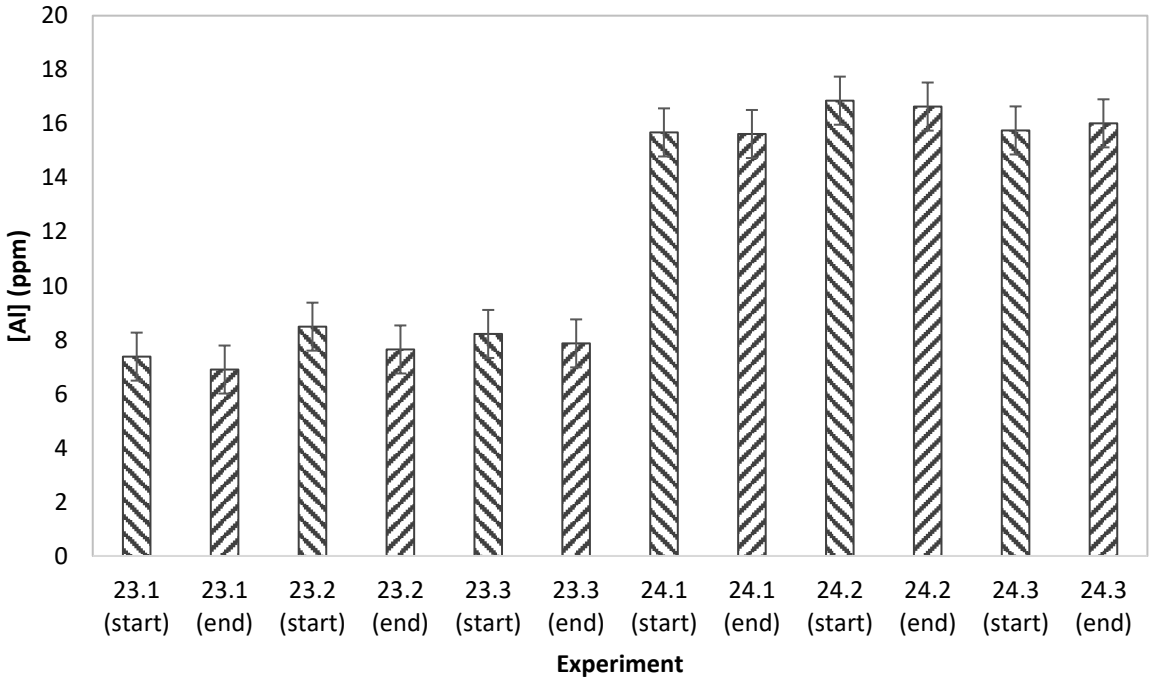

Figure 4.31: *Initial and final aluminum concentration of experiments 23 (9 ppm Al) and 24 (18 ppm Al), where (1) is the first seed crystal re-use, (2) the second, and (3) the third seed crystal re-use.*

4.4.2.1 Significant difference

An analysis of variance (ANOVA) was done on the average calcium removed, calculated from the four runs as well as the control, to determine if there is a significant difference between the values. The ANOVA table (Table 4.23) shows a p-value of 4.38×10^{-14}, which shows that at least one significant difference was found between 2 values.

Table 4.23: *ANOVA results for the average percentage calcium removal of the control runs and the 4 experiments in the presence of aluminum*

Source of Variation	*SS*	*df*	*MS*	*F*	*P-value*	*F crit*
Between Groups	1805.00	5	361.00	940.77	4.38×10^{-14}	3.20
Within Groups	4.22	11	0.38			
Total	1809.22	16				

To specifically see if there is a significant difference between the control in the presence of antiscalant and experiment 23 (9 ppm Al), a t-test was performed with a significance level of 0.05. The t-test had a p-value of 2.52×10^{-6}, which is smaller than 0.05, confirming that there is a significant difference between the two sets of data. A t-test with a significance level of 0.05 was also performed to determine if there is a significant difference between the control without antiscalant and experiment 23 (9 ppm Al). The t-test had a p-value of 0.0063, which is smaller than 0.05 and confirms that there is a significant difference between these two experiments. The full results of the t-test can be seen in Appendix D.

4.4.2.2 Repeatability in the presence of aluminum

To increase confidence in the data obtained in the presence of aluminum, a repeat of experiment 23 was done to see if the results can be repeated. The percentage calcium removal of each experimental run, as well as the average calcium removal, were compared (Table 4.24). The data obtained from the repeat run of the experiment showed that there is a slight difference in the third run, but the data still falls within the uncertainty of the average calcium removal.

Table 4.24: *The concentration of aluminum, initial and final calcium concentrations, percentage calcium removed and the average percentage calcium removed for the three runs where seed crystals were re-used for experiment 23 and the repeat of the experiment (experiment 23').*

Exp.	**Aluminum**	**Calcium conc. (ppm) @ 5 min**	**Calcium Conc. (ppm) @ 150 min**	**% Calcium removed**	**Average % Calcium removal**
23.1	9 ppm Al (1 mg/mg antiscalant)	1620.64	986.03	39.2	38.9
23.2		1628.42	1005.29	38.3	
23.3		1658.57	1006.72	39.3	
23.1'	9 ppm Al (1 mg/mg antiscalant)	1652.91	992.97	39.9	38.0
23.2'		1704.07	1045.73	38.6	
23.3'		1642.24	1061.83	35.3	

The desupersaturation curves of the three different runs for each of the experiments were also compared (Figure 4.32). The data show fairly good repeatability for the first two runs, with the data falling within the uncertainty calculate. Some deviation was found for the third experimental run. The

desupersaturation curve, as well as the calcium removal calculated for the different runs (Table 4.24), show a slight deviation.

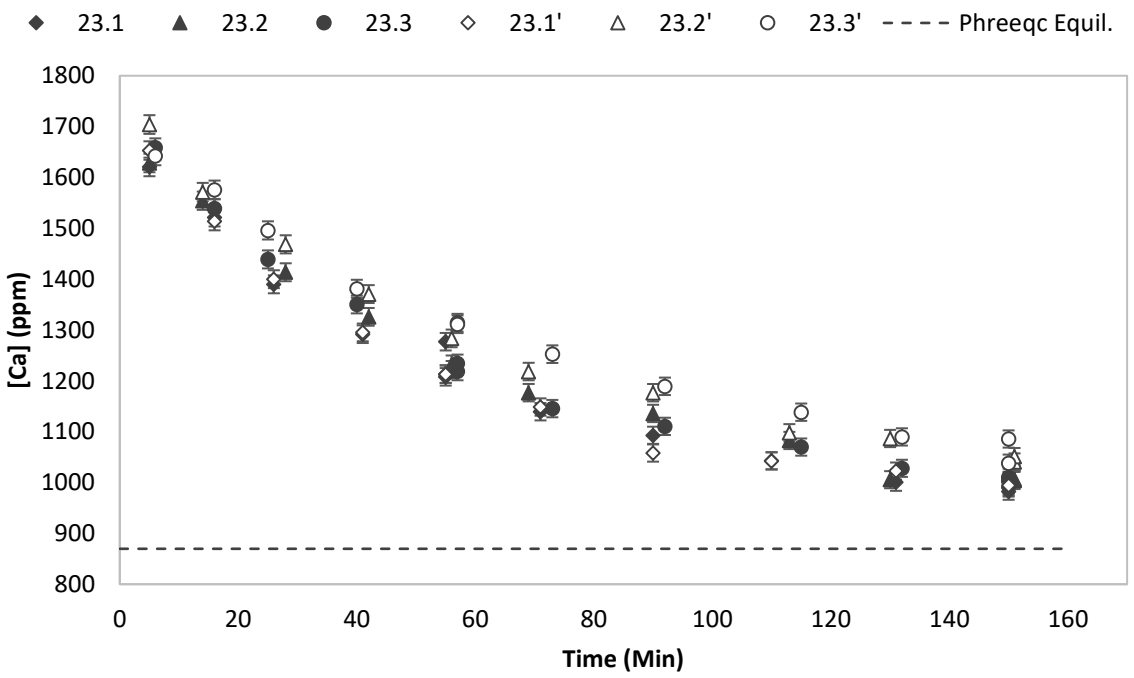

Figure 4.32: *The desupersaturation curve for experiment 23 and the repeat of the experiment (23') at three times gypsum saturation (with 2000 ppm seeding) where (1), (2) and (3) are the number of seed crystal re-uses, in the presence of 9 ppm aluminum, including the equilibrium concentration calculated by Phreeqc.*

4.4.3 In the presence of both hydrogen peroxide and aluminum

The crystallisation in the presence of aluminum was successful (Experiments 22 – 25), and this was also true for the crystallisation in the presence of hydrogen peroxide (Experiments 19 – 21). Therefore, the possibility of obtaining an even more desirable result in the presence of a combination of hydrogen peroxide and aluminum was investigated (Experiment 28). The percentage calcium removed for each run, as well as the average percentage calcium removed between the three runs, were calculated (Table 4.25). Table 4.25 contains the data for experiment 20 (90 ppm H_2O_2) and 22 (4.5 ppm Al). These two experiments gave the best results in the two previous chemical treatment studies, and therefore their results were compared to the result obtained in the presence of both these chemicals. Table 4.25 shows the concentration of chemicals added, the initial and final calcium concentration, the percentage calcium removed, the average percentage calcium removed for the three runs where seed crystals were re-used, and the growth rate constant and pH of the control experiments and the experiments performed in the presence of hydrogen peroxide, in the presence of aluminum and in the presence of both hydrogen peroxide and aluminum.

Table 4.25: *Experimental data to evaluate crystallisation in the presence of both hydrogen peroxide and aluminum.*

Exp	Chemicals added	Calcium conc. (ppm) @ 5 min	Calcium Conc. (ppm) @ 150 min	% Calcium removed	Average % Calcium removal
C.1'	No antiscalant	1717.51	986.84	42.5	42.8
C.2'		1718.67	988.08	42.5	
C.3'		1738.99	985.88	43.3	
C.1	9 ppm antiscalant	1606.10	1305.68	18.7	15.3
C.2		1634.14	1391.21	14.9	
C.3		1647.09	1445.15	12.3	
20.1	90 ppm H_2O_2 (10 mg/mg antiscalant)	1713.32	1165.52	32.0	25.3
20.2		1768.33	1311.03	25.9	
20.3		1754.69	1436.09	18.2	
22.1	4.5 ppm Al (0.5 g m/mg antiscalant)	1623.93	936.41	42.3	41.2
22.2		1639.39	955.40	41.7	
22.3		1645.34	992.91	39.7	
28.1	90 ppm H_2O_2 4.5 ppm Al ($AlCl_3$)	1670.37	1025.93	38.6	38.0
28.2		1680.15	1038.62	38.2	
28.3		1723.11	1080.80	37.3	

From Table 4.25 and Figure 4.33, it can be seen that for experiment 28 (90 ppm H_2O_2 and 4.5 ppm Al) the calcium removal decreased slightly with the re-use of seed crystals. It decreased from 38.6% calcium removal the first time the seed crystals were re-used to 38.2% when the seed crystals were re-used for a second time, and then to 37.3% after the third time they were re-used. These values are all within the uncertainty of the data. Since there is only a slight decrease in the crystal effectivity, it can be said that the antiscalant was made nearly ineffective. It is not possible to say for certain whether it was due to the hydrogen peroxide or the aluminum. However, the data tends to resemble the results found previously in the presence of aluminum.

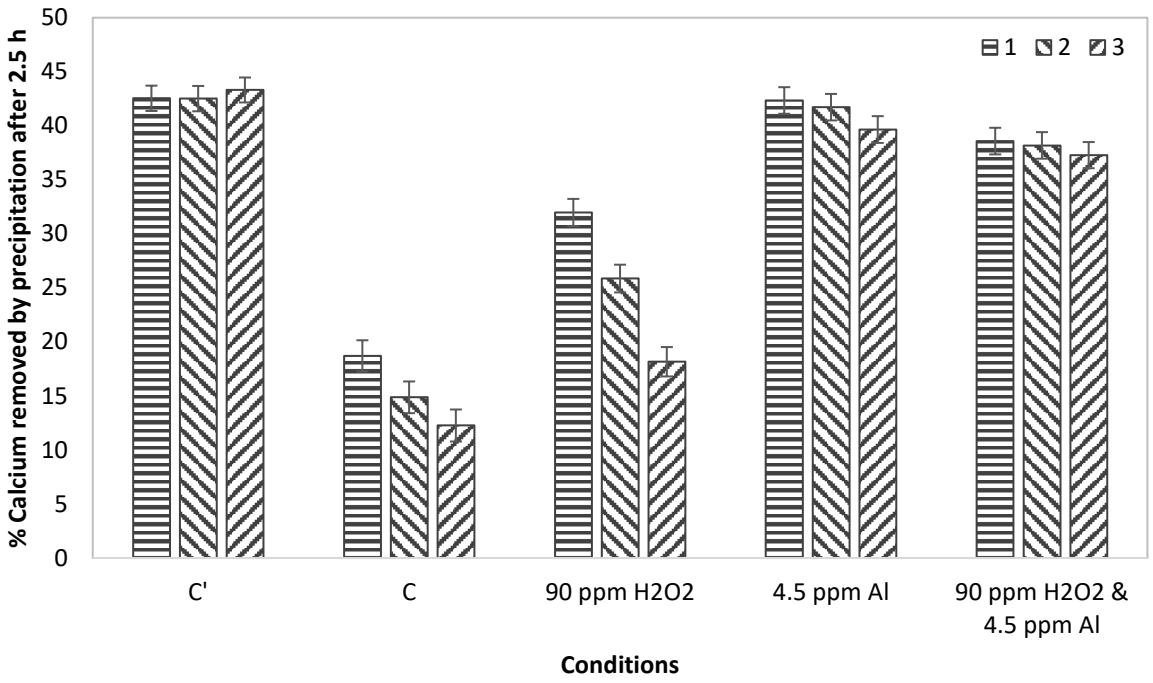

Figure 4.33: *The percentage calcium removed from solution (SS3) by means of precipitation after 2.5 hours of the control runs and the experiments performed in the presence of hydrogen peroxide, in the presence of aluminum, in the presence of both hydrogen peroxide and aluminum and 9 ppm antiscalant, with 2000 ppm seeding where (1) was the first re-use of seed crystals, (2) the second and (3) the third re-use of seed crystals.*

The average percentage calcium removed for the three runs done for each experiment was compared to both control runs where no treatments were done and in both the presence and absence of antiscalant (Figure 4.34). The average calcium removal of experiment 28 (90 ppm H_2O_2 and 4.5 ppm Al), when a combination of hydrogen peroxide and aluminum was present was found to be 38.0%. This is higher than the 25.3% calcium removal when hydrogen peroxide was present in experiment 20 (90 ppm H_2O_2) as well as the average calcium removal of 15.3% during the control run in the presence of antiscalant. However, this was lower than the average calcium removal of 42.8% of the control run in the absence of antiscalant, as well as the average calcium removal of 41.2% of experiment 22 (4.5 ppm Al) when aluminum was present.

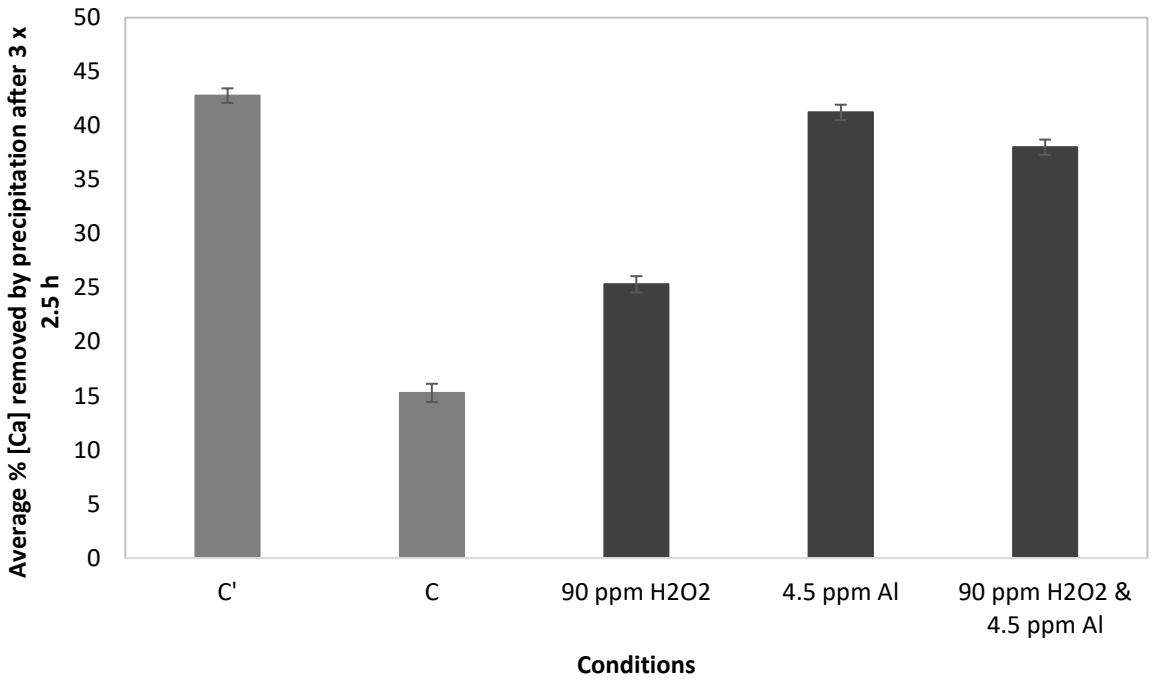

Figure 4.34: *The average percentage calcium removed from solution (SS3) by means of precipitation after 2.5 hours of the control runs and the experiments performed in the presence of hydrogen peroxide, in the presence of aluminum, in the presence of both hydrogen peroxide and aluminum and 9 ppm antiscalant, with 2000 ppm re-used seeding crystals.*

It was expected that the presence of both hydrogen peroxide and aluminum would increase the calcium removal to be similar to the calcium removal of the control run in the absence of antiscalant. Furthermore, it was also expected that the combination of hydrogen peroxide and aluminum in the system would degrade the antiscalant entirely and make it completely ineffective. It was also expected that the flocculation behaviour that was caused by the aluminum would also increase the calcium removal. However, this did not occur. The calcium removal was found to be between that of experiment 20 (90 ppm H_2O_2), where hydrogen peroxide was present, and experiment 22 (4.5 ppm Al) where aluminum was present. It is possible that the hydrogen peroxide and the aluminum competed against one another to degrade the antiscalant, resulting in the antiscalant not being degraded to the degree it would have been if there was no competition. Due to this competition effect the crystallisation process was not favoured.

4.5 Physical treatments vs. chemical treatments

The two control runs, in both the absence and presence of antiscalants, were compared to the best results of the two physical treatment methods as well as the two best results of the chemical treatments (Table 4.26). The best results for mixing as a physical treatment method was found in experiment 6 (G* = 1.13) where the seed-crystal mixture was mixed for 10 minutes at 188 s^{-1}. The best results for air scouring as treatment method were found in experiment 14 (F* = 5.20 m) where air was

sparged through the seed crystal mixture at 62.4 m/h for 5 minutes. For the chemical treatments, the best results were found for experiments 20 and 22, in the presence of 90 ppm hydrogen peroxide and 4.5 ppm aluminum, respectively. Table 4.26 shows the concentration of chemicals added, the initial and final calcium concentration, the percentage calcium removed, the average percentage calcium removed for the three runs where seed crystals were re-used, and the growth rate constant and pH of the control experiments and the best experiments of each treatment.

Table 4.26: Summative experimental data for a comparison of physical and chemical treatment methods.

Exp.	Conditions	Calcium conc. (ppm) @ 5 min	Calcium Conc. (ppm) @ 150 min	% Calcium removed	Average % Calcium removal	k' ($l.mol^{-1}.min^{-1}$)
C.1'	No antiscalant	1717.51	986.84	42.5	42.8	1.927
C.2'		1718.67	988.08	42.5		1.917
C.3'		1738.99	985.88	43.3		1.856
C.1	9 ppm antiscalant	1606.10	1305.68	18.7	15.3	0.259
C.2		1634.14	1391.21	14.9		0.168
C.3		1647.09	1445.15	12.3		0.125
6.1	Mixing: 188 s^{-1}; 10 minutes	1740.35	1036.93	40.6	31.4	1.335
6.2		1738.94	1225.85	27.6		0.458
6.3		1757.63	1290.21	25.9		0.346
14.1	Air scouring: 62.4 m/h; 5 minutes	1684.24	1305.68	22.5	18.6	0.295
14.2		1686.55	1407.40	16.6		0.176
14.3		1720.23	1433.86	16.7		0.165
20.1	90 ppm H_2O_2 (10 mg/mg antiscalant)	1713.32	1165.52	32.0	25.3	0.607
20.2		1768.33	1311.03	25.9		0.319
20.3		1754.69	1436.09	18.2		0.176
22.1	4.5 ppm Al (0.5mg/mg antiscalant)	1623.93	936.41	42.3	41.2	3.776
22.2		1639.39	955.40	41.7		2.866
22.3		1645.34	992.91	39.7		1.887

From Table 4.26 and Figure 4.35 it can be seen that all the treatment methods increased the average calcium removal compared to the control run in the presence of antiscalant. However, no treatment method increased the average calcium removal to such an extent that it removed more calcium than the control run in the absence of antiscalant. For the physical treatments (experiments 6 and 14) it was found that the best results were obtained with mixing as a treatment method, having an average calcium removal of 31.4 % when the seed crystal mixture was mixed at 188 s^{-1} for 10 minutes. Between the chemical treatments (experiments 20 and 22) the best calcium removal was found in the presence of 4.5 ppm aluminum, having an average calcium removal of 41.2%. Between these two treatments, the chemical treatment in the presence of aluminum performed the best, almost reaching the average

calcium removal of 42.8% in the absence of antiscalant. These results show that the chemical dosing delivered much better results compared to the results of the physical treatment methods.

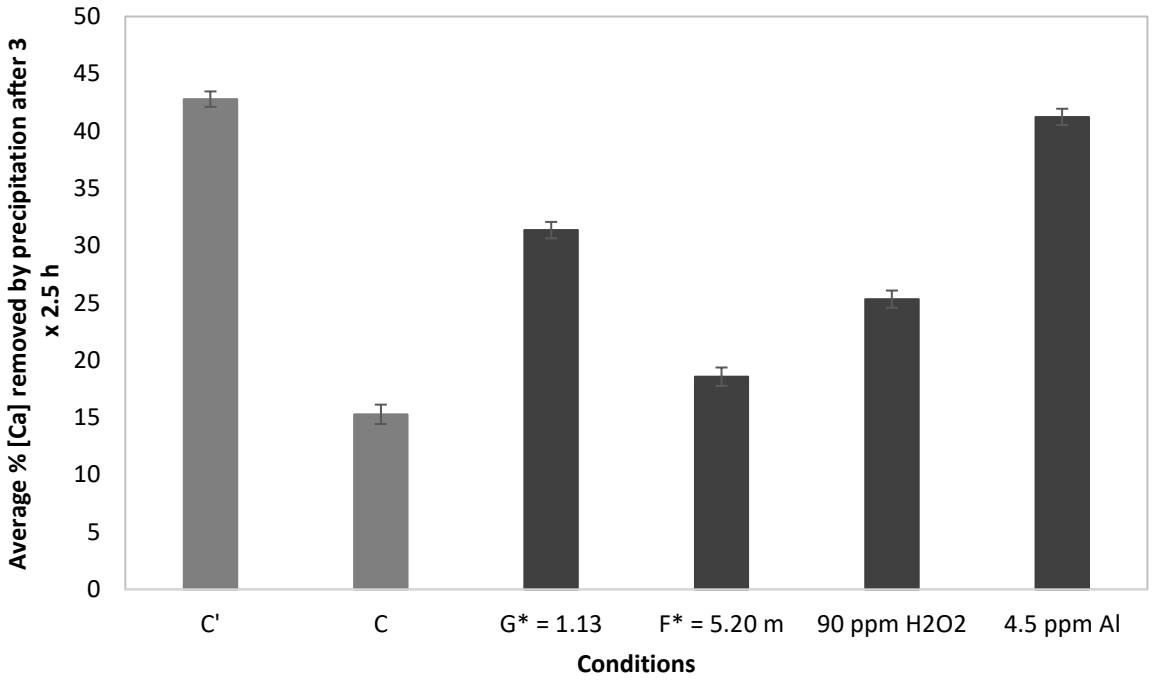

Figure 4.35: *The average percentage calcium removed from solution (SS3) after 2.5 hours of the control runs and the best experiments of the different treatments in the presence of 9 ppm antiscalant, with 2000 ppm re-used seeding crystals.*

The SEM images of the seed crystals of these experiments were compared to one another (Figure 4.36) to determine if there are differences between the seed crystals of the control experiments (Figure 4.36 [a] and [b]), the physical treatment experiments (Figure 4.36 [c] and [d]) and the chemical treatment experiments (Figure 4.36 [e] and [f]).

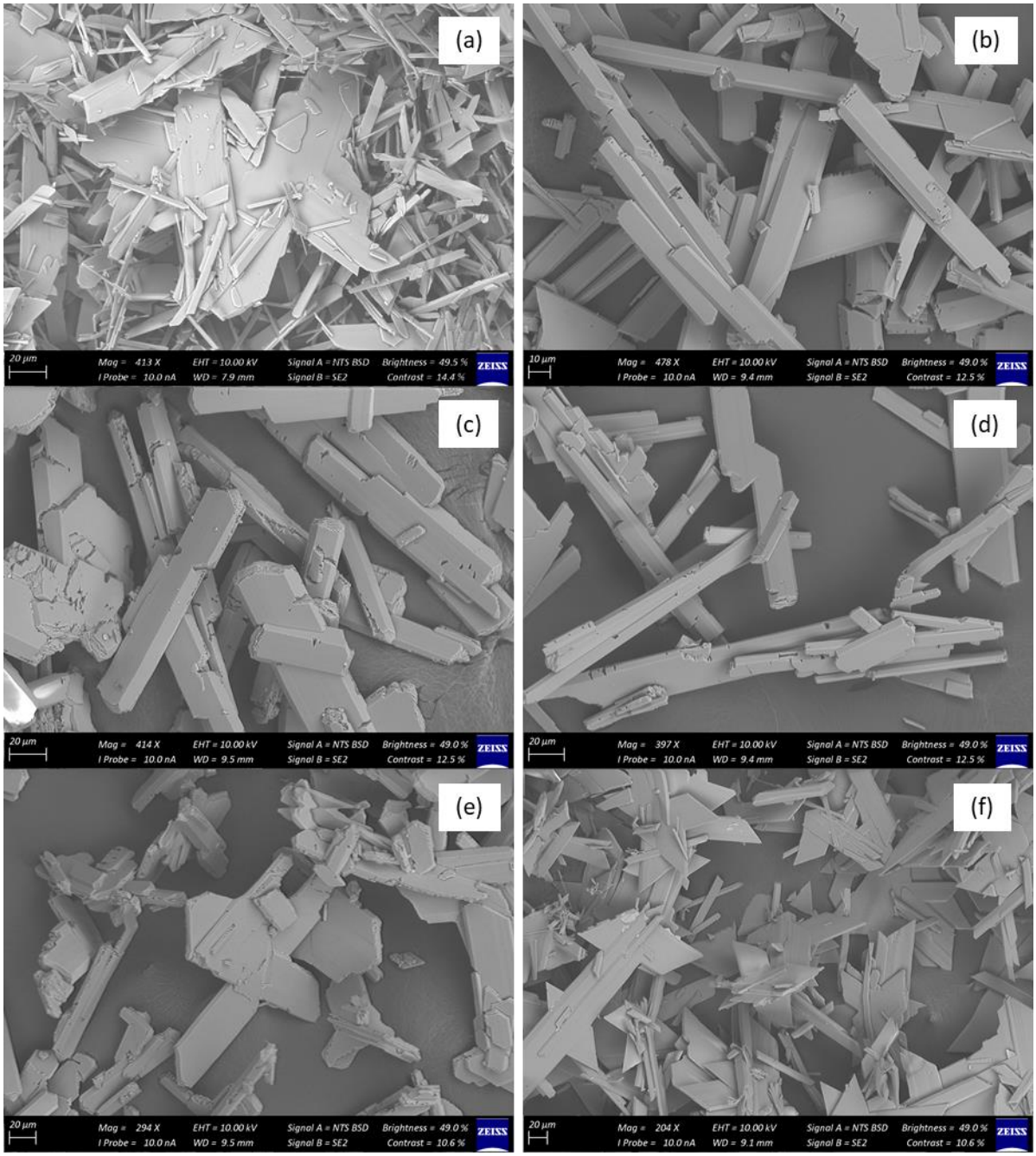

Figure 4.36: *SEM analysis of pure gypsum crystals formed in the absence of antiscalant (a), gypsum crystals formed in the presence of antiscalant (b), gypsum crystals formed in the presence of antiscalant treated with mixing (c), gypsum crystals formed in the presence of antiscalant treated with air (d), gypsum crystals formed in the presence of hydrogen peroxide and antiscalant (e) and gypsum crystals formed in the presence of aluminum and antiscalant (f).*

It can be seen that the seed crystals in the absence of antiscalant (Figure 4.36 [a]) have a different shape compared to the seed crystals of the control experiment in the presence of antiscalant (Figure 4.36 [b]). In the absence of antiscalant, the crystals were found to be more plate-shaped compared to the more tubular shape in the presence of antiscalant. The difference in the shape is due

to the absence and presence of the antiscalant, and this is why there is such a big difference in the average calcium removal of these experiments.

For the physical treatments, the seed crystals were found to have the same tubular shape, but cavities were found on the seed crystals of experiment 4 (Figure 4.36 [c]) when the seed crystal mixture was mixed as treatment. These cavities were not found on the seed crystals of experiment 14 (Figure 4.36 [d]) when the air was sparged through the seed crystal mixture. The cavities found on the seed crystals when mixing was applied as physical treatment could be the reason why there was a difference between the average calcium removal when mixing was applied compared to when air scouring was applied as physical treatment.

The seed crystals for the chemical treatment, when hydrogen peroxide was added (Figure 4.36 [e]) and when aluminum was added (Figure 4.36 [f]) were found to both have similar plate-shaped seed crystals. The seed crystal of experiment 22 (Figure 4.36 [f]) in the presence of 4.5 ppm aluminum was, however, found to be thinner plates than the seed crystals of experiment 20 (Figure 4.36 [e]) in the presence of 90 ppm hydrogen peroxide. The seed crystals of these two experiments have the same plate shape as the control experiment in the absence of antiscalant (Figure 4.36 [a]), showing that the chemicals degraded the antiscalant, leaving it ineffective. The seed crystals of the control run in the absence of antiscalant (Figure 4.36 [a]) also had the thinner plates, similar to the seed crystals of experiment 22 (Figure 4.36 [f]) in the presence of 4.5 ppm aluminum. This shows that more antiscalant was degraded and left ineffective in the presence of aluminum than in the presence of hydrogen peroxide.

Chapter 5: Conclusions

Based on the findings in literature and the experimental results obtained during this study, the following conclusions can be drawn.

Effect of re-used seed crystals.

In the absence of an antiscalant, it was found that there was no effect on the crystallisation process when seed crystals were re-used. However, in the presence of antiscalants, the efficiency of the seed crystals decreased with each run. The average calcium removal of the three runs when the crystals were re-used decreased from 42.8% to 15.3% when antiscalant was added. Different crystal shapes were also found: tubular/needle-shaped gypsum crystals in the presence of antiscalants compared to the plate-shaped crystal in the absence of antiscalants. This indicated that the presence of antiscalants influenced not only the crystallisation process but affected the crystals formed in the process as well.

Effect of re-used seed crystals with physical seed-crystal treatment methods.

An increase was found in the average calcium removal of all the experiments where the seed crystal mixture was treated by mixing compared to the control experiment in the presence of antiscalants where no such treatment took place. At a constant mixing speed, the average calcium removal increased as the treatment duration increased, until a maximum was reached after which it started to decrease. Similarly, it was found that at a constant treatment duration, the average calcium removal increased as the mixing speed increased, until a maximum was reached after which it started to decrease. Both these factors can be combined into the G-factor. The average calcium removal increased as the specific G-factor (G*) increased up until a specific G-factor of 1.13, after which a further increase in the G-factor led to a decrease in average calcium removal. The maximum average calcium removal of 31.4% was found at a G* = 1.13 when the seed-crystal mixture was mixed for 10 minutes at a G-factor of 188 s^{-1}. This removed 16.1% more calcium than the control run where no treatment took place. Upon further investigation by means of SEM, it was found that the seed crystals that were treated by mixing had cavities, whereas hardly any cavities were found on the control seed crystals. The increase in the average calcium removal could possibly be due to these cavities that increased the number of active growth sites. Mixing as seed crystal treatment removed more than double the amount of calcium compared to the control run where the seed crystals were re-used, thus showing that the treatment was successful.

Little difference was found between the calcium removal of the control run in the presence of antiscalant and the runs that were treated by means of air scouring. The maximum average calcium removal of 18.6% was found when air was sparged through the seed crystal mixture at 62.4 m/h for 5

minutes — removing only 3.3% more calcium than the control run in the presence of antiscalant. SEM analysis results and the seed crystal sizes were also found to be similar for the control run and the air treatment runs. These results show that the air treatment did not do anything to increase the calcium removal and was unsuccessful as a seed crystal treatment.

Effect of re-used seed crystals with chemical dosing.

An increase was found in the average calcium removal of all the experiments that had chemical dosing compared to the control experiment where no such dosing took place in the presence of antiscalants. The average calcium removal increased when the amount of hydrogen peroxide present increased from 45 ppm to 90 ppm, reaching a maximum average calcium removal of 25.3%. The average calcium removal then decreased when the hydrogen peroxide concentration was further increased to 135 ppm. In the presence of 90 ppm hydrogen peroxide, 10.1% more calcium was removed compared to the control run where no treatment took place. Upon further investigation by SEM analysis, a physical difference in the seed crystal shape was found between the seed crystals formed in the presence of hydrogen peroxide and antiscalant compared to the seed crystals formed in the presence of antiscalant, indicating that the antiscalant was degraded. Therefore, this approach showed positive results as a treatment method to increase calcium removal.

In the presence of aluminum, the average calcium removal stayed relatively constant at the different concentrations of aluminum. The average calcium removal decreased slightly from 41.2% to 38.9% when the amount of aluminum was increased from 4.5 ppm to 9 ppm, but it was still within the calculated uncertainty. When the aluminum was further increased to 18 ppm, the average calcium removal did not change. In the presence of 4.5 ppm aluminum, 26.0% more calcium was removed compared to the control run where no treatment took place. Further SEM analysis also found a physical difference between the seed crystals formed in the presence of aluminum and antiscalant and the seed crystals formed in the presence of antiscalant, indicating that the antiscalant had degraded. Flocculation behaviour was also found due to the presence of aluminum. The presence of aluminum almost tripled the calcium removal of the control run in the presence of antiscalant. Therefore, it was successful as a treatment.

The combined presence of 90 ppm hydrogen peroxide and 4.5 ppm aluminum did not increase the average calcium removal compared to the maximum removal obtained in the presence of only 4.5 ppm aluminum.

Physical treatments vs. chemical dosing.

It can be concluded that the physical treatment that delivered the best results was mixing and that the presence of aluminum provided the best result of the chemical treatments. Comparing these two with one another, the highest average calcium removal was found in the presence of 4.5 ppm aluminum. However, from this study, it was found that the presence of hydrogen peroxide, the presence of aluminum and mixing as seed-crystal treatment method increased the average calcium removal significantly when seed crystals were re-used. These are therefore viable options to improve the crystallisation process in the presence of antiscalant.

Chapter 6: Recommendations

In this study the effect of various seed crystal treatment methods (for re-used seed crystals) on gypsum precipitation in the presence of antiscalants was investigated. From the results of this investigation the following recommendations for future work are made:

- A pilot plant study to determine if the crystal treatment methods increase calcium removal on a large scale.
- A study into the combination of physical treatment and chemical dosing.
- A study on the effect of hydrogen peroxide and UV-light on the re-used seed crystals and the resulting effect on gypsum precipitation in the presence of antiscalants.
- A study on the effect of other various treatment methods on re-used seed crystals and the resulting effect of this on gypsum precipitation in the presence of antiscalants and other impurities.
- A study on the effect of various types of mixing on gypsum precipitation.
- A study on the effect of different types of mixing as a seed crystal treatment method.
- A study on the effect of temperature on the chemical dosing.
- Study the effect of doing the chemical treatment experiments under conditions where the pH is controlled.

Chapter 7: References

Abdel-Aal, E. A., Rashed, M. M. & El-Shall, H., 2004. Crystallization of calcium sulfate dihydrate at different supersaturation ratios and different free sulfate concentrations. *Crystal Research Technology,* 39(4), pp. 313-321.

Ahmed, S. B., Tlili, M. M., Amami, M. & b, A. M., 2014. Gypsum Precipitation Kinetics and Solubility in the NaCl-MgCl2-CaSO4-H2O System. *Industrial & Engineering Chemistry Research,* Volume 53, pp. 9554-9560.

Amjad, Z., 1988. Kinetics of crystal growth of calcium sulfate dihydrate: The influence of polymer composition, molecular weight, and solution pH. *Canadian Journal of Chemistry,* Volume 66, pp. 1529-1536.

Amjad, Z., 1988. Seeded Growth of Calcium-containing scale forming minerals in the presence of inhibitors. *Corrosion/88,* Volume 421, pp. 1-11.

Amjad, Z., 2004. Gypsum Scale Formation on Heat Exchanger Surfaces: The Influence of Natural and Synthetic Polyelectrolytes. *Tenside Surfactants Detergents,* 41(5), pp. 214-219.

Amjad, Z., 2013. Gypsum scale formation on heated metal surfaces: The Influence of polymer type and polymer stability on gypsum inhibition. *Desalination and Water Treatment,* Volume 51, pp. 4709-4718.

Amjad, Z. & Hooley, J., 1986. Influence of Polyelectrolytes on the Crystal Growth of Calcium Sulfate Dihydrate. *Journal of Colloid and Interface Science,* 111(2), pp. 496-503.

Andreozzi, R., Caprio, V., Insola, A. & Marotta, R., 1999. Advanced oxidation processes (AOP) for water purification and recovery. *Catalysis Today,* 53(1), pp. 51-59.

BCF, 2015. *BCF Technion.* [Online]
Available at: https://bcf.technion.ac.il/portfolio/rcfrpm-conversion/
[Accessed 23 July 2019].

Bock, E., 1961. On the Solubility of Anhydrous Calcium sulphate and of gypsum in concentrated solutions of sodium chloride at 25C, 30C, 40C and 50C. *Canadian Journal of Chemistry,* Volume 39, pp. 1746-1751.

Bock, H., 2017. *The effect of humic substances on the crystallisation of gypsum,* Stellenbosch: Stellenbosch University.

Brandse, W. P. & van Rosmalen, G. M., 1977. The influence of sodium chloride on the crystallization rate of gypsum. *Journal of Inorganic and Nuclear Chemistry,* 39(11), pp. 2007-2010.

Bratby, J., 2016. *Coagulation and Flocculation in Water and Wastewater Treatment.* 3rd ed. Seattle: IWA Publishing.

Callister, W. D. J. & Rethwisch, D. G., 2015. *Material Science and Engineering.* 9th ed. s.l.:John Wiley & Sons.

CerCell, 2019. *CerCell.* [Online]
Available at: https://cercell.com/support/cellvessel-details/impeller-power/
[Accessed 23 July 2019].

Degremont, s., 2007. *Water Treatment Handbook.* 7 ed. New York: Degremont.

Frost, J. W., Loo, S., Cordeiro, M. L. & Li, D., 1987. Radical-based dephosphorylation and organophosphonate biodegradation. *Journal of the American Chemical Society,* 109(7), pp. 2166-2171.

Gerber, D. H., 2011. *The chemical manipulation of meta-stable brine supersaturated with gypsum: forcing precipitation by overriding the inhibitory effect of antiscalants on crystal formation,* Stellenbosch: Stellenbosch University .

Hamdona, S. K. & Al Hadad, U. A., 2007. Crystallization of calcium sulfate dihydrate in the presence of some metal ions. *Journal of Crystal Growth ,* Issue 229, pp. 145-151.

Hamdona, S., Nessim, R. & Hamza, S., 1993. Spontaneous precipitation of calcium sulphate dihydrate in the presence of some metal ions. *Desalination,* Issue 93, pp. 69-80.

Hughes, I. G. & Hase, T. P. A., 2010. *Measurements and their Uncertainties.* 1st ed. New York: Oxford University Press.

Jones, C., 2000. Applications of hydrogen peroxide and derivatives.. *Journal of Chemical Technology & Biotechnology,* 75(11), p. 1083.

Klima, W. F. & Nancollas, G. H., 1987. The Growth of Gypsum. *AiChe Symposium Series,* Volume 83, pp. 23-30.

Kucera, J., 2015. *Reverse Osmosis - Industrial Processes and Applications.* 2nd ed. Hoboken: John Wiley & Sons, Inc.

Lancia, A., Musmarra, D. M. & Prisciandaro, M., 1999. Measuring Induction Period for Calcium Sulfate Dihydrate Precipitation. *AlChE Journal,* 45(2), pp. 390-397.

Lawler, D. F., Cobb, M., Freeman, B. & Greenlee, L. F., 2010. *Improving Recovery: A Concentrate Management Strategy for Inland Desalination,* Texas: Texas Water Development Board.

Lewis, A. & Nathoo, J., 2006. *Prevention of calcium sulphate crystallization in water desalination plants using slurry precipitation and recycle reverse osmosis (SPARRO),* s.l.: Water research commission.

Liu, S. & Nancillas, G., 1970. The kinetics of crystal growth of calcium sulfate dihydrate. *Journal of crystal growth ,* Volume 6, pp. 281-289.

Liu, S. & Nancollas, G., 1973. Linear crystallization and induction-period studies of the growth of calcium sulphate dihydrate crystals. *Talanta,* 20(1), pp. 211-216.

Liu, S.-T. & Nancollas, G. H., 1970. The kinetics of crystal growth of calcium sulfate dihydrate. *Journal of Crystal Growth ,* 6(3), pp. 281-289.

Liu, S. T. & Nancollas, G. H., 1970. The Kinetics of Crystal Growth of Calcium Sulfate Dihydrate. *Journal of Crystal Growth,* Volume 6, pp. 281-289.

Liu, S. T. & Nancollas, G. H., 1975. A Kinetic and Morphological Study of the Seeded Growth of Calcium Sulfate Dihydrate in the Presence of Additives. *Journal of Colloid and Interface Science,* 52(3), pp. 593-601.

Marshall, W. & Slusher, R., 1966. Thermodynamics of Calcium Sulfate Dihydrate in Aqueous Sodium Chloride Solutions, 0-110C. *The Journal of Physical Chemistry,* 70(12), pp. 4015-4027.

McCartney, E. & Alexander, A., 1958. The effect of additives upon the process of crystallisation. *Journal of Colloid Science ,* Issue 13, pp. 383-396.

Minerals.net, 2018. *Minerals.net.* [Online]
Available at: http://www.minerals.net/mineral/gypsum.aspx
[Accessed 12 April 2018].

Mullin, J. W., 1972. *Crystallisation.* 2nd ed. London: Butterworths.

Nagata, S., 1975. *Mixing - Principles and applications.* 1 ed. New York: John Wiley & Sons, Inc..

Nancollas, G. H., Reddy, M. M. & Tsai, F., 1973. Calcium sulfate dihydrate crystal growth in aqueous solution at elevated temperatures. *Journal of Crystal Growth,* 20(2), pp. 125-25.

Nyvlt, J., 1971. *Industrial crystallisation from solutions.* 1st ed. London: Butterworths.

Oldshue, J. Y., 1983. *Fluid Mixing Technology.* 1 ed. New York: McGraw-Hill Publications Co..

Ostroff, A. G. & Metler, A. A., 1966. Solubility of Calcium Sulfate Dihydrate in the System NaCl-MgCl2-H2O from 28° to 70° C.. *Journal of Chemical and Engineering Data,* 11(3), pp. 346-350.

Pandey, A., 2019. *Radial Impellers Axial Impellers.* [Online]
Available at:
https://webcache.googleusercontent.com/search?q=cache:9c6xOERnnXoJ:https://4.imimg.com/data4/BT/HN/MY-6907292/radial-turbine-impellers.pdf+&cd=1&hl=en&ct=clnk&gl=za
[Accessed 23 July 2019].

Parkhurst, D. L. & Appelo, C. A. J., 1999. *User's Guide to PHREEQC,* Colorado: U.S. Department of Interior.

Partridge, E. P. & White, A. H., 1929. The solubility of calcium sulfate from 0 to 200˚C. *Journal of the American Chemical Society,* 51(2), pp. 360-370.

Power, W. H., Fabuss, B. M. & Satterfield, C. N., 1964. Transient Solubilities in the Calcium Sulfate-Water System. *Journal of Chemical and Engineering Data,* 9(3), pp. 437-442.

Power, W. H., Fabuss, B. M. & Satterfield, C. N., 1966. Transient Solute Concentrations and Phase Changes of Calcium Sulfate in Aqueous Sodium Chloride. *Journal of Chemical and Engineering Data ,* 11(2), pp. 149-154.

Rahardianto, A., Gao, J. & Gabelich, C. J., 2007. High recovery membrane desalting of low-salinity brackish water: Integration of accelerated precipitation softening with membrane RO. *Journal of Membrane Science,* 289(1-2), pp. 123-137.

Rashad, M., Mahmoud, M., Ibrahim, I. & Abdel-Aal, E., 2004. Crystallization of calcium sulfate dihydrate under simulated conditions of phosphoric acid production in the presence of aluminum and magnesium ions. *Journal of crystal growth ,* Issue 267, pp. 372-379.

Rautenbach, R. & Habbe, R., 1991. Seeding Technique for "Zero-Discharge" Processes, Adaption to Electrodialysis. *Desalination,* Issue 84, pp. 153-161.

Rosenberg, Y. O., Reznk, I. J., Zmora-Nahum, S. & Ganor, J., 2012. The effect of pH on the formation of a gypsum scale in the presence of a phosphonate antiscalant. *Desalination,* Volume 284, pp. 207-220.

Sarig, S., Kahana, F. & Leshem, R., 1975. Selection of threshold agents for calcium sulfate scale control on the basis of chemical structure. *Desalination ,* Volume 17, pp. 215-229.

Schram, C. J., Smyth, R. J., Taylor, L. S. & Beaudoin, S. P., 2016. Understanding Crystal Growth Kinetics in the Absence and Presence of a Polymer Using a Rotating Disk Apparatus. *Crystal Growth & Design ,* Volume 16, pp. 2640-2645.

Seader, J., Henley, E. J. & Keith, R. D., 2011. *Separation Process Principles.* 3rd ed. Hoboken: John Wiley & Sons, Inc..

Shih, W., Gao, J., Rahardianto, A. & Glater, J., 2006. Ranking of antiscalant performance for gypsum scale suppression in the presence of residual aluminum.. *Desalination,* Issue 196, pp. 280-292.

Smedley, T., 2017. *BBC.* [Online]
Available at: http://www.bbc.com/future/story/20170412-is-the-world-running-out-of-fresh-water
[Accessed 5 August 2019].

Smith, B. R. & Sweett, F., 1971. The Crystallization of Calcium Sulfate Dihydrate. *Journal of Colloid and Interface Science,* 37(3), pp. 612-618.

Sohnel, O. & Garside, J., 1981. On Supersaturation Evaluation for solution growth. *Journal of Crystal Growth,* Volume 54, pp. 358-360.

Söhnel, O. & Garside, J., 1992. *Precipitation: Basic principles and industrial application.* 1st ed. s.l.:Butterworth-Heinemann Ltd.

Tait, S., Clarke, W. P., Keller, J. & Batstone, D., 2009. Removal of sulfate from high-strength wastewater by crystallisation. *Water research,* Issue 43, pp. 762-772.

von Gunten, U., 2003. Ozonation of drinking water: Part I. Oxidation kinetics and product formation. *Water Research,* 37(7), pp. 1443-1467.

Witkamp, G. J., Van Der Eerden, J. P. & Rosemalen, G. M., 1990. Growth of Gypsum: I. Kinetics. *Journal of Crystal Growth ,* 120(1-2), pp. 281-289.

Yang, Q., Ma, Z., Hasson, D. & Semiat, R., 2004. Destruction of anti-scalants in RO concentrates by electrochemical oxidation. *Journal of Chemical Industry and Engineering (China),* 55(2), p. 339340.

Zeng, D. & Wang, W., 2011. Solubility phenomena involving CaSO4 in hydrometallurgical processes concerning heavy metals. *Pure and Applied Chemistry,* 83(5), pp. 1045-1061.

Zwietering, T. N., 1985. Suspending of solid particles in liquid by agitators. *Chemical Engineering Science,* 8(3), pp. 244-253.

Appendix A: Detailed experimental procedure

The experimental procedure was done similar to work done by Bock (2017), as detailed below.

A.1. Solution and crystal preparation

This step by step procedure was followed to prepare the stock solutions:

1. Measure 8 L of RO-water into two 10 L containers.
2. Measure 2 L of RO-water, add roughly 500 ml into a 1 L glass container.
3. Weigh 133.02 g of calcium chloride dihydrate.
4. Add the calcium chloride into the 1 L glass container.
5. Mix the solution with a magnetic stirrer until all the calcium chloride is dissolved.
6. Add the calcium chloride mixture into one of the 10 L containers, and use the remainder of the 2 L to rinse the 1 L glass beaker, also adding it to the 10 L container.
7. Mark the container '*calcium chloride solution'.*
8. Measure 2 L of RO-water and add roughly 500 ml into a 1 L glass container.
9. Put the 1 L glass container into hot water to heat up the RO-water.
10. Weigh 128.52 g of sodium sulphate anhydrous.
11. Add the sodium sulphate anhydrous into the 1 L glass container that has been warmed.
12. Mix the solution with a magnetic stirrer until all sodium sulphate is dissolved.
13. Add the sodium sulphate mixture into one of the 10 L containers, and use the remainder of the 2 L to rinse the 1 L glass beaker, also adding it to the 10 L container.
14. Mark the container '*sodium sulphate solution'.*

This step by step procedure was followed to prepare pure gypsum crystals:

1. Add 1 L of both the calcium chloride and sodium sulphate solutions into a 2 L glass beaker.
2. Stir the solution at 400 rpm for 8 hours by using a magnetic stirrer.
3. Switch off the stirrer and allow the crystals to settle.
4. Filter the crystal mixture using a Buchner-filter.
5. Let the crystals dry at room temperature.

A.2. Seed crystal generation

This step by step procedure is done the day prior to the experiment to generate the seed crystals that are used in the first experiment.

1. Set the water bath on 25˚C to heat up overnight.
2. Add 500 ml of both the calcium chloride and sodium sulphate solutions into a 1 L glass beaker.
3. Add 2000 ppm gypsum seed crystals into the mixture.
4. Add 9 ppm antiscalant to the mixture.
5. Set to stir overnight at 400 rpm using a magnetic stirrer.

A.3. Experimental procedure

This step by step procedure includes liquid removal, seed crystal treatment, experimental crystallisation and cleaning.

1. Fill 36 x 15 ml centrifugal tubes with 7.5 ml of RO-water for sample dilutions.
2. Turn on the air-conditioning unit to get constant room temperature.
3. Stop the stirrer of the crystal mixture that was mixed overnight and let crystals settle for 3 min while steps 4 – 6 is performed.
4. Connect the reactor to the heating bath, and let the heating jacket fill with water.
5. Add 500 ml of the sodium sulphate solution into the reactor.
6. Add 9 ppm antiscalant to the reactor.
7. Remove the water above the settled crystals in the 1L glass beaker with the pump; pump it to a small waste container.
8. Transfer the remaining crystals to a 250 ml glass beaker.
9. In the case of physical treatment, apply treatment – detailed below*****
10. Extract 50 ml of the seed crystal mixture in the 250 ml glass beaker using a 60 ml syringe.
11. Weigh the syringe containing the seed crystal mixture.
12. Add 500 ml of the calcium chloride solution to the reactor.
13. Add the 50 ml of seed crystal solution to the reactor.
14. Set the overhead stirrer to 180 rpm.
15. Start the overhead stirrer as well as the stopwatch.
16. Submerge the temperature and pH probe into the solution in the reactor.
17. In the case of chemical treatment – detailed below******
18. Take a 2.5 ml sample using a micropipette at 5 minutes.
19. Record the time the sample is taken as well as the pH and temperature.

20. Eject the sample into a 5 ml syringe attached to a $0.22\ \mu m$ syringe filter.
21. Filter the sample with the $0.22\ \mu m$ syringe filter into a 4 ml vial.
22. Add 0.4 μL of the filtered sample to a centrifugal tube prepared using a micropipette.
23. Label the centrifugal tube with the sample number.
24. Repeat steps 18 – 23 using new pipette tips, syringes and filters at time 15, 25, 45, 55, 70, 90, 110, 130 and 150 minutes. Take duplicate samples at 55 minutes and 150 minutes.
25. After the sample was taken at 150 minutes, stop the overhead stirrer and let the crystals settle for 3 minutes while steps 26 – 28 is performed.
26. Remove the pH and temperature probes from the reactor.
27. Stop the water circulation from the water bath to the reactor.
28. Drain the heating jacket of the reactor.
29. Remove the water above the settled crystals with the pump; pump it to a small waste container.
30. Transfer the seed crystal mixture to a 250 ml glass beaker.
31. * In the case of physical treatment, apply treatment – detailed below.
32. Connect a clean reactor to the heating bath, and let the heating jacket fill with water.
33. Add 500 ml of the sodium sulphate solution into the reactor.
34. Add 9 ppm antiscalant to the reactor.
35. Repeat from step 10 – 34 (Second experimental run)
36. Rinse the reactor used during the first experiment 5 times with RO-water to ensure it is clean, and let it dry for the next experiment.
37. Repeat from step 10 – 30 (Third experimental run)
38. Filter the seed-crystal mixture using a Buchner-filter.
39. Place the filtered seed crystals in an open container to dry, and label the container.
40. Rinse the reactor used during the first experiment 10 times with RO-water to ensure it is clean.
41. Rinse all the glassware used during the experimental procedure 5 times with RO-water to ensure it is clean.
42. Wash the syringes and 4 ml vials used with RO-water.
43. Let all the syringes, 4 ml vials and glassware dry for the next experimental run.
44. Empty the waste container of the water removal pump into a big waste container.
45. Clean the workspace.

*Physical treatment procedure – Mixing as seed crystal treatment method:

1. Add a magnetic stirrer-bar to the seed crystal mixture.
2. Set the magnetic stirrer on the required stirrer speed.
3. Start the magnetic stirrer and stopwatch.
4. Record the type of treatment, stirrer speed and duration.
5. Run the treatment for the required duration.
6. Stop the magnetic stirrer.
7. Remove the magnetic stirrer-bar using a large magnet.

*Physical treatment procedure – Air scouring as seed crystal treatment method:

1. Open the valve allowing air flow to the air scouring set-up.
2. Open the needle valve allowing flow to the air sparger.
3. Set the required air flow by adjusting the air flow meter.
4. Place the air sparger at the bottom of the 250 ml glass beaker and start the stopwatch.
5. Record the type of treatment, air flow rate, pressure in the line and the duration.
6. Run the treatment for the required duration.
7. Remove the sparger from the 250 ml glass beaker.
8. Close the valve allowing air to the air scouring set-up.

**Chemical treatment procedure:

1. Add the required amount of hydrogen peroxide or aluminum to the reactor using a micropipette 2.5 minutes after the experiment has started.

Appendix B: Experimental data

All the experimental data generated during the study is presented in this Appendix.

B.1. Verification data

The data generated to compare gypsum crystallisation to the data obtained from Bock (2017) as well as the data generated to verify the repeatability of the reactor are detailed in Tables B.1 to B.3.

Table B. 1: *Verification experiments data*

Experiment	V1	Experiment	V2	Experiment	V3
Seed crystals	-	Seed crystals	-	Seed crystals	-
Antiscalant	-	Antiscalant	-	Antiscalant	-
Temperature	25	Temperature	25	Temperature	25
Time (min)	Ca Conc. (ppm)	Time (min)	Ca Conc. (ppm)	Time (min)	Ca Conc. (ppm)
0	1915.74	10	2000.30	10	2048.87
5	2058.41	20	1964.91	20	2003.14
9	2067.96	30	1978.17	40	1899.37
20	2097.17	44	1842.19	58	1635.24
40	1891.55	61	1661.37	80	1403.00
63	1618.48	118	1210.34	101	1255.00
80	1431.98	144	1120.35	126	1150.10
110	1058.62	160	1071.14	-	-
141	1144.03	180	1010.86	-	-
170	1112.50	180	1025.45	-	-

Table B. 2: *Data by Bock (2017) used for verification*

Experiment	Bock (2017)
Seed crystals	-
Antiscalant	-
Temperature	25
Time (min)	Ca Conc. (ppm)
0	1902.161
10	1900.632
14	1903.059
19	1913.966
29	1893.813
44	1735.414
59	1475.624
89	1167.487
119	1043.789
179	938.661

Table B. 3: *Reactor verification data*

Experiment	Reactor 1	Experiment	Reactor 1'	Experiment	Reactor 2
Seed crystals	2000 ppm	Seed crystals	2000 ppm	Seed crystals	2000 ppm
Antiscalant	-	Antiscalant	-	Antiscalant	-
Temperature	25	Temperature	25	Temperature	25
Time (min)	Ca Conc. (ppm)	Time (min)	Ca Conc. (ppm)	Time (min)	Ca Conc. (ppm)
5	1671.28	6	1618.76	5	1639.67
15	1506.54	16	1524.14	17	1547.42
25	1441.95	25	1445.57	26	1471.90
40	1284.57	39	1333.05	49	1299.12
58	1168.03	57	1222.71	67	1221.47
81	1082.20	82	1116.47	88	1145.82
103	1018.76	114	1048.01	137	1038.24
125	976.76	135	1008.48	157	997.96
146	939.70	159	984.27	235	933.19
177	919.53	191	968.53	250	938.11
202	904.86	214	939.62	319	908.04
223	900.05	234	927.20	321	912.14
232	893.57	234	943.21	-	-

B.2. Baseline experiments data

The data generated during the baseline experiments are detailed in Tables B.4 to B.6.

Table B. 4: *Baseline experiments on supersaturation data.*

Experiment	SS3	Experiment	SS4
Super sat.	SS3	Super sat.	SS4
Seed crystals	-	Seed crystals	-
Stirrer speed	180 rpm	Stirrer speed	180 rpm
Temperature	25	Temperature	25
Time (min)	Ca Conc. (ppm)	Time (min)	Ca Conc. (ppm)
5	1719.25	5	2371.32
10	1744.90	10	2403.49
20	1754.68	20	2241.04
40	1739.35	40	1675.59
60	1718.00	59	1386.15
80	1643.31	80	1213.62
100	1459.69	99	1110.72
119	1328.15	99	1116.41
141	1219.10	120	1032.17
160	1115.24	139	1018.70
181	1061.84	167	978.28

Table B. 5: *Baseline experiments on seeding data*

Experiment	SS3 + S	Experiment	SS3 + S +A
Super sat.	SS3	Super sat.	SS3
Seed crystals	2000 ppm	Seed crystals	2000 ppm
Antiscalant	-	Antiscalant	9 ppm
Stirrer speed	180 rpm	Stirrer speed	180 rpm
Temperature	25	Temperature	25
Time (min)	Ca Conc. (ppm)	Time (min)	Ca Conc. (ppm)
5	1648.85	5	1652.49
10	1499.28	10	1567.69
20	1349.30	20	1498.82
30	1260.95	30	1442.95
50	1124.79	50	1334.19
70	1051.73	69	1277.62
89	988.09	94	1218.87
111	945.44	111	1165.98
131	924.43	133	1162.24
143	932.75	150	1145.68
143	927.38	177	1126.73
-	-	187	1130.24

Table B. 6: *Baseline experiments on antiscalant data*

Experiment	SS3 + A
Super sat.	SS3
Seed crystals	-
Antiscalant	9 ppm
Stirrer speed	180 rpm
Temperature	25
Time (min)	Ca Conc. (ppm)
5	1813.47
31	1776.05
85	1770.78
122	1797.82
185	1800.97

B.3. Control experiments data

The data generated during the control experiments are detailed in Tables B.7 to B.9.

Table B. 7: *Control experiment in the absence of antiscalant data*

Experiment: Control in the absence of antiscalant					
Super sat.	3	Antiscalant	0 ppm	Stirrer speed	180 rpm
Experiment	C.1'	Experiment	C.2'	Experiment	C.3'
Seed crystals	2000 ppm	Seed crystals	2000 ppm	Seed crystals	2000 ppm
Average pH		Average pH		Average pH	
Temperature	25	Temperature	25	Temperature	25
Time (min)	Ca Conc. (ppm)	Time (min)	Ca Conc. (ppm)	Time (min)	Ca Conc. (ppm)
6	1717.51	5	1718.67	6	1738.99
16	1524.14	17	1547.42	14	1593.87
25	1445.57	26	1471.90	27	1455.44
39	1333.05	49	1299.12	48	1331.05
57	1222.71	67	1221.47	66	1237.47
82	1116.47	88	1145.82	85	1159.38
114	1048.01	137	1038.24	109	1101.15
135	1008.48	157	988.08	134	1046.42
159	986.84	-	-	167	985.88

Table B. 8: *Control experiment in the presence of antiscalant data*

Experiment: Control in the presence of antiscalant					
Super sat.	3	Antiscalant	9 ppm	Stirrer speed	180 rpm
Experiment	C.1	Experiment	C.2	Experiment	C.3
Seed crystals	2000 ppm	Seed crystals	2000 ppm	Seed crystals	2000 ppm
Average pH	4.96	Average pH	4.94	Average pH	4.95
Temperature	25	Temperature	25	Temperature	25
Time (min)	Ca Conc. (ppm)	Time (min)	Ca Conc. (ppm)	Time (min)	Ca Conc. (ppm)
5	1606.10	7	1634.14	5	1647.09
15	1586.58	16	1613.60	15	1630.79
25	1567.14	26	1608.58	26	1633.57
43	1526.68	40	1615.01	41	1606.14
56	1478.28	40	1593.83	55	1565.84
56	1469.28	55	1575.85	55	1580.60
70	1455.26	72	1525.06	65	1562.56
90	1400.99	90	1482.84	92	1511.43
112	1366.36	112	1443.09	110	1481.14
130	1353.05	131	1422.34	132	1446.99
150	1301.80	150	1390.97	150	1440.20
150	1309.56	150	1391.46	150	1450.09

Table B. 9: *Control experiment in the presence of antiscalant repeat data*

Experiment: Control in the presence of antiscalant (Repeat)					
Super sat.	3	Antiscalant	9 ppm	Stirrer speed	180 rpm
Experiment	C.1	Experiment	C.2	Experiment	C.3
Seed crystals	2000 ppm	Seed crystals	2000 ppm	Seed crystals	2000 ppm
Average pH	4.98	Average pH	4.94	Average pH	4.95
Temperature	25	Temperature	25	Temperature	25
Time (min)	Ca Conc. (ppm)	Time (min)	Ca Conc. (ppm)	Time (min)	Ca Conc. (ppm)
5	1652.06	4	1675.14	5	1708.43
15	1617.89	15	1635.64	17	1684.97
25	1591.80	25	1610.59	26	1664.28
40	1535.58	41	1569.18	37	1632.30
54	1509.71	54	1546.67	55	1595.07
54	1504.08	54	1539.96	55	1598.99
69	1461.18	72	1504.51	71	1571.36
93	1429.95	93	1476.02	91	1540.02
110	1395.69	113	1450.27	110	1502.31
125	1390.22	131	1420.27	133	1491.92
152	1359.82	154	1378.47	156	1461.21
152	1337.05	154	1378.47	156	1471.39

B.4. Mixing as seed crystal treatment method experimental data

The data generated during the experiments with mixing as seed crystal treatment method are detailed in Tables B.10 to B.22.

Table B. 10: *Experiment 1 data*

Experiment: 1					
Treatment: Mixing @ G-factor of 93 s^{-1} for 1 minute					
Super sat.	3	Antiscalant	9 ppm	Stirrer speed	180 rpm
Experiment	1.1	Experiment	1.2	Experiment	1.3
Seed crystals	2000 ppm	Seed crystals	2000 ppm	Seed crystals	2000 ppm
Average pH	4.94	Average pH	4.93	Average pH	4.93
Temperature	25	Temperature	25	Temperature	25
Time (min)	Ca Conc. (ppm)	Time (min)	Ca Conc. (ppm)	Time (min)	Ca Conc. (ppm)
5	1658.14	7	1696.96	5	1739.91
15	1616.95	16	1671.85	15	1725.49
25	1585.79	26	1662.93	26	1709.59
43	1550.75	40	1614.75	41	1683.17
56	1500.46	40	1627.75	55	1646.90
56	1535.39	55	1590.08	55	1679.40
70	1438.77	72	1573.10	65	1634.06
90	1410.06	90	1568.14	92	1619.52
112	1398.03	112	1527.55	110	1570.47
130	1265.26	131	1521.22	132	1575.93
150	1326.95	150	1490.16	150	1547.35
150	1330.42	150	1503.92	150	1553.80

Table B. 11: *Experiment 2 data*

Experiment: 2					
Treatment: Mixing @ G-factor of 93 s^{-1} for 5 minutes					
Super sat.	3	Antiscalant	9 ppm	Stirrer speed	180 rpm
Experiment	2.1	Experiment	2.2	Experiment	2.3
Seed crystals	2000 ppm	Seed crystals	2000 ppm	Seed crystals	2000 ppm
Average pH	4.93	Average pH	4.93	Average pH	4.93
Temperature	25	Temperature	25	Temperature	25
Time (min)	Ca Conc. (ppm)	Time (min)	Ca Conc. (ppm)	Time (min)	Ca Conc. (ppm)
5	1657.23	5	1698.82	5	1681.84
15	1599.49	15	1653.08	15	1646.97
25	1551.69	25	1607.23	25	1630.17
40	1485.38	40	1562.78	41	1579.16
56	1402.05	55	1516.63	56	1560.59
56	1402.34	55	1521.69	56	1564.54
70	1373.64	71	1461.49	68	1531.26
91	1320.25	92	1415.76	89	1479.01
111	1282.88	113	1357.94	110	1448.46
131	1241.41	133	1337.42	130	1415.20
151	1165.98	150	1314.63	150	1387.48
151	1163.76	150	1300.94	150	1380.96

Table B. 12: *Experiment 3 data.*

Experiment: 3					
Treatment: Mixing @ G-factor of 93 s^{-1} for 10 minutes					
Super sat.	3	Antiscalant	9 ppm	Stirrer speed	180 rpm
Experiment	3.1	Experiment	3.2	Experiment	3.3
Seed crystals	2000 ppm	Seed crystals	2000 ppm	Seed crystals	2000 ppm
Average pH	4.92	Average pH	4.92	Average pH	4.93
Temperature	25	Temperature	25	Temperature	25
Time (min)	Ca Conc. (ppm)	Time (min)	Ca Conc. (ppm)	Time (min)	Ca Conc. (ppm)
7	1683.40	5	1707.19	7	1725.68
15	1621.22	17	1649.13	15	1689.63
25	1586.45	32	1585.01	25	1658.67
40	1498.73	41	1544.92	42	1608.38
61	1430.07	56	1502.57	56	1587.66
61	1414.21	56	1490.08	56	1590.53
75	1374.52	69	1427.30	69	1568.08
93	1321.89	91	1410.50	90	1506.76
112	1263.48	111	1376.98	110	1492.79
131	1196.32	131	1341.70	134	1450.81
150	1095.10	149	1260.09	150	1458.39
150	1086.95	149	1265.11	150	1450.75

***Table B. 13**: Experiment 27 data*

Experiment: 27					
Treatment: Mixing @ G-factor of 93 s^{-1} for 15 minutes					
Super sat.	3	Antiscalant	9 ppm	Stirrer speed	180 rpm
Experiment	27.1	Experiment	27.2	Experiment	27.3
Seed crystals	2000 ppm	Seed crystals	2000 ppm	Seed crystals	2000 ppm
Average pH	4.88	Average pH	4.88	Average pH	4.88
Temperature	25	Temperature	25	Temperature	25
Time (min)	Ca Conc. (ppm)	Time (min)	Ca Conc. (ppm)	Time (min)	Ca Conc. (ppm)
5	1695.71	5	1753.13	5	1732.81
15	1676.27	16	1700.68	16	1708.98
27	1586.59	33	1674.82	25	1696.50
40	1548.02	43	1637.11	45	1656.98
55	1494.51	56	1543.35	57	1631.82
55	1511.50	56	1544.55	57	1616.67
71	1439.05	72	1538.59	75	1593.16
90	1391.22	93	1500.78	92	1548.32
120	1323.08	116	1454.87	114	1517.31
134	1319.48	130	1452.74	135	1473.36
151	1261.34	150	1447.89	152	1477.68
151	1263.80	150	1437.58	152	1469.23

***Table B. 14:** Experiment 4 data*

Experiment: 4					
Treatment: Mixing @ G-factor of 188 s^{-1} for 1 minute					
Super sat.	3	Antiscalant	9 ppm	Stirrer speed	180 rpm
Experiment	4.1	Experiment	4.2	Experiment	4.3
Seed crystals	2000 ppm	Seed crystals	2000 ppm	Seed crystals	2000 ppm
Average pH	4.92	Average pH	4.92	Average pH	4.92
Temperature	25	Temperature	25	Temperature	25
Time (min)	Ca Conc. (ppm)	Time (min)	Ca Conc. (ppm)	Time (min)	Ca Conc. (ppm)
5	1628.71	6	1661.45	5	1718.44
16	1534.08	16	1635.16	15	1697.13
26	1495.78	26	1623.13	27	1664.04
41	1330.27	40	1466.49	41	1585.85
60	1274.03	56	1495.36	57	1566.10
60	1296.67	56	1522.81	57	1604.11
78	1239.47	71	1451.42	75	1539.71
92	1247.45	90	1424.34	94	1494.79
113	1172.91	111	1369.23	111	1488.96
130	1161.87	130	1357.89	130	1447.18
150	1145.28	150	1348.99	149	1412.99
150	1135.06	150	1353.34	149	1417.88

Table B. 15: *Experiment 5 data.*

Experiment: 5					
Treatment: Mixing @ G-factor of 188 s^{-1} for 5 minutes					
Super sat.	3	Antiscalant	9 ppm	Stirrer speed	180 rpm
Experiment	5.1	Experiment	5.2	Experiment	5.3
Seed crystals	2000 ppm	Seed crystals	2000 ppm	Seed crystals	2000 ppm
Average pH	4.87	Average pH	4.89	Average pH	4.89
Temperature	25	Temperature	25	Temperature	25
Time (min)	Ca Conc. (ppm)	Time (min)	Ca Conc. (ppm)	Time (min)	Ca Conc. (ppm)
5	1626.54	5	1626.15	5	1633.25
16	1578.86	15	1620.58	14	1586.78
25	1501.66	26	1523.91	27	1558.36
40	1401.86	41	1463.69	44	1487.91
55	1235.10	56	1423.72	53	1468.41
55	1300.97	56	1409.19	53	1483.96
71	1273.34	72	1378.21	69	1437.39
92	1233.68	90	1340.81	95	1389.30
111	1173.66	112	1280.36	110	1335.58
130	1130.98	130	1250.16	130	1288.46
150	1096.80	150	1212.51	150	1274.88
150	1119.61	150	1201.25	150	1281.33

Table B. 16: *Experiment 6 data.*

Experiment: 6					
Treatment: Mixing @ G-factor of 188 s^{-1} for 10 minutes					
Super sat.	3	Antiscalant	9 ppm	Stirrer speed	180 rpm
Experiment	6.1	Experiment	6.2	Experiment	6.3
Seed crystals	2000 ppm	Seed crystals	2000 ppm	Seed crystals	2000 ppm
Average pH	4.86	Average pH	4.87	Average pH	4.88
Temperature	25	Temperature	25	Temperature	25
Time (min)	Ca Conc. (ppm)	Time (min)	Ca Conc. (ppm)	Time (min)	Ca Conc. (ppm)
5	1740.35	6	1738.94	6	1757.63
16	1647.30	15	1682.69	16	1710.00
26	1582.30	26	1610.59	26	1657.80
40	1484.72	43	1533.92	41	1594.93
58	1400.68	55	1479.61	56	1551.46
58	1379.06	55	1469.87	56	1550.96
70	1323.47	73	1418.56	70	1475.44
89	1203.70	91	1360.09	93	1408.96
110	1133.24	111	1313.41	112	1355.45
133	1057.25	130	1265.11	130	1326.05
151	1035.97	150	1227.28	151	1279.49
151	1037.89	150	1224.42	151	1300.94

Table B. 17: *Experiment 6 repeat data*

Experiment: 6 (Repeat)					
Treatment: Mixing @ G-factor of 188 s^{-1} for 10 minutes					
Super sat.	3	Antiscalant	9 ppm	Stirrer speed	180 rpm
Experiment	6.1'	Experiment	6.2'	Experiment	6.3'
Seed crystals	2000 ppm	Seed crystals	2000 ppm	Seed crystals	2000 ppm
Average pH	4.91	Average pH	4.92	Average pH	4.92
Temperature	25	Temperature	25	Temperature	25
Time (min)	Ca Conc. (ppm)	Time (min)	Ca Conc. (ppm)	Time (min)	Ca Conc. (ppm)
5	1707.37	6	1670.50	5	1687.65
16	1637.82	16	1645.85	15	1664.57
27	1536.61	26	1566.51	25	1627.20
42	1476.22	41	1548.54	40	1603.19
58	1400.85	56	1493.64	57	1547.58
58	1411.54	56	1497.51	57	1555.39
70	1355.33	69	1475.84	70	1500.58
85	1273.72	95	1370.59	91	1457.91
110	1115.85	115	1324.51	113	1348.62
130	1065.67	138	1283.94	130	1322.58
152	1013.95	150	1213.49	151	1249.49
152	1015.52	150	1204.63	151	1252.53

Table B. 18: *Experiment 26 data*

Experiment: 26					
Treatment: Mixing @ G-factor of 188 s^{-1} for 15 minutes					
Super sat.	3	Antiscalant	9 ppm	Stirrer speed	180 rpm
Experiment	26.1	Experiment	26.2	Experiment	26.3
Seed crystals	2000 ppm	Seed crystals	2000 ppm	Seed crystals	2000 ppm
Average pH	4.85	Average pH	4.87	Average pH	4.87
Temperature	25	Temperature	25	Temp.	25
Time (min)	Ca Conc. (ppm)	Time (min)	Ca Conc. (ppm)	Time (min)	Ca Conc. (ppm)
5	1740.94	6	1734.63	6	1739.92
15	1648.64	17	1697.34	16	1712.55
26	1628.54	26	1668.99	27	1674.89
44	1549.19	45	1614.35	42	1646.19
59	1479.96	55	1584.86	56	1630.16
59	1487.55	55	1615.37	56	1626.05
74	1452.73	75	1553.12	85	1552.85
92	1411.73	100	1483.65	110	1515.11
110	1384.80	121	1427.32	125	1492.70
132	1327.29	136	1402.68	136	1446.07
150	1288.31	150	1369.60	151	1415.74
150	1300.54	150	1378.04	151	1404.73

Table B. 19: *Experiment 7 data.*

Experiment: 7					
Treatment: Mixing @ G-factor of 533 s^{-1} for 1 minute					
Super sat.	3	Antiscalant	9 ppm	Stirrer speed	180 rpm
Experiment	7.1	Experiment	7.2	Experiment	7.3
Seed crystals	2000 ppm	Seed crystals	2000 ppm	Seed crystals	2000 ppm
Average pH	4.88	Average pH	4.87	Average pH	4.87
Temperature	25	Temperature	25	Temperature	25
Time (min)	Ca Conc. (ppm)	Time (min)	Ca Conc. (ppm)	Time (min)	Ca Conc. (ppm)
5	1647.64	7	1606.65	5	1683.09
16	1549.71	16	1597.21	16	1638.68
30	1488.60	26	1566.60	27	1621.18
41	1428.12	40	1533.03	42	1551.48
56	1366.50	55	1480.18	58	1501.19
56	1349.75	55	1472.33	58	1504.31
77	1300.49	70	1423.80	74	1450.70
98	1232.23	97	1375.72	92	1442.89
110	1223.00	111	1356.90	115	1395.60
131	1165.45	136	1299.00	132	1373.26
151	1134.38	151	1267.09	150	1327.60
151	1140.40	151	1268.64	150	1320.48

Table B. 20: *Experiment 8 data.*

Experiment: 8					
Treatment: Mixing @ G-factor of 533 s^{-1} for 5 minutes					
Super sat.	3	Antiscalant	9 ppm	Stirrer speed	180 rpm
Experiment	8.1	Experiment	8.2	Experiment	8.3
Seed crystals	2000 ppm	Seed crystals	2000 ppm	Seed crystals	2000 ppm
Average pH	4.89	Average pH	4.89	Average pH	4.9
Temperature	25	Temperature	25	Temperature	25
Time (min)	Ca Conc. (ppm)	Time (min)	Ca Conc. (ppm)	Time (min)	Ca Conc. (ppm)
5	1729.78	6	1696.98	7	1695.68
15	1677.16	15	1632.00	16	1675.36
26	1601.68	26	1581.62	25	1578.26
42	1542.84	39	1527.39	41	1550.61
55	1478.85	56	1440.61	55	1536.32
55	1487.52	56	1446.81	55	1547.55
70	1442.56	73	1400.70	71	1505.85
90	1384.00	90	1350.11	92	1449.36
109	1343.35	118	1281.86	115	1406.35
131	1272.97	131	1277.77	135	1368.85
150	1172.28	150	1250.16	151	1348.28
150	1180.67	150	1240.61	151	1350.41

Table B. 21: *Experiment 9 data.*

Experiment: 9					
Treatment: Mixing @ G-factor of 533 s^{-1} for 10 minutes					
Super sat.	3	Antiscalant	9 ppm	Stirrer speed	180 rpm
Experiment	9.1	Experiment	9.2	Experiment	9.3
Seed crystals	2000 ppm	Seed crystals	2000 ppm	Seed crystals	2000 ppm
Average pH	4.87	Average pH	4.89	Average pH	4.89
Temperature	25	Temperature	25	Temperature	25
Time (min)	Ca Conc. (ppm)	Time (min)	Ca Conc. (ppm)	Time (min)	Ca Conc. (ppm)
5	1724.70	6	1746.16	5	1762.34
15	1683.24	16	1711.46	17	1754.83
25	1627.87	26	1666.72	26	1708.09
40	1556.90	40	1588.97	42	1657.44
56	1491.84	56	1529.09	57	1635.82
56	1497.77	56	1560.50	57	1639.65
77	1425.28	71	1535.05	72	1592.82
90	1405.49	93	1493.07	91	1492.27
111	1361.06	118	1459.87	110	1491.83
137	1301.00	131	1435.07	129	1448.82
151	1275.98	150	1411.29	151	1421.36
151	1275.86	150	1411.46	-	-

Table B. 22: *Experiment 9 repeat data.*

Experiment: 9 (Repeat)					
Treatment: Mixing @ G-factor of 533 s^{-1} for 10 minutes					
Super sat.	3	Antiscalant	9 ppm	Stirrer speed	180 rpm
Experiment	9.1'	Experiment	9.2'	Experiment	9.3'
Seed crystals	2000 ppm	Seed crystals	2000 ppm	Seed crystals	2000 ppm
Average pH	4.89	Average pH	4.9	Average pH	4.9
Temperature	25	Temperature	25	Temperature	25
Time (min)	Ca Conc. (ppm)	Time (min)	Ca Conc. (ppm)	Time (min)	Ca Conc. (ppm)
5	1679.62	5	1693.89	8	1670.79
16	1638.62	17	1674.81	14	1679.69
25	1576.07	27	1615.78	28	1658.28
41	1535.31	43	1557.19	41	1630.66
55	1488.36	57	1541.52	56	1589.01
55	1485.17	57	1530.26	56	1586.93
70	1456.11	73	1487.48	72	1554.06
93	1326.17	88	1475.17	90	1542.14
112	1346.16	114	1342.01	112	1491.00
131	1290.18	141	1373.09	129	1473.31
150	1281.67	149	1357.07	150	1449.67
150	1292.27	149	1379.38	150	1450.87

B.5. Air scouring as seed crystal treatment method experimental data

The data generated during the experiments with aeration as seed crystal treatment method is detailed in Tables B.23 to B.32.

Table B. 23: *Experiment 10 data*

Experiment: 10					
Treatment: Aeration @ air flux of 15.6 m/h for 1 minute					
Super sat.	3	Antiscalant	9 ppm	Stirrer speed	180 rpm
Experiment	10.1	Experiment	10.2	Experiment	10.3
Seed crystals	2000 ppm	Seed crystals	2000 ppm	Seed crystals	2000 ppm
Average pH	4.94	Average pH	4.95	Average pH	4.95
Temperature	25	Temperature	25	Temperature	25
Time (min)	Ca Conc. (ppm)	Time (min)	Ca Conc. (ppm)	Time (min)	Ca Conc. (ppm)
5	1614.92	5	1655.51	5	1667.90
15	1641.92	15	1669.08	16	1645.62
25	1585.33	25	1603.17	26	1655.91
41	1527.47	41	1600.26	40	1638.87
56	1554.56	56	1581.51	56	1600.45
56	1474.24	56	1572.92	56	1604.61
70	1423.05	80	1540.47	71	1592.31
90	1394.02	92	1483.28	91	1572.81
110	1315.46	111	1449.82	112	1538.16
130	1308.41	130	1394.01	132	1497.10
150	1279.54	151	1395.54	150	1475.67
150	1267.99	151	1401.95	150	1462.61

Table B. 24: *Experiment 11 data*

Experiment: 11					
Treatment: Aeration @ air flux of 15.6 m/h for 5 minutes					
Super sat.	3	Antiscalant	9 ppm	Stirrer speed	180 rpm
Experiment	11.1	Experiment	11.2	Experiment	11.3
Seed crystals	2000 ppm	Seed crystals	2000 ppm	Seed crystals	2000 ppm
Average pH	4.93	Average pH	4.93	Average pH	4.93
Temperature	25	Temperature	25	Temperature	25
Time (min)	Ca Conc. (ppm)	Time (min)	Ca Conc. (ppm)	Time (min)	Ca Conc. (ppm)
5	1677.33	6	1640.06	6	1638.44
15	1659.54	15	1604.88	17	1616.83
25	1580.82	26	1609.60	25	1620.64
41	1545.00	42	1525.96	41	1589.57
56	1441.81	56	1511.06	55	1542.89
56	1454.09	56	1461.56	55	1523.14
69	1400.12	73	1498.89	70	1527.80
91	1405.25	91	1465.49	91	1489.47
110	1311.32	113	1405.42	111	1457.04
130	1309.73	138	1368.76	130	1426.79
150	1275.68	150	1383.12	150	1421.02
150	1277.36	150	1366.67	150	1421.89

Table B. 25: *Experiment 12 data*

Experiment: 12					
Treatment: Aeration @ air flux of 15.6 m/h for 10 minutes					
Super sat.	3	Antiscalant	9 ppm	Stirrer speed	180 rpm
Experiment	10.1	Experiment	10.2	Experiment	10.3
Seed crystals	2000 ppm	Seed crystals	2000 ppm	Seed crystals	2000 ppm
Average pH	4.87	Average pH	4.88	Average pH	4.89
Temperature	25	Temperature	25	Temperature	25
Time (min)	Ca Conc. (ppm)	Time (min)	Ca Conc. (ppm)	Time (min)	Ca Conc. (ppm)
5	1699.74	5	1718.82	6	1720.73
14	1646.89	15	1650.09	16	1686.80
25	1636.82	25	1656.25	26	1655.81
39	1587.01	41	1598.33	43	1635.53
55	1545.75	56	1572.43	60	1614.10
55	1538.33	56	1592.94	60	1621.41
71	1494.39	71	1556.67	73	1603.80
92	1455.01	89	1524.05	90	1583.57
110	1423.13	116	1484.39	115	1539.67
130	1396.11	131	1460.83	136	1527.37
151	1354.22	151	1442.82	149	1504.25
151	1340.76	151	1453.45	149	1516.60

Table B. 26: *Experiment 13 data*

Experiment: 13					
Treatment: Aeration @ air flux of 62.4 m/h for 1 minute					
Super sat.	3	Antiscalant	9 ppm	Stirrer speed	180 rpm
Experiment	13.1	Experiment	13.1	Experiment	13.1
Seed crystals	2000 ppm	Seed crystals	2000 ppm	Seed crystals	2000 ppm
Average pH	4.90	Average pH	4.90	Average pH	4.91
Temperature	25	Temperature	25	Temperature	25
Time (min)	Ca Conc. (ppm)	Time (min)	Ca Conc. (ppm)	Time (min)	Ca Conc. (ppm)
5	1665.70	5	88.66	5	1744.29
15	1578.29	17	83.32	16	1686.39
26	1548.36	28	82.06	27	1691.21
42	1467.71	44	78.50	43	1583.08
56	1402.63	56	139.83	58	1548.37
56	1401.60	71	74.85	58	1558.86
69	1340.85	90	68.28	70	1510.36
91	1273.32	115	67.73	91	1467.77
111	1233.35	135	65.48	112	1421.56
131	1181.65	151	63.54	130	1392.68
149	1136.75	151	63.61	151	1368.32
149	1143.58	-	-	151	1341.91

Table B. 27: *Experiment 13 repeat data*

Experiment: 13 (Repeat)					
Treatment: Aeration @ air flux of 62.4 m/h for 1 minute					
Super sat.	3	Antiscalant	9 ppm	Stirrer speed	180 rpm
Experiment	13.1'	Experiment	13.3'	Experiment	13.3'
Seed crystals	2000 ppm	Seed crystals	2000 ppm	Seed crystals	2000 ppm
Average pH	4.87	Average pH	4.89	Average pH	4.89
Temperature		Temperature	25	Temperature	25
Time (min)	Ca Conc. (ppm)	Time (min)	Ca Conc. (ppm)	Time (min)	Ca Conc. (ppm)
5	1586.70	5	1647.17	5	1680.03
15	1578.29	17	1670.93	16	1674.07
25	1548.36	28	1640.12	27	1654.80
42	1467.71	44	1583.83	43	1630.63
56	1402.63	56	1555.77	58	1591.43
56	1401.60	71	1506.49	58	1610.51
71	1340.85	90	1385.72	70	1565.88
90	1273.32	115	1333.18	91	1487.20
111	1233.35	135	1306.98	112	1454.22
133	1201.40	151	1301.50	130	1429.16
150	1176.25	151	1301.93	151	1410.06
150	1183.08	-	-	151	1420.68

Table B. 28: *Experiment 14 data*

Experiment: 14					
Treatment: Aeration @ air flux of 62.4 m/h for 5 minutes					
Super sat.	3	Antiscalant	9 ppm	Stirrer speed	180 rpm
Experiment	14.1	Experiment	14.1	Experiment	14.1
Seed crystals	2000 ppm	Seed crystals	2000 ppm	Seed crystals	2000 ppm
Average pH	4.94	Average pH	4.95	Average pH	4.95
Temperature	25	Temperature	25	Temperature	25
Time (min)	Ca Conc. (ppm)	Time (min)	Ca Conc. (ppm)	Time (min)	Ca Conc. (ppm)
5	1684.24	5	1686.55	5	1720.23
15	1662.40	16	1681.13	16	1702.95
25	1627.42	25	1670.10	27	1688.67
40	1552.83	40	1660.63	40	1671.59
56	1523.33	58	1602.34	55	1633.07
56	1527.20	58	1572.44	55	1602.64
69	1454.09	68	1537.95	68	1573.12
92	1420.39	92	1484.06	90	1551.13
110	1354.03	116	1422.00	111	1478.66
130	1326.69	136	1389.38	127	1472.63
150	1290.51	150	1400.55	150	1430.61
150	1320.84	150	1414.26	150	1437.11

Table B. 29: *Experiment 15 data*

Experiment: 15					
Treatment: Aeration @ air flux of 62.4 m/h for 10 minutes					
Super sat.	3	Antiscalant	9 ppm	Stirrer speed	180 rpm
Experiment	15.1	Experiment	15.2	Experiment	15.3
Seed crystals	2000 ppm	Seed crystals	2000 ppm	Seed crystals	2000 ppm
Average pH	4.96	Average pH	4.95	Average pH	4.96
Temperature	25	Temperature	25	Temperature	25
Time (min)	Ca Conc. (ppm)	Time (min)	Ca Conc. (ppm)	Time (min)	Ca Conc. (ppm)
5	1737.89	5	1751.35	5	1764.00
14	1699.37	15	1730.67	17	1723.93
25	1640.52	28	1680.00	26	1694.16
41	1607.49	42	1651.90	41	1667.48
49	1534.63	55	1619.98	57	1657.23
49	1546.67	55	1631.04	57	1657.40
70	1509.95	71	1582.88	70	1621.72
93	1461.96	89	1569.13	91	1621.12
110	1444.43	110	1474.99	110	1600.38
132	1361.82	130	1512.24	131	1601.85
150	1351.84	150	1482.07	151	1569.91
150	1345.53	150	1489.55	151	1541.19

Table B. 30: *Experiment 16 data*

Experiment: 16					
Treatment: Aeration @ air flux of 155.9 m/h for 1 minute					
Super sat.	3	Antiscalant	9 ppm	Stirrer speed	180 rpm
Experiment	16.1	Experiment	16.2	Experiment	16.3
Seed crystals	2000 ppm	Seed crystals	2000 ppm	Seed crystals	2000 ppm
Average pH	4.94	Average pH	4.95	Average pH	4.94
Temperature	25	Temperature	25	Temperature	25
Time (min)	Ca Conc. (ppm)	Time (min)	Ca Conc. (ppm)	Time (min)	Ca Conc. (ppm)
5	1691.61	6	1735.32	5	1739.05
15	1694.70	15	1685.97	16	1709.10
26	1636.83	29	1655.20	26	1698.61
42	1575.11	41	1644.50	41	1674.96
55	1564.37	56	1597.74	56	1619.48
55	1567.25	56	1616.82	56	1626.30
70	1530.44	71	1605.36	69	1492.34
89	1475.42	91	1532.92	91	1596.34
111	1410.84	110	1549.64	115	1546.44
131	1406.33	127	1513.12	131	1533.15
150	1383.65	150	1455.97	150	1519.64
150	1385.91	150	1467.10	150	1522.48

Table B. 31: *Experiment 17 data*

Experiment: 17					
Treatment: Aeration @ air flux of 155.9 m/h for 5 minutes					
Super sat.	3	Antiscalant	9 ppm	Stirrer speed	180 rpm
Experiment	17.1	Experiment	17.2	Experiment	17.3
Seed crystals	2000 ppm	Seed crystals	2000 ppm	Seed crystals	2000 ppm
Average pH	4.97	Average pH	4.96	Average pH	4.97
Temperature	25	Temperature	25	Temperature	25
Time (min)	Ca Conc. (ppm)	Time (min)	Ca Conc. (ppm)	Time (min)	Ca Conc. (ppm)
5	1718.96	5	1732.97	6	1763.85
15	1694.31	16	1751.19	15	1792.74
27	1616.02	25	1731.79	26	1767.78
42	1601.04	41	1691.72	39	1751.22
56	1547.78	55	1658.00	56	1712.43
56	1533.06	55	1667.91	56	1723.14
70	1515.36	69	1632.02	71	1699.76
93	1438.30	90	1570.59	90	1654.99
111	1409.32	111	1536.10	111	1642.02
130	1334.02	134	1521.54	135	1626.35
151	1307.29	150	1485.09	150	1593.10
151	1308.39	150	1494.08	150	1601.65

Table B. 32: *Experiment 18 data*

Experiment: 18					
Treatment: Aeration @ air flux of 155.9 m/h for 10 minutes					
Super sat.	3	Antiscalant	9 ppm	Stirrer speed	180 rpm
Experiment	18.1	Experiment	18.2	Experiment	18.3
Seed crystals	2000 ppm	Seed crystals	2000 ppm	Seed crystals	2000 ppm
Average pH	4.95	Average pH	4.94	Average pH	4.94
Temperature	25	Temperature	25	Temperature	25
Time (min)	Ca Conc. (ppm)	Time (min)	Ca Conc. (ppm)	Time (min)	Ca Conc. (ppm)
5	1801.64	5	1769.51	5	1795.22
16	1748.43	15	1770.20	16	1802.73
26	1717.85	26	1750.12	30	1747.44
42	1668.97	41	1716.46	41	1740.11
56	1559.59	56	1686.54	55	1715.54
56	1570.28	56	1687.06	55	1710.50
71	1571.11	70	1648.68	71	1702.12
92	1516.98	91	1603.64	90	1692.67
111	1426.62	111	1568.36	110	1643.94
129	1428.27	131	1540.24	129	1599.62
150	1393.06	151	1528.24	150	1596.74
150	1397.36	151	1531.01	150	1619.16

B.6. Crystallisation in the presence of hydrogen peroxide experimental data

The data generated during the experiments in the presence of hydrogen peroxide are detailed in Tables B.33 to B.36.

Table B. 33: *Experiment 19 data*

Experiment: 19					
Treatment: Presence of 45 ppm hydrogen peroxide					
Super sat.	3	Antiscalant	9 ppm	Stirrer speed	180 rpm
Experiment	19.1	Experiment	19.2	Experiment	19.3
Seed crystals	2000 ppm	Seed crystals	2000 ppm	Seed crystals	2000 ppm
Average pH	4.75	Average pH	4.75	Average pH	4.75
Temperature	25	Temperature	25	Temperature	25
Time (min)	Ca Conc. (ppm)	Time (min)	Ca Conc. (ppm)	Time (min)	Ca Conc. (ppm)
5	1718.01	5	1719.04	5	1722.53
16	1671.46	16	1698.32	16	1729.95
26	1565.70	25	1635.39	26	1691.87
42	1448.13	42	1545.07	41	1687.42
55	1423.22	57	1528.22	58	1630.07
55	1430.33	57	1545.49	58	1684.00
71	1361.30	72	1499.78	71	1616.88
90	1303.11	93	1441.48	92	1557.59
114	1224.24	106	1388.76	113	1546.25
131	1182.92	129	1324.49	131	1507.17
151	1153.45	151	1253.51	150	1488.47
151	1161.84	151	1255.33	150	1494.01

Table B. 34: *Experiment 20 data*

Experiment: 20					
Treatment: Presence of 90 ppm hydrogen peroxide					
Super sat.	3	Antiscalant	9 ppm	Stirrer speed	180 rpm
Experiment	20.1	Experiment	20.2	Experiment	20.3
Seed crystals	2000 ppm	Seed crystals	2000 ppm	Seed crystals	2000 ppm
Average pH	4.73	Average pH	4.73	Average pH	4.73
Temperature	25	Temperature	25	Temperature	25
Time (min)	Ca Conc. (ppm)	Time (min)	Ca Conc. (ppm)	Time (min)	Ca Conc. (ppm)
5	1713.32	5	1768.33	6	1754.69
16	1623.24	14	1754.68	16	1734.87
26	1555.89	26	1670.73	26	1710.67
41	1477.27	39	1599.60	47	1608.12
59	1373.79	59	1515.46	58	1634.52
59	1388.46	59	1516.69	58	1631.93
80	1322.54	80	1457.28	72	1591.97
94	1279.75	107	1403.14	93	1547.83
112	1243.40	116	1388.47	113	1524.57
131	1212.68	135	1333.63	133	1461.73
150	1167.70	151	1305.54	150	0.00
150	1163.33	151	1316.52	150	1436.09

Table B. 35: *Experiment 20 repeat data*

Experiment: 20 (Repeat)					
Treatment: Presence of 90 ppm hydrogen peroxide					
Super sat.	3	Antiscalant	9 ppm	Stirrer speed	180 rpm
Experiment	20.1'	Experiment	20.2'	Experiment	20.3'
Seed crystals	2000 ppm	Seed crystals	2000 ppm	Seed crystals	2000 ppm
Average pH	4.75	Average pH	4.74	Average pH	4.76
Temperature	25	Temperature	25	Temperature	25
Time (min)	Ca Conc. (ppm)	Time (min)	Ca Conc. (ppm)	Time (min)	Ca Conc. (ppm)
5	1752.47	5	1724.25	5	1766.56
16	1703.80	16	1692.98	15	1747.73
26	1609.90	26	1625.57	26	1694.07
40	1596.94	41	1556.59	40	1680.65
55	1442.67	60	1484.77	55	1632.41
55	1433.57	60	1503.92	55	1584.74
69	1316.19	92	1414.79	68	1543.08
82	1234.10	115	1356.20	94	1493.49
112	1170.37	131	1301.00	117	1479.71
130	1119.20	152	1264.16	131	1416.30
150	1080.95	152	1278.01	150	1501.23
150	1097.67	-	-	150	1443.59

Table B. 36: *Experiment 21 data*

Experiment: 21					
Treatment: Presence of 45 ppm hydrogen peroxide					
Super sat.	3	Antiscalant	9 ppm	Stirrer speed	180 rpm
Experiment	21.1	Experiment	21.2	Experiment	21.3
Seed crystals	2000 ppm	Seed crystals	2000 ppm	Seed crystals	2000 ppm
Average pH	4.75	Average pH	4.77	Average pH	4.77
Temperature	25	Temperature	25	Temperature	25
Time (min)	Ca Conc. (ppm)	Time (min)	Ca Conc. (ppm)	Time (min)	Ca Conc. (ppm)
5	1737.10	5	1757.25	5	1750.00
15	1670.25	16	1740.31	16	1748.19
29	1627.08	26	1718.32	27	1720.67
42	1603.52	43	1679.29	40	1698.31
56	1561.47	56	1649.51	59	1670.06
56	1572.45	56	1676.82	59	1675.21
71	1524.94	71	1605.72	72	1644.80
91	1477.72	92	1580.62	90	1629.44
110	1441.49	116	1514.64	111	1572.59
140	1380.91	131	1534.89	135	1558.75
151	1385.69	152	1498.32	150	1558.81
151	1367.42	152	1501.54	150	1564.90

B.7. Crystallisation in the presence of aluminum experimental data

The data generated during the experiments in the presence of aluminum are detailed in Tables B.37 to B.41.

Table B. 37: *Experiment 22 data*

Experiment: 22					
Treatment: Presence of 4.5 ppm aluminum					
Super sat.	3	Antiscalant	9 ppm	Stirrer speed	180 rpm
Experiment	22.1	Experiment	22.2	Experiment	22.3
Seed crystals	2000 ppm	Seed crystals	2000 ppm	Seed crystals	2000 ppm
Average pH	4.56	Average pH	4.55	Average pH	4.54
Temperature	25	Temperature	25	Temperature	25
Time (min)	Ca Conc. (ppm)	Time (min)	Ca Conc. (ppm)	Time (min)	Ca Conc. (ppm)
5	1623.93	6	1639.39	5	1645.34
15	1463.04	16	1492.99	16	1525.88
26	1341.74	25	1408.88	25	1430.69
41	1267.37	40	1277.92	41	1302.24
56	1175.92	55	1207.07	56	1229.10
56	1154.52	55	1189.06	56	1255.20
73	1081.98	70	1146.75	73	1177.35
91	1065.59	89	1097.15	91	1113.08
112	961.49	111	1019.93	111	1075.92
130	935.29	123	1003.36	131	1034.13
150	942.60	151	957.62	151	989.10
150	930.23	151	953.18	151	996.72

Table B. 38: *Experiment 23 data*

Experiment: 23					
Treatment: Presence of 9 ppm aluminum					
Super sat.	3	Antiscalant	9 ppm	Stirrer speed	180 rpm
Experiment	23.1	Experiment	23.2	Experiment	23.3
Seed crystals	2000 ppm	Seed crystals	2000 ppm	Seed crystals	2000 ppm
Average pH	4.23	Average pH	4.24	Average pH	4.27
Temperature	25	Temperature	25	Temperature	25
Time (min)	Ca Conc. (ppm)	Time (min)	Ca Conc. (ppm)	Time (min)	Ca Conc. (ppm)
5	1620.64	5	1628.42	6	1658.57
16	1521.48	14	1554.26	16	1538.86
26	1389.76	28	1413.54	25	1438.78
41	1291.77	42	1325.83	40	1350.15
55	1207.81	56	1221.79	57	1218.35
55	1276.96	56	1232.62	57	1234.39
71	1139.24	69	1176.76	73	1145.38
90	1092.94	90	1135.84	92	1110.48
110	1042.91	113	1082.70	115	1069.75
131	1000.52	130	1005.56	132	1027.92
150	982.87	151	1003.99	150	1010.42
150	989.19	151	1006.60	150	1003.03

Table B. 39: *Experiment 23 repeat data*

Experiment: 23 (Repeat)					
Treatment: Presence of 9 ppm aluminum					
Super sat.	3	Antiscalant	9 ppm	Stirrer speed	180 rpm
Experiment	23.1'	Experiment	23.2'	Experiment	23.3'
Seed crystals	2000 ppm	Seed crystals	2000 ppm	Seed crystals	2000 ppm
Average pH	4.31	Average pH	4.32	Average pH	4.31
Temperature	25	Temperature	25	Temperature	25
Time (min)	Ca Conc. (ppm)	Time (min)	Ca Conc. (ppm)	Time (min)	Ca Conc. (ppm)
1	1652.91	5	1704.07	6	1642.24
2	1513.89	14	1571.27	16	1575.78
3	1399.87	28	1468.44	25	1495.83
4	1295.21	42	1370.67	40	1381.15
5	1213.05	56	1283.43	57	1314.32
6	1213.26	56	1281.18	57	1311.34
7	1148.49	69	1218.26	73	1252.42
8	1058.00	90	1176.66	92	1189.21
9	1042.41	113	1097.87	115	1138.34
10	1022.56	130	1086.61	132	1089.70
11	991.42	151	1040.43	150	1085.58
12	994.52	151	1051.04	150	1038.08

Table B. 40: *Experiment 24 data*

Experiment: 24					
Treatment: Presence of 18 ppm aluminum					
Super sat.	3	Antiscalant	9 ppm	Stirrer speed	180 rpm
Experiment	24.1	Experiment	24.2	Experiment	24.3
Seed crystals	2000 ppm	Seed crystals	2000 ppm	Seed crystals	2000 ppm
Average pH	4.41	Average pH	4.41	Average pH	4.41
Temperature	25	Temperature	25	Temperature	25
Time (min)	Ca Conc. (ppm)	Time (min)	Ca Conc. (ppm)	Time (min)	Ca Conc. (ppm)
5	1604.45	5	1587.28	5	1617.84
15	1480.69	15	1493.54	19	1490.67
26	1355.13	25	1401.91	26	1426.56
41	1246.41	41	1294.39	41	1344.98
55	1186.77	57	1232.96	55	1269.32
55	1175.60	57	1203.16	55	1240.17
73	1099.88	67	1174.37	71	1209.80
91	1030.35	87	1113.57	90	1127.26
112	1002.26	115	1028.58	111	1058.82
133	970.56	128	1026.80	131	1020.86
152	949.82	151	976.04	151	1015.23
152	963.14	151	973.54	151	1024.89

Table B. 41: *Experiment 25 data*

Experiment: 25					
Treatment: Presence of 4.5 ppm aluminum					
Super sat.	3	Antiscalant	9 ppm	Stirrer speed	180 rpm
Experiment	25.1	Experiment	25.2	Experiment	25.3
Seed crystals	2000 ppm	Seed crystals	2000 ppm	Seed crystals	2000 ppm
Average pH	4.27	Average pH	4.27	Average pH	4.26
Temperature	25	Temperature	25	Temperature	25
Time (min)	Ca Conc. (ppm)	Time (min)	Ca Conc. (ppm)	Time (min)	Ca Conc. (ppm)
6	1686.13	6	1667.87	5	1647.80
15	1520.44	17	1520.50	15	1549.91
23	1443.57	31	1369.09	25	1495.00
43	1250.68	49	1269.19	42	1382.00
55	1189.99	57	1240.21	58	1318.09
55	1186.63	57	1245.14	58	1292.38
70	1113.96	82	1148.25	72	1258.48
90	1064.22	94	1124.27	91	1188.02
114	1004.17	114	1071.78	112	1148.75
134	969.82	133	1048.09	133	1077.16
151	951.37	150	1015.58	151	1059.64
151	963.65	150	1018.05	151	1064.43

B.8. Crystallisation in the presence of hydrogen peroxide and aluminum

The data generated during the experiment in the presence of hydrogen peroxide and aluminum is detailed in Table 42.

Table B. 42: *Experiment 28 data*

Experiment: 28					
Treatment: Presence of 90 ppm hydrogen peroxide and 4.5 ppm aluminum					
Super sat.	3	Antiscalant	9 ppm	Stirrer speed	180 rpm
Experiment	28.1	Experiment	28.2	Experiment	28.3
Seed crystals	2000 ppm	Seed crystals	2000 ppm	Seed crystals	2000 ppm
Average pH	4.41	Average pH	4.41	Average pH	4.41
Temperature	25	Temperature	25	Temperature	25
Time (min)	Ca Conc. (ppm)	Time (min)	Ca Conc. (ppm)	Time (min)	Ca Conc. (ppm)
5	1670.37	5	1680.15	5	1723.11
16	1560.18	19	1546.66	15	1599.83
26	1448.75	28	1459.34	27	1502.82
40	1334.60	44	1363.04	41	1398.39
55	1254.28	55	1280.64	56	1329.00
55	1263.68	55	1274.02	56	1323.96
70	1226.04	75	1208.77	69	1270.15
91	1140.28	91	1172.87	92	1166.78
113	1094.73	109	1136.56	120	1149.67
129	1067.39	131	1100.34	140	1072.94
151	1028.68	151	1040.62	151	1085.06
151	1023.18	151	1036.63	151	1076.55

Appendix C: Uncertainty

C.1. Uncertainty propagation of the calcium concentration

The calcium concentration is a function of the concentration of the diluted sample measured by the ICP-OES (c_{ICP}), the volume of the diluted sample (V_{RO}) and the volume of the undiluted sample added (V_{sample}) as shown in equation 3.9.

$$f(c_{Ca}) = c_{ICP}(1 + \frac{V_{RO}}{2V_{sample}}) \quad [3.3]$$

The uncertainty propagation is a function of the derivatives of the dependent functions (Equation 2.26)

$$\Delta_y = \sqrt{\left(\sum_{i=1}^{m}\left(\frac{\partial f}{\partial x_i}\right)\Delta_{xi}\right)^2} \quad [2.26]$$

Thus, the derivatives are:

$$\frac{df}{dc_{ICP}} = 1 + \frac{V_{RO}}{2V_{sample}} \quad [C.1]$$

$$\frac{df}{dV_{RO}} = \frac{c_{ICP}}{2V_{sample}} \quad [C.2]$$

$$\frac{df}{dV_{sample}} = -\frac{c_{ICP}V_{RO}}{2V_{sample}^2} \quad [C.3]$$

By substituting the derivatives (Equations C.1 – C.3) into equation 2.13, the propagated uncertainty of the calcium concentration can be calculated by equation 3.9.

$$\Delta c_{Ca} = \sqrt{\left[\left(1 + \frac{V_{RO}}{2V_{sample}}\right)\Delta c_{ICP}\right]^2 + \left[\frac{c_{ICP}}{2V_{sample}}.\Delta V_{RO}\right]^2 + \left[-\frac{c_{ICP}V_{RO}}{2V_{sample}^2}.\Delta V_{sample}\right]^2} \quad [3.9]$$

C.2. Uncertainty propagation of the percentage calcium removal

The percentage calcium removal is a function of the initial calcium concentration ($x_{Ca-inital}$) and the final calcium concentration ($x_{Ca-final}$) as shown in equation 3.5.

$$f(\%\, Ca_{removed}) = \left(1 - \frac{x_{Ca-final}}{x_{Ca-initial}}\right)100 \quad [3.5]$$

The uncertainty propagation is a function of the derivatives of the dependent functions (Equation 2.26)

$$\Delta_y = \sqrt{\left(\sum_{i=1}^{m}\left(\frac{\partial f}{\partial x_i}\right)\Delta_{xi}\right)^2} \quad [2.26]$$

Thus, the derivatives are:

$$\frac{df}{dx_{Ca-final}} = \frac{100}{-x_{Ca-inital}} \quad [C.4]$$

$$\frac{df}{dx_{Ca-initial}} = \frac{100\ x_{Ca-final}}{x^2_{Ca-inital}} \quad [C.5]$$

By substituting the derivatives (Equations C.4 – C.5) into equation 2.13, the propagated uncertainty of the percentage calcium removal can be calculated by equation 3.10.

$$\Delta\%Ca_{removed} = \sqrt{\left[\frac{100}{-x_{Ca-inital}}.\Delta x_{Ca-final}\right]^2 + \left[\frac{100\ x_{Ca-final}}{x^2_{Ca-inital}}.\Delta x_{Ca-inital}\right]^2} \quad [3.10]$$

C.3. Uncertainty propagation of the average percentage calcium removal

The average percentage calcium removal is a function of the different percentage calcium removals ($\%Ca_{removed,1}$) as shown in equation 3.6.

$$f(\%Ca_{Average}) = \frac{\%Ca_{removed,1} + \%Ca_{removed,2} + \%Ca_{removed,3}}{3} \quad [3.6]$$

The uncertainty propagation is a function of the derivatives of the dependent functions (Equation 2.26)

$$\Delta_y = \sqrt{\left(\sum_{i=1}^{m}\left(\frac{\partial f}{\partial x_i}\right)\Delta_{xi}\right)^2} \quad [2.26]$$

Thus, the derivatives are:

$$\frac{df}{d\%Ca_{removed,1}} = \frac{1}{3} \quad [C.6]$$

$$\frac{df}{d\%Ca_{removed,2}} = \frac{1}{3} \quad [C.7]$$

$$\frac{df}{d\%Ca_{removed,3}} = \frac{1}{3} \quad [C.8]$$

By substituting the derivatives (Equations C.6 – C.8) into equation 2.23, the propagated uncertainty of the average percentage calcium removal can be calculated by equation 3.11.

$$\Delta\%Ca_{Average} = \sqrt{\left[\frac{\Delta\%Ca_{removed,1}}{3}\right]^2 + \left[\frac{\Delta\%Ca_{removed,2}}{3}\right]^2 + \left[\frac{\Delta\%Ca_{removed,3}}{3}\right]^2} \quad [3.11]$$

C.4. Uncertainty propagation of the growth rate constant

The growth rate constant is a function of the calcium concentration at time t (c_{Ca}), the initial calcium concentration ($c_{Ca,i}$) and the equilibrium calcium concentration (x_{Ca-eq}) as shown in equation 3.8.

$$f(k') = \left(\frac{1}{c_{Ca} - c_{Ca-eq}} - \frac{1}{c_{Ca,i} - c_{Ca-eq}}\right).\frac{1}{t} \quad [3.8]$$

The uncertainty propagation is a function of the derivatives of the dependent functions (Equation 2.26)

$$\Delta_y = \sqrt{\left(\sum_{i=1}^{m}\left(\frac{\partial f}{\partial x_i}\right)\Delta_{xi}\right)^2} \quad [2.26]$$

Thus, the derivatives are:

$$\frac{df}{dc_{Ca}} = \frac{1}{t.(c_{Ca} - c_{Ca-eq})^2} \quad [C.9]$$

$$\frac{df}{dc_{Ca,i}} = \frac{-1}{t.(c_{Ca,i} - c_{Ca-eq})^2} \quad [C.10]$$

By substituting the derivatives (Equations C.9 – C.10) into equation 2.26 the propagated uncertainty of the growth rate constant can be calculated by equation 3.16.

$$\Delta k' = \sqrt{\left[\frac{\Delta c_{Ca}}{t.(c_{Ca} - c_{Ca-eq})^2}\right]^2 + \left[\frac{-\Delta c_{Ca,i}}{t.(c_{Ca,i} - c_{Ca-eq})^2}\right]^2} \quad [3.16]$$

C.5. Uncertainty parameters

The uncertainty parameters calculated using multiple samples for the different volumes used during the sample dilution and the uncertainty parameter of the ICP measurements are shown in Table C.1.

Table C. 1: *Uncertainty parameters calculated.*

		V_{RO}	V_{sample}	c_{ICP}
Data used for calculations		7.4440	0.2031	78.845
		7.4363	0.1995	78.965
		7.4862	0.2058	80.602
		7.4516	0.2000	80.965
		7.4868	0.1992	81.434
		7.4530	0.1998	80.650
		7.4988	0.1996	80.999
		7.4522	0.1993	78.203
		7.4383	0.1998	80.594
		7.4600	0.1996	81.564
		7.4767	0.1990	78.081
		7.4361	0.1992	81.033
		7.4417	0.1997	-
		7.4526	0.1990	-
Number of cells	n	14	14	12
Average	$\bar{x}$	7.46	0.20	80.16
Standard dev	s	0.0207	0.0019	1.2665
Standard error	sn	0.0055	0.0005	0.3656
Sig level	α	0.05	0.05	0.05
Students t-stat	t(α, n-1)	2.160	2.160	2.201
Uncertainty parameter	$\Delta_{x,i}$	0.012	0.001	0.805

C.6. Uncertainty calculated for the experimental data

The uncertainty calculated for the control experiments can be seen in Tables C.2 – C.3.

Table C. 2: *Uncertainty of the initial and final calcium concentrations during the control experiments.*

Experiment	Initial @ 5 min		Final @ 150 min	
	Calcium conc. (ppm)	**Uncertainty (ppm)**	**Calcium conc. (ppm)**	**Uncertainty (ppm)**
C.1'	1717.51	18.93	986.84	16.96
C.2'	1718.67	18.93	988.08	16.96
C.3'	1738.99	19.00	985.88	16.95
C.1	1606.10	18.58	1305.68	17.71
C.2	1634.14	18.66	1391.21	17.94
C.3	1647.09	18.70	1445.15	18.10

Table C. 3: *Uncertainty of calcium removal and average calcium removal for the control experiments.*

Experiment	% Calcium removed		% Average Calcium removed	
	% removed	Uncertainty	% removed	Uncertainty
C.1'	42.54	1.17		
C.2'	42.51	1.17	42.79	0.67
C.3'	43.31	1.16		
C.1	18.70	1.45		
C.2	14.87	1.47	15.28	0.85
C.3	12.26	1.48		

The uncertainty calculated for the data where mixing as seed crystal treatment was applied can be seen in Tables C.4 – C.5.

Table C. 4: *Uncertainty of the initial and final calcium concentrations during the experiments with mixing as seed crystal treatment.*

Experiment	Initial @ 5 min		Final @ 150 min	
	Calcium conc. (ppm)	Uncertainty (ppm)	Calcium conc. (ppm)	Uncertainty (ppm)
1.1	1658.14	18.74	1328.68	17.77
1.2	1696.96	18.86	1497.04	18.25
1.3	1739.91	19.00	1550.57	18.41
2.1	1657.23	18.74	1164.87	17.36
2.2	1698.82	18.87	1307.78	17.72
2.3	1681.84	18.81	1384.22	17.92
3.1	1683.40	18.82	1091.02	17.18
3.2	1707.19	18.90	1262.6	17.60
3.3	1725.68	18.96	1454.57	18.12
27.1	1695.71	18.86	1262.57	17.60
27.2	1753.13	19.05	1442.73	18.09
27.3	1732.81	18.98	1473.45	18.18
4.1	1628.71	18.65	1140.17	17.30
4.2	1661.45	18.75	1351.16	17.83
4.3	1718.44	18.93	1415.44	18.01
5.1	1626.54	18.64	1108.21	17.22
5.2	1626.15	18.64	1206.88	17.46
5.3	1633.25	18.66	1278.10	17.64
6.1	1740.35	19.00	1036.93	17.06
6.2	1738.94	19.00	1225.85	17.51
6.3	1757.63	19.06	1290.21	17.67
26.1	1740.94	19.01	1294.42	17.68
26.2	1734.63	18.99	1373.82	17.90
26.3	1739.92	19.00	1410.23	18.00

Experiment	Initial @ 5 min		Final @ 150 min	
	Calcium conc. (ppm)	Uncertainty (ppm)	Calcium conc. (ppm)	Uncertainty (ppm)
7.1	1647.64	18.71	1137.39	17.29
7.2	1606.65	18.58	1267.87	17.61
7.6	1702.84	18.88	1324.04	17.76
8.1	1729.78	18.97	1176.47	17.38
8.2	1696.98	18.86	1245.39	17.56
8.3	1695.68	18.86	1349.34	17.83
9.1	1665.45	18.76	1275.92	17.63
9.2	1746.16	19.02	1411.38	18.00
9.3	1762.34	19.08	1421.36	18.03

Table C. 5: *Uncertainty of the calcium removal and average calcium removal for the experiments with mixing as seed crystal treatment.*

Experiment	% Calcium removed		% Average Calcium removed	
	% removed	Uncertainty	% removed	Uncertainty
1.1	19.87	1.40		
1.2	11.78	1.46	14.18	0.83
1.3	10.88	1.44		
2.1	29.71	1.31		
2.2	23.02	1.35	23.47	0.78
2.3	17.70	1.41		
3.1	35.19	1.25		
3.2	26.04	1.32	25.65	0.76
3.3	15.71	1.40		
27.1	25.54	1.33		
27.2	17.71	1.37	19.41	0.79
27.3	14.97	1.40		
4.1	30.00	1.33		
4.2	18.68	1.41	22.10	0.79
4.3	17.63	1.39		
5.1	31.87	1.32		
5.2	25.78	1.37	26.47	0.79
5.3	21.74	1.40		
6.1	40.57	1.18		
6.2	27.62	1.27	31.35	0.72
6.3	25.87	1.28		
26.1	25.65	1.30		
26.2	20.80	1.35	21.80	0.77
26.3	18.95	1.36		
7.1	30.97	1.31	24.46	0.79

Experiment	% Calcium removed		% Average Calcium removed	
	% removed	Uncertainty	% removed	Uncertainty
7.2	21.09	1.43		
7.6	22.25	1.35		
8.1	31.99	1.25		
8.2	26.61	1.32	26.34	0.76
8.3	20.42	1.37		
9.1	23.39	1.37		
9.2	19.17	1.36	20.64	0.78
9.3	19.35	1.34		

The uncertainty calculated for the data where aeration as seed crystal treatment was applied can be seen in Tables C.6. – C.7.

Table C. 6: *Uncertainty of the initial and final calcium concentrations during the experiments with aeration as seed crystal treatment.*

Experiment	Initial @ 5 min		Final @ 150 min	
	Calcium conc. (ppm)	Uncertainty (ppm)	Calcium conc. (ppm)	Uncertainty (ppm)
10.1	1614.92	18.60	1273.77	17.63
10.2	1655.51	18.73	1398.75	17.96
10.3	1667.90	18.77	1469.14	18.16
11.1	1677.33	18.80	1276.52	17.64
11.2	1640.06	18.68	1374.89	17.90
11.3	1638.44	18.68	1421.45	18.03
12.1	1699.74	18.87	1347.49	17.82
12.2	1718.82	18.93	1448.13	18.10
12.3	1720.73	18.94	1516.60	18.30
13.1	1639.25	18.68	1250.05	17.57
13.2	1651.18	18.72	1360.97	17.86
13.3	1678.05	18.80	1484.49	18.21
14.1	1684.24	18.82	1305.68	17.71
14.2	1686.55	18.83	1407.40	17.99
14.3	1720.23	18.94	1433.86	18.06
15.1	1737.89	19.00	1348.68	17.83
15.2	1751.35	19.04	1485.81	18.21
15.3	1764.00	19.08	1555.55	18.42
16.1	1691.61	18.85	1384.78	17.93
16.2	1735.32	18.99	1461.54	18.14
16.3	1739.05	19.00	1521.06	18.32
17.1	1718.96	18.93	1307.84	17.72
17.2	1732.97	18.98	1489.58	18.22
17.3	1763.85	19.08	1597.38	18.55

18.1	1801.64	19.21	1395.21	17.95
18.2	1769.51	19.10	1529.62	18.34
18.6	1795.22	19.19	1607.95	18.58

Table C. 7: *Uncertainty of the calcium removal and average calcium removal for the experiments with aeration as seed crystal treatment.*

Experiment	% Calcium removed		% Average Calcium removed	
	% removed	Uncertainty	% removed	Uncertainty
10.1	21.13	1.42		
10.2	15.51	1.45	16.18	0.84
10.3	11.92	1.47		
11.1	23.90	1.35		
11.2	16.17	1.45	17.77	0.82
11.3	13.24	1.48		
12.1	20.72	1.37		
12.2	15.75	1.40	16.11	0.81
12.3	11.86	1.44		
13.1	23.74	1.38		
13.2	17.58	1.43	17.62	0.82
13.3	11.53	1.47		
14.1	22.48	1.36		
14.2	16.55	1.42	18.56	0.80
14.3	16.65	1.39		
15.1	22.4	1.33		
15.2	15.16	1.39	16.46	0.80
15.3	11.82	1.41		
16.1	18.14	1.40		
16.2	15.78	1.39	15.48	0.81
16.3	12.53	1.42		
17.1	23.92	1.33		
17.2	14.04	1.41	15.80	0.80
17.3	9.44	1.44		
18.1	22.56	1.29		
18.2	13.56	1.39	15.52	0.79
18.6	10.43	1.41		

The uncertainty calculated for the data in the presence of hydrogen peroxide can be seen in Tables C.8 – C.9.

Table C. 8: *Uncertainty of the initial and final calcium concentrations during the experiments in the presence of hydrogen peroxide.*

Experiment	Initial @ 5 min		Final @ 150 min	
	Calcium conc. (ppm)	Uncertainty (ppm)	Calcium conc. (ppm	Uncertainty (ppm)
19.1	1718.01	18.93	1157.65	17.34
19.2	1719.04	18.93	1254.42	17.58
19.3	1722.53	18.95	1491.24	18.23
20.1	1713.32	18.92	1165.52	17.36
20.2	1768.33	19.10	1311.03	17.73
20.3	1754.69	19.05	1436.09	18.07
21.1	1737.10	18.99	1376.56	17.90
21.2	1757.25	19.06	1499.93	18.25
21.3	1750.00	19.04	1561.86	18.44

Table C. 9: *Uncertainty of calcium removal and average calcium removal for the experiments in the presence of hydrogen peroxide.*

Experiment	% Calcium removed		% Average Calcium removed	
	% removed	Uncertainty	% removed	Uncertainty
19.1	32.62	1.25		
19.2	27.03	1.30	24.36	0.77
19.3	13.43	1.42		
20.1	31.97	1.26		
20.2	25.86	1.28	25.33	0.75
20.3	18.16	1.36		
21.1	20.76	1.35		
21.2	14.64	1.39	15.38	0.80
21.3	10.75	1.43		

The uncertainty calculated for the data in the presence of aluminum can be seen in Tables C.10 – C.11.

Table C. 10: *Uncertainty of the initial and final calcium concentrations during the experiments in the presence of aluminum.*

Experiment	Initial @ 5 min		Final @ 150 min	
	Calcium conc. (ppm)	Uncertainty (ppm)	Calcium conc. (ppm)	Uncertainty (ppm)
22.1	1623.93	18.63	936.41	16.85
22.2	1639.39	18.68	955.40	16.89
22.3	1645.34	18.70	992.91	16.97
23.1	1620.64	18.62	986.03	16.95
23.2	1628.42	18.65	1005.29	16.99
23.3	1658.57	18.74	1006.72	17.00
24.1	1604.45	18.57	956.48	16.89
24.2	1587.28	18.52	974.79	16.93
24.3	1617.84	18.61	1020.06	17.03
25.1	1686.13	18.83	957.51	16.90
25.2	1667.87	18.77	1016.82	17.02
25.3	1647.8	18.71	1062.04	17.12

Table C. 11: *Uncertainty of calcium removal and average calcium removal for the experiments in the presence of aluminum.*

Experiment	% Calcium removed		% Average Calcium removed	
	% removed	Uncertainty	% removed	Uncertainty
22.1	42.34	1.23		
22.2	41.72	1.23	41.24	0.71
22.3	39.65	1.24		
23.1	39.16	1.26		
23.2	38.27	1.26	38.91	0.72
23.3	39.30	1.23		
24.1	40.39	1.26		
24.2	38.59	1.28	38.64	0.74
24.3	36.95	1.28		
25.1	43.21	1.19		
25.2	39.03	1.23	39.27	0.71
25.3	35.55	1.27		

The uncertainty calculated for the data in the presence of hydrogen peroxide and aluminum can be seen in Table C.12. – C.13.

Table C. 12: *Uncertainty of the initial and final calcium concentrations during the experiments in the presence of hydrogen peroxide and aluminum.*

Experiment	Initial @ 5 min		Final @ 150 min	
	Calcium conc. (ppm)	Uncertainty (ppm)	Calcium conc. (ppm)	Uncertainty (ppm)
28.1	1670.37	18.78	1025.93	17.04
28.2	1680.15	18.81	1038.62	17.07
28.3	1723.11	18.95	1080.8	17.16

Table C. 13: *Uncertainty of calcium removal and average calcium removal for the experiments in the presence of hydrogen peroxide and aluminum.*

Experiment	% Calcium removed		% Average Calcium removed	
	% removed	Uncertainty	% removed	Uncertainty
28.1	38.58	1.23		
28.2	38.18	1.23	38.01	0.71
28.3	37.28	1.21		

Appendix D: Statistical tests

The t-test results tables for the different tests done are detailed below.

Table D. 1: *T-test between the control experiment in the presence of antiscalant and experiment 6.*

	C	***6***
Mean	16.02	31.76
Variance	0.82	0.25
Observations	4	4
Pearson Correlation	0.97	
df	3	
t Stat	-71.82	
P(T<=t) one-tail	2.97E-06	
t Critical one-tail	2.35	
P(T<=t) two-tail	5.95E-06	
t Critical two-tail	3.18	

Table D. 2: *T-test between the control experiment in the presence of antiscalant and experiment 20.*

	C	***20***
Mean	16.02	26.06
Variance	0.82	0.81
Observations	4	4
Pearson Correlation	-0.92	
df	3	
t Stat	-11.34	
P(T<=t) one-tail	0.00074	
t Critical one-tail	2.35	
P(T<=t) two-tail	0.00147	
t Critical two-tail	3.18	

Table D. 3: *T-test between the control experiment in the presence of antiscalant and experiment 23.*

	C	***23***
Mean	16.02	38.44
Variance	0.82	0.38
Observations	4	4
Pearson Correlation	0.76	
df	3	
t Stat	-75.88	
P(T<=t) one-tail	2.52E-06	
t Critical one-tail	2.35	
P(T<=t) two-tail	5.05E-06	
t Critical two-tail	3.18	

Table D. 4: *T-test between the control experiment in the absence of antiscalant and experiment 23.*

	C'	***23***
Mean	42.79	38.71
Variance	0.21	0.12
Observations	3	3
Pearson Correlation	-1.00	
df	2	
t Stat	8.86	
P(T<=t) one-tail	0.0063	
t Critical one-tail	2.92	
P(T<=t) two-tail	0.0125	
t Critical two-tail	4.30	

Appendix E: Sample calculations

All sample calculations were done using the data of experiment 6. The raw data obtained from the ICP-OES is detailed in Table E.1.

***Table E. 1**: Raw data obtained from experiment 6 for sample calculations.*

Run	Crystal treatment		Calcium conc. (ppm) @ 5 min		Calcium Conc. (ppm) @ 150 min	
	Speed (rpm)	Time (Min)	ICP-OES	Actual	ICP-OES	Actual
6.1			86.45	1707.37	51.42	1014.73
6.2	400	10	84.58	1670.50	61.00	1209.06
6.3			85.41	1687.65	63.42	1251.01

E.1. Calcium concentration

The calcium concentration was calculated for experiment 6.1 at 5 minutes using equation 3.2, where $V_{7.5} = 7.5\ ml$, $V_{0.2} = 0.2\ ml$ and $x_{ICP} = 86.45\ ppm$.

$$x_{Ca} = x_{ICP}\left(1 + \frac{V_{7.5}}{2V_{0.2}}\right) \qquad [3.2]$$

$$x_{Ca} = 86.45\left(1 + \frac{7.5}{2\times0.2}\right)$$

$$x_{Ca} = 1707.37\ ppm$$

Once the calcium concentration was calculated, the uncertainty was calculated using equation 3.10, where $V_{7.5} = 7.5\ ml$, $V_{0.2} = 0.2\ ml$ and $x_{ICP} = 86.45\ ppm$ and the uncertainty parameters where $\Delta x_{ICP} = 0.805$, $\Delta V_{7.5} = 0.012$ and $\Delta V_{0.2} = 0.001$ as calculated in Appendix C.

$$\Delta x_{Ca} = \sqrt{\left[\left(1 + \frac{V_{7.5}}{2V_{0.2}}\right)\Delta x_{ICP}\right]^2 + \left[\frac{x_{ICP}}{2V_{0.2}}.\Delta V_{7.5}\right]^2 + \left[-\frac{x_{ICP}V_{7.5}}{2V_{0.2}^2}.\Delta V_{0.2}\right]^2} \qquad [3.10]$$

$$\Delta x_{Ca} = \sqrt{\left[\left(1 + \frac{7.5}{2\times0.2}\right)0..805\right]^2 + \left[\frac{88.12}{2\times0.2}.0.012\right]^2 + \left[-\frac{86.45\times7.5}{2\times0.2^2}.0.001\right]^2}$$

$$\Delta x_{Ca} = 19.00\ ppm$$

$$\therefore x_{Ca} = 1707.38 \pm 19.00\ ppm$$

E.2. Percentage calcium removed

The percentage calcium was calculated for experiment 6.1 using equation 3.3, where $x_{Ca-final} = 1014.73\ ppm$ and $x_{Ca-initial} = 1707.37\ ppm$.

$$\% \, Ca_{removed} = \left(1 - \frac{x_{Ca-final}}{x_{Ca-initial}}\right) 100 \qquad [3.3]$$

$$\% \, Ca_{removed} = \left(1 - \frac{1014.73}{1707.37}\right) 100$$

$$\% \, Ca_{removed} = 40.57\%$$

Once the calcium concentration was calculated, the uncertainty was calculated using equation 3.12, where $x_{Ca-final} = 1014.73\, ppm$ and $x_{Ca-initial} = 1707.37\, ppm$ and the uncertainty parameters where $\Delta x_{Ca-final} = 17.06$ and $. \Delta x_{Ca-inital} = 19.00$

$$\Delta\%Ca_{removed} = \sqrt{\left[\frac{100}{-x_{Ca-inital}} . \Delta x_{Ca-final}\right]^2 + \left[\frac{100 \; x_{Ca-final}}{x^2_{Ca-inital}} . \Delta x_{Ca-inital}\right]^2} \qquad [3.12]$$

$$\Delta\%Ca_{removed} = \sqrt{\left[\frac{100}{-1707.37} \times 17.06\right]^2 + \left[\frac{100 \times 1014.73}{1707.37^2} \times 19.00\right]^2}$$

$$\Delta\%Ca_{removed} = 1.18\%$$

$$\therefore \% \, Ca_{removed} = 40.57 \pm 1.18\%$$

E.3. Average calcium removed

The average percentage calcium was calculated for experiment 6.1 using equation 3.4, where $\%Ca_{removed,1} = 40.57\%$, $\%Ca_{removed,2} = 27.62\%$, $\%Ca_{removed,3} = 25.57\%$.

$$\%Ca_{Average} = \frac{\%Ca_{removed,1} + \%Ca_{removed,2} + \%Ca_{removed,3}}{3} \qquad [3.4]$$

$$\%Ca_{Average} = \frac{40.57+27.62+25.87}{3}$$

$$\%Ca_{Average} = 31.35\%$$

Once the average calcium concentration was calculated, the uncertainty was calculated using equation 3.14, where the uncertainty parameters where $\Delta\%Ca_{removed,1} = 1.18\%$, $\Delta\%Ca_{removed,2} = 1.27\%$, $\Delta\%Ca_{removed,3} = 1.28\%$.

$$\Delta\%Ca_{Average} = \sqrt{\left[\frac{\Delta\%Ca_{removed,1}}{3}\right]^2 + \left[\frac{\Delta\%Ca_{removed,2}}{3}\right]^2 + \left[\frac{\Delta\%Ca_{removed,3}}{3}\right]^2} \qquad [3.14]$$

$$\Delta\%Ca_{Average} = \sqrt{\left[\frac{1.18}{3}\right]^2 + \left[\frac{1.27}{3}\right]^2 + \left[\frac{1.28}{3}\right]^2}$$

$$\Delta\%Ca_{Average} = 0.72\%$$

$$\%Ca_{Average,6} = 31.35 \pm 0.72\%$$

E.4. Growth rate constant

The growth rate constant was calculated for experiment 6.1 using equation 3.6, where $x_{Ca} = 1014.73\ ppm$, $x_{Ca,i} = 1707.37\ ppm$ and $x_{Ca-eq} = 868.69\ ppm$ at t = 145 minutes.

$$k' = \left(\frac{1}{x_{Ca} - x_{Ca-eq}} - \frac{1}{x_{Ca,i} - x_{Ca-eq}}\right).\frac{1}{t} \quad [3.6]$$

For the growth rate constant the concentration should be in mol. Therefore, the values were converted using the molar mass of calcium $M_{Ca} = 40.078\ g/mol$.

$$n = \frac{m}{M}$$

$$n = \frac{1014.73/1000}{40.078}$$

$$n_{Ca} = 0.0253\ mol/l$$

After all the values were converted, the growth rate constant was calculated using equation 3.16, where $x_{Ca} = 0.0253\ mol/l$, $x_{Ca,i} = 0.0426\ mol/l$ and $x_{Ca-eq} = 0.0217\ mol/l$ at t = 145 minutes.

$$k' = \left(\frac{1}{x_{Ca} - x_{Ca-eq}} - \frac{1}{x_{Ca,i} - x_{Ca-eq}}\right).\frac{1}{t} \quad [3.16]$$

$$k' = \left(\frac{1}{0.0253 - 0.0217} - \frac{1}{0.0426 - 0.0217}\right).\frac{1}{145}$$

$$k' = 1.576\frac{l}{mol.min}$$

E.5. Relative Centrifugal Force

The Relative Centrifugal Force (RCF) calculations were done for experiment 6, where the seed crystal mixture was mixed for 10 minutes at 400 rpm.The RCF was calculated using equation 2.20, where $RPM = 400$ and $r = 0.015\ m$.

$$RFC = RPM^2 \times 1.118 \times 10^{-5} \times r \quad [2.20]$$

$$RFC = 400^2 \times 1.118 \times 10^{-5} \times 0.015$$

$$RFC = 0.0268 \times g$$

E.6. G-factor

The G-factor calculations were done for experiment 6, where the seed crystal mixture was mixed for 10 minutes at 400 rpm. Before the G-factor could be calculated, the impeller power was firstly calculated, where N_P = 0.5, $\rho = 1052.718\ kg/m^3$, $n = 6.66\ rps$ and $d = 0.03\ m$

$$P = N_P \times \rho \times n^3 \times d^5 \qquad [2.22]$$

$$P = 0.5 \times 1052.718 \times 6.66^3 \times 0.03^5$$

$$P = 0.0038\ W$$

Now the G-factor could be calculated using equation 2.21, where $P = 0.0038W$, $V = 0.00012\ m^3$ and $\mu = 0.00089\ Pa.s$.

$$G = \sqrt{\frac{P/V}{\mu}} \qquad [2.21]$$

$$G = \sqrt{\frac{0.0038/0.00012}{0.00089}}$$

$$G = 118.37\ 1/s$$